https://doi.org/10.5194/essd-2022-239
Preprint. Discussion started: 1 August 2022

Open Access Earth System Science Data Discussions

Heat stored in the Earth system 1960-2020: Where does the energy go?

Authors: Karina von Schuckmann[1], Audrey Minère[1], Flora Gues[1,2], Francisco José Cuesta Valero[3,36], Gottfried Kirchengast[4], Susheel Adusumilli[5], Fiamma Straneo[5], Richard P. Allan[6], Paul M. Barker[7], Hugo Beltrami[8,51], Tim Boyer[9], Lijing Cheng[10,11], John A. Church[7], Damien Desbruyeres[12], Han Dolman[13], Catia M. Domingues[14], Almudena García-García[3,36], Donata Giglio[15], John E. Gilson[5], Maximilian Gorfer[16,4], Leopold Haimberger[17], Stefan Hendricks[18], Shigeki Hosoda[19], Gregory C. Johnson[20], Rachel Killick[21], Brian King[14], Nicolas Kolodziejczyk[22], Anton Korosov[23], Gerhard Krinner[24], Mikael Kuusela[25], Moritz Langer[26,27], Thomas Lavergne[28], Isobel Lawrence[29], Yuehua Li[30], John Lyman[20], Ben Marzeion[21], Michael Mayer[17,31], Andrew H. MacDougall[32], Trevor McDougall[7], Didier Paolo Monselesan[33], Jan Nitzbon[26,34], Inès Otosaka[35], Jian Peng[3,36], Sarah Purkey[5], Dean Roemmich[5], Kanako Sato[19], Katsunari Sato[37], Abhishek Savita[38], Axel Schweiger[39], Andrew Shepherd[35], Sonia I. Seneviratne[40], Leon Simons[41], Donald A. Slater[42], Thomas Slater[35], Noah Smith[43], Andrea Steiner[4], Toshio Suga[44,19], Tanguy Szekely[45], Wim Thiery[46], Mary-Louise Timmermans[47], Inne Vanderkelen[46], Susan E. Wjiffels[33,48], Tonghua Wu[49], Michael Zemp[50]

Corresponding author: Karina von Schuckmann, karina.von.schuckmann@mercator-ocean.fr

1 Mercator Ocean International, Toulouse, France
2 CELAD, Toulouse, France
3 Department of Remote Sensing, Helmholtz Centre for Environmental Research, Leipzig, 04318, Germany
4 Wegener Center for Climate and Global Change and Institute of Physics, University of Graz, Graz, Austria
5 Scripps Institution of Oceanography, University of California San Diego, San Diego, California, USA
6 University of Reading, UK
7 University of New South Wales, Sydney, Australia
8 Climate & Atmospheric Sciences Institute and Department of Earth Sciences, St. Francis Xavier University, Antigonish, B2G 2W5, Canada
9 NOAA's National Centers for Environmental Information, Silver Spring, Maryland, USA
10 Institute of Atmospheric Physics, Chinese Academy of Sciences, Beijing, China
11 Center for Ocean Mega-Science, Chinese Academy of Sciences, Qingdao, 266071, China
12 Ifremer, University of Brest, CNRS, IRD, Laboratoire d'Océanographie Physique et Spatiale, Brest, France
13 Netherlands Institute for Sea Research, Den Burg, Texel, Netherlands
14 National Oceanographic Centre, Southampton, UK
15 University of Colorado, Boulder, USA
16 Center for Climate Systems Modeling, ETH Zurich, Zurich, Switzerland
17 Department of Meteorology and Geophysics, University of Vienna, Vienna, Austria
18 Alfred Wegener Institute Helmholtz Centre for Polar and Marine Research, Germany
19 Japan Marine-Earth Science and Technology (JAMSTEC), Japan
20 NOAA, Pacific Marine Environmental Laboratory, Seattle, USA
21 Met Office Hadley Centre, Exeter, UK
22 University of Brest, CNRS, IRD, Ifremer, Laboratoire d'Océanographie Physique et Spatiale, IUEM, Brest, France
23 Nansen Environmental and Remote Sensing Center, Norway
24 Institut des Géosciences de l'Environnement, CNRS, Université Grenoble Alpes, Grenoble, France
25 Carnegie Mellon University, Pittsburg, USA
26 Alfred Wegener Institute Helmholtz Centre for Polar and Marine Research, Permafrost Research Section, Potsdam, Germany
27 Humboldt-Universität zu Berlin, Geography Department, Berlin, Germany
28 Norwegian Meteorological Institute, Norway
29 European Space Agency, ESRIN, Via Galileo Galilei, 1, 00044 Frascati RM, Italy
30 University of Bremen, Germany

https://doi.org/10.5194/essd-2022-239
Preprint. Discussion started: 1 August 2022

Open Access Earth System Science Data Discussions

31 European Centre for Medium-Range Weather Forecasts (ECMWF), Reading, UK
32 Climate & Environment Program, St. Francis Xavier University Antigonish, Nova Scotia, Canada B2G 2W5
33 CSIRO Oceans and Atmosphere, Hobart, Tasmania, Australia
34 Alfred Wegener Institute Helmholtz Centre for Polar and Marine Research, Paleoclimate Dynamics Section, Bremerhaven, Germany.
35 Centre for Polar Observation and Modelling, University of Leeds, UK
36 Remote Sensing Centre for Earth System Research, Leipzig University, 04103, Leipzig, Germany
37 Japan Meteorological Agency, Japan
38 GEOMAR, Kiel, Germany
39 Polar Science Center, Applied Physics Laboratory, University of Washington, Seattle, WA, USA
40 Institute for Atmospheric and Climate Science, ETH Zurich, Zurich, 8092, Switzerland
41 The Club of Rome, The Netherlands Association, 's-Hertogenbosch, The Netherlands
42 Glaciology and Oceanography, Univ. of Edinburgh, UK
43 Department of Mathematics, University of Exeter, Exeter, United Kingdom
44 Tohoku University, Japan
45 Ocean Scope, Brest, France
46 Department of Hydrology and Hydraulic Engineering, Vrije Universiteit Brussel, Brussels, 1050, Belgium
47 Department of Earth and Planetary Sciences, Yale University, New Haven, Connecticut, USA
48 Woods Hole Oceanographic Institution, Massachusetts, USA
49 Cryosphere Research Station on Qinghai–Xizang Plateau, State Key Laboratory of Cryospheric Science, Northwest Institute of Eco–Environment and Resources (NIEER), Chinese Academy of Sciences (CAS), Lanzhou, 730000, China
50 Department of Geography, University of Zurich, Switzerland
51 Département des sciences de la Terre et de l'atmosphère, Université du Québec à Montréal, Montréal, Québec, Canada.

Abstract. The Earth climate system is out of energy balance and heat has accumulated continuously over the past decades, warming the ocean, the land, the cryosphere and the atmosphere. According to the 6th Assessment Report of the Intergovernmental Panel on Climate Change, this planetary warming over multiple decades is human-driven and results in unprecedented and committed changes to the Earth system, with adverse impacts for ecosystems and human systems. The Earth heat inventory provides a measure of the Earth energy imbalance, and allows for quantifying how much heat has accumulated in the Earth system, and where the heat is stored. Here we show that 380 ± 62 ZJ of heat has accumulated in the Earth system from 1971 to 2020, at a rate of 0.48 ± 0.1 W m^{-2}, with 89 ± 17 % of this heat stored in the ocean, 6 ± 0.1 % on land, 4 ± 1% in the cryosphere and 1 ± 0.2 % in the atmosphere. Over the most recent decade (2006-2020), the Earth heat inventory shows increased warming at rate of 0.48 ± 0.3 W m^{-2}/decade, and the Earth climate system is out of energy balance by 0.76 ± 0.2 Wm^{-2}. The Earth heat inventory is the most fundamental global climate indicator that the scientific community and the public can use as the measure of how well the world is doing in the task of bringing anthropogenic climate change under control. We call for an implementation of the Earth heat inventory into the Paris agreement's global stocktake based on best available science. The Earth heat inventory in this study, updated from von Schuckmann et al, 2020, is underpinned by worldwide multidisciplinary collaboration and demonstrates the critical importance of concerted international efforts for climate change monitoring and community-based recommendations as coordinated by the Global Climate Observing System (GCOS). We also call for urgently needed actions for enabling continuity, archiving, rescuing and calibrating efforts to assure improved and long-term monitoring capacity of the relevant GCOS Essential Climate Variables (ECV) for the Earth heat inventory.

https://doi.org/10.5194/essd-2022-239
Preprint. Discussion started: 1 August 2022

Open Access Earth System Science Data Discussions

Introduction

Since a recent international quantification of the Earth heat inventory (von Schuckmann et al., 2020), three main reports of the 6th assessment cycle of the Intergovernmental Panel for Climate Change (IPCC)[1] have been published. The IPCC report of Working Group III (WGIII) 'Climate Change 2022: Mitigation of Climate Change' (IPCC, 2022b) states that '*options available now in every sector that can at least halve emissions by 2030*' and that '*accelerated climate action is critical to sustainable development*'[2]. The IPCC report of Working Group II (WGII) 'Climate Change 2022: Impacts, Adaptation and Vulnerability' (IPCC, 2022a) offers solutions, while pointing out that '*every small increase in warming will result in increased risks*', and that *'it is essential to make rapid, deep cuts in greenhouse gas emissions to keep the maximum number of adaptation options open*[3]. The IPCC report of Working Group I (WGI) 'Climate Change 2022: The Physical Science Basis' (IPCC, 2021) concluded that '*recent human-induced changes in the climate are widespread, rapid, and intensifying, and unprecedented in thousands of years'*, and '*that there is no going back from some changes in the climate system, from which some changes could be slowed and others could be stopped by limiting warming*'[4].

These assessment outcomes further emphasize the need to extend the Global Climate Observing System (GCOS) beyond the strict scientific observation of the climate state to also supporting policy and planning (GCOS, 2021). The GCOS was established in 1992 to aid in developing and coordinating a GCOS that supported scientific understanding of climate change. More recently it has broadened its focus to include policy development, public information and planning for adaptation and mitigation (GCOS, 2016). GCOS started assessments of the Earth's heat inventory in 2018, and the carbon and the water cycles, to identify potential gaps and inconsistencies in existing observation systems (Crisp et al., 2022; Dorigo et al., 2021; von Schuckmann et al., 2020). The first call for concerted international collaboration on the Earth's energy imbalance and the associated Earth heat inventory had been established in a perspective paper in 2016 (von Schuckmann et al., 2016), initiating a research focus activity under WCRP/CLIVAR[5]. One of the outcomes was the development of an internationally and multidisciplinary driven publication on the Earth heat inventory, now under the auspices of GCOS (von Schuckmann et al., 2020), which further continues with this study. With this second study we aim to contribute to a more frequent and regular update of the state of the Earth heat inventory as an important indicator of climate change.

The Earth heat inventory provides a quantitative measure of the heat accumulated in the Earth system, which results from the anthropogenically perturbed planetary radiation budget – i.e., a positive Earth Energy Imbalance (EEI) forced by increasing atmospheric concentrations of radiatively active greenhouse gasses from human-induced emissions (Forster et al., 2022; Hansen et al., 2011) (Fig. 1). Estimates of the Earth heat inventory can be obtained by analyzing several

1 https://www.ipcc.ch/
2 https://report.ipcc.ch/ar6wg3/pdf/IPCC_AR6_WGIII_PressConferenceSlides.pdf
3 https://report.ipcc.ch/ar6wg2/pdf/IPCC_AR6_WGII_PressConferenceSlides.pdf
4 https://www.ipcc.ch/report/ar6/wg1/resources/presentations-and-multimedia
5 https://www.clivar.org/research-foci/heat-budget

https://doi.org/10.5194/essd-2022-239
Preprint. Discussion started: 1 August 2022

Open Access Earth System Science Data Discussions

Essential Climate Variables (ECVs) of GCOS, complemented by model and reanalysis outputs to fill the gaps, through the quantification of increases in heat content of the ocean, the land, the atmosphere, and the heat used to melt ice (Forster et al., 2022; von Schuckmann et al., 2020). This assessment allows for evaluating the total heat accumulated in the Earth system and where and how much heat is stored in the different Earth system components (Fig. 1). The derivative of the Earth heat inventory over time provides then an estimate of the global heating rate, and hence, the absolute value of the EEI (Loeb et al., 2012; Trenberth et al., 2016). A recent quantification of the Earth heat inventory (von Schuckmann et al., 2020) revealed a consistent long-term Earth system heat gain over the period 1971–2018, with a total heat gain of 358±37 ZJ, which is equivalent to a global heating rate of 0.47±0.1 W m^{-2}. Over the period 1971–2018, the majority of heat gain is reported for the global ocean, with 89 % of the excess heat in the climate system stored there, and for 2010–2018 that was 90%. 52 % of the excess heat was stored in the upper 700 m of the ocean for both time periods, with 28 % stored in the 700–2000 m depth layer and 9 % below 2000 m depth for 1971–2018 (30% in the 700–2000 m layer and 8% below 2000 m for 2010–2018). For 1971–2018, heat gain by the land amounts to 6 % of the total, 4 % is used for the melting of grounded and floating ice, and 1 % goes to atmospheric warming. Those fractions are 5%, 3%, and 2% respectively for 2010–2018. The results are consistent within uncertainty ranges with the assessment outcomes as obtained in the recent IPCC report (Forster et al., 2022).

The rate of change in the Earth heat inventory, and hence, the EEI, is the portion of the forcing that the Earth has not yet realized as warming (Hansen et al., 2005). The Earth system responds to an imposed radiative forcing through a number of feedbacks, which operate on various different timescales. Earth's radiative response is complex, comprising a variety of climate feedbacks (e.g., water vapor feedback, cloud feedbacks, ice-albedo feedback) (Forster et al., 2022). Conceptually, the relationships between EEI, radiative forcing and surface temperature change can be expressed as (Gregory & Andrews, 2016):

$$\Delta N_{TOA} = \Delta F_{ERF} - |\alpha_{FP}| \Delta T_S , \quad (1)$$

where ΔN_{TOA} is the Earth's net energy imbalance at the Top Of the Atmosphere (TOA) (in W m^{-2}), ΔF_{ERF} is the effective radiative forcing (W m^{-2}), ΔT_S is the global surface temperature anomaly (K) relative to the equilibrium state and α_{FP} is the net total feedback parameter (W m^{-2} K^{-1}), which represents the combined effect of the various climate feedbacks. Essentially, α_{FP} in Eq. (1) can be viewed as a measure of how efficient the system is at restoring radiative equilibrium for a unit surface temperature rise. Thus, ΔN_{TOA} represents the difference between the applied radiative forcing and Earth's radiative response through climate feedbacks associated with surface temperature increase (e.g., Hansen et al., 2011). Observation-based estimates of ΔN_{TOA} are therefore crucial both to our understanding of past climate change and for refining projections of future climate change (Gregory & Andrews, 2016; Kuhlbrodt & Gregory, 2012). The long atmospheric lifetime of carbon dioxide means that ΔN_{TOA}, ΔF_{ERF} and ΔT_S will remain positive for centuries, even with substantial reductions in greenhouse gas emissions, and lead to substantial sea-level rise, ocean warming and ice shelf loss (Cheng et al., 2019; Forster et al., 2022; Hansen et al., 2017; IPCC, 2021; Nauels et al., 2017). In other words, warming will continue even if atmospheric greenhouse gas (GHG) amounts are stabilized at today's level, and the EEI defines additional global warming that will occur without further change in forcing (Hansen et al., 2017). The EEI is less subject to decadal variations associated with internal climate variability than global

https://doi.org/10.5194/essd-2022-239
Preprint. Discussion started: 1 August 2022

surface temperature and therefore represents a robust measure of the rate of climate change, and its future commitment (Cheng et al., 2017; Forster et al., 2022; Palmer & McNeall, 2014; von Schuckmann et al., 2016).

https://doi.org/10.5194/essd-2022-239
Preprint. Discussion started: 1 August 2022

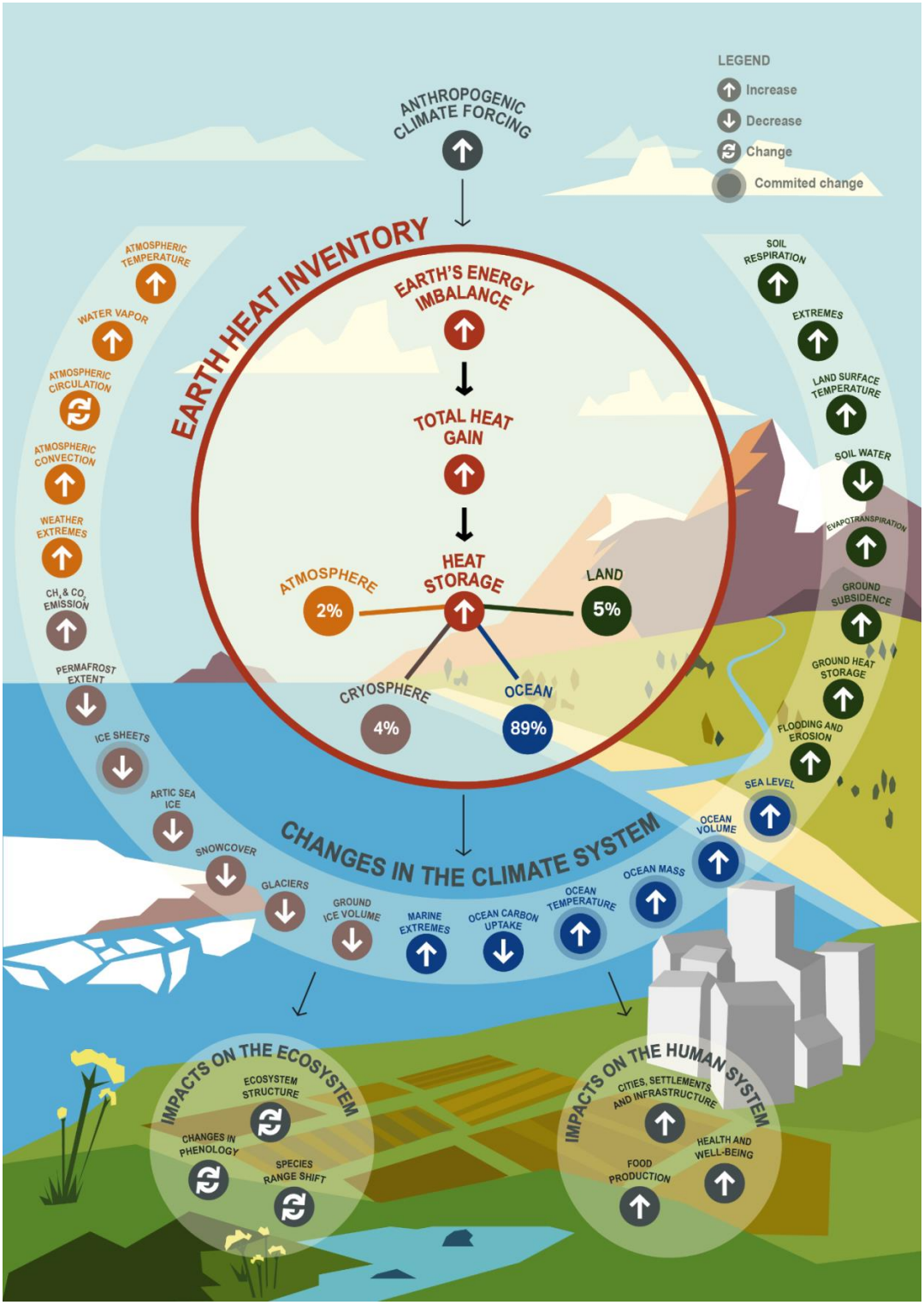

https://doi.org/10.5194/essd-2022-239
Preprint. Discussion started: 1 August 2022

Fig. 1: *Schematic overview on the central role of the Earth heat inventory and its linkage to anthropogenic emissions, the Earth energy imbalance, change in the Earth system and implications for ecosystems and human systems. The Earth heat inventory plays a central role for climate change monitoring as it provides information on the absolute value of the Earth energy imbalance, the total Earth system heat gain, and how much and where heat is stored in the different Earth system components. Examples of associated global-scale changes in the Earth system as assessed in (Gulev et al., 2021) are drawn, together with major implications for the ecosystem and human systems (IPCC, 2022c). Upward arrows indicate increasing change, downward arrows indicate decreasing change, and turning arrows indicate change in both directions. The % for heat stored in the Earth system are provided over the period 2006-2020 (see section 6).*

The heat gain in the Earth system from a positive EEI results in directly and indirectly triggered changes in the climate system, with a variety of implications for the environment and human systems (Fig. 1). One of the most direct implications from a positive EEI is the rise of Global Mean Surface Temperature (GMST). The accumulation and storage of surplus anthropogenic heat leads to ocean warming and thermal expansion of the water column, which together with terrestrial ice melt leads to sea level rise (WCRP Global Sea Level Budget Group, 2018). Moreover, there are various facets of impacts from ocean warming such as on climate extremes, which are provided in more detail in a recent review (Cheng et al., 2022). The heat accumulation in the Earth system also leads to warming of the atmosphere, particularly to a temperature increase in the troposphere, leading to water vapor increase and changes in atmospheric circulation (Gulev et al., 2021).

On land, the heat accumulation leads to an increase in ground heat storage, which in turn triggers an increase in ground surface temperature that may increase soil respiration, and evaporation, and may lead to a decrease in soil water, depending on the climatic and meteorological conditions and factors such as land cover and soil characteristics (Cuesta-Valero et al., 2022; Gulev et al., 2021). Moreover, inland water heat storage increases, which in turn leads to increases in lake water temperature that may result in algal blooms and lake stratification, and typically leads to a decrease in ice cover. Heat gain in the Earth system also induces an increase in permafrost heat content, which in turn increases ground subsidence, CH_4 and CO_2 emissions, and a decrease in permafrost extent and ground ice volume. More details are synthesized in (Cuesta-Valero et al., 2022). In the cryosphere associated changes include a loss of glaciers, ice sheets and Arctic sea ice (IPCC, 2019). These human-induced changes have already impacted terrestrial, freshwater and ocean ecosystems, and have adverse impacts on human systems (Fig.1). Particularly, they have emerged for ecosystem structure, species ranges and phenology (timing of life cycles), and include adverse impacts such as for water security and food production, health and wellbeing, cities, settlements and infrastructures as assessed in detail in the recent IPCC Working Group II report (IPCC, 2022c, see their Fig. SPM.2).

In summary, the Earth heat inventory is a global climate indicator integrating fundamental aspects of the Earth system under global warming. Particularly, the global climate indicator of the Earth heat inventory

- provides the best available current estimate of the absolute value of the Earth Energy Imbalance (Cheng et al., 2017; Cheng et al., 2019; Hakuba et al., 2021; Hansen et al., 2011; Loeb et al., 2012, 2022; Trenberth et al., 2016; von Schuckmann et al., 2020),

https://doi.org/10.5194/essd-2022-239
Preprint. Discussion started: 1 August 2022

- enables an integrated view of the effective radiative climate forcing, Earth's surface temperature response and the climate sensitivity (Forster et al., 2022; Hansen et al., 2011; Hansen et al., 2005; Palmer & McNeall, 2014; Smith et al., 2015),

- informs about the status of global warming in the Earth system as it integrates the heat 'in the pipeline' that will ultimately warm the deep ocean and melt ice sheets in the long term (Hansen et al., 2011; Hansen et al., 2005; IPCC, 2021),

- reveals how much and where surplus anthropogenic heat is available for melting the cryosphere and warming the ocean, land and atmosphere, which in turn allows for an evaluation of associated changes in the climate system and is essential to improve seasonal-to-decadal climate predictions and projections on century timescales to enable improved planning for and adaptation to climate change (Hansen et al., 2011; von Schuckmann et al., 2016, 2020),

- provides a tool for assessing the status of the GCOS, the identification of its strength and gaps, and the development of crucial recommendations of its future evolution (GCOS, 2021; von Schuckmann et al., 2020),

- creates an opportunity for a safe climate pathway while evaluating an atmospheric CO_2 reduction amount to bring Earth back towards energy balance (Hansen et al., 2000; von Schuckmann et al., 2020).

- Enables concerted international and multidisciplinary collaboration and advancements in climate science.

Hence, regularly assessing, quantifying and evaluating the Earth heat inventory creates a unique opportunity to support the call of action and solution pathways as assessed during the 6th assessment cycle of the IPCC. Moreover, the Earth heat inventory allows for a regular stock taking of the implementation of the Paris Agreement[6] while monitoring progress towards achieving the purpose of the agreement and its long-term goals based on best available science.

Based on the quantification of the Earth heat inventory published in 2020 (von Schuckmann et al., 2020), we will present the updated results of the Earth heat inventory over the period 1960-2020, along with the long-term Earth's system heat gain over this period, and the partitions of where the heat goes for the ocean, atmosphere, land and cryosphere. Section 2 provides the updates for ocean heat content, which is based on improved evaluations and the addition of further international data products of subsurface temperature. Updated estimates and refinements for atmospheric heat content are discussed in Section 3. For the land component in section 4, an improved uncertainty framework is proposed for the ground heat storage estimate, and new evaluations for inland freshwater heat storage and thawing of permafrost have been included (Cuesta-Valero et al., 2022). Heat available to melt the cryosphere is described in section 5. In section 6, the updated Earth heat inventory is established and discussed based on the results of sections 2-5. In the final section,

[6] https://unfccc.int/process-and-meetings/the-paris-agreement/the-paris-agreement

https://doi.org/10.5194/essd-2022-239
Preprint. Discussion started: 1 August 2022

challenges and recommendations for future improved estimates are discussed for each Earth system component, with associated recommendations for future evolutions of the GCOS.

2. Heat stored in the ocean

Estimating global Ocean Heat Content (OHC) directly depends on the variables of the in situ component of the Global Ocean Observing System (GOOS), which has continued to evolve during the past century (Abraham et al., 2013; Gould et al., 2013; Moltmann et al., 2019). Many global OHC estimates for the historical period start from about the 1950s and 1960s, i.e., when shipboard Nansen bottle and mechanical bathythermograph (MBT) instruments, conductivity–temperature–depth (CTD) instruments and the expendable bathythermograph (XBT) became available (Abraham et al., 2013; Goni et al., 2019). In the 1980s and 1990s, the GOOS (GOOS, 2019) started to further evolve, including programs for moored arrays in the tropical ocean basins, and the international World Ocean Circulation Experiment (WOCE) (Gould et al., 2013; King et al., 2001). Estimates of global OHC are, however, challenged by various factors, such as limited global coverage and data quality. The international community, especially under the auspices of the International qualiy-controlled Ocean Database project (IQuOD[7]), works together to face these obstacles through data and meta-data recovery and improved observational uncertainty specification, bias correction methods, and data processing techniques (Boyer et al., 2016; Castelao, 2020; Castelão, 2021; Cheng et al., 2018; Cowley et al., 2021; Goni et al., 2019; Gouretski & Cheng, 2020; Leahy et al., 2018; Mieruch et al., 2021; Palmer et al., 2018; Savita et al., 2022). Satellite altimeter measurements of sea surface height began in 1993 and are used to complement in situ-derived OHC estimates, either for validation purposes (Cabanes et al., 2013) or for establishing global gridded ocean temperature fields (Guinehut et al., 2012; Willis et al., 2004). Indirect estimates of OHC from remote sensing through the global sea-level budget became possible with satellite-derived ocean mass information in 2002 (Dieng et al., 2017; Hakuba et al., 2021; Llovel et al., 2014; Marti et al., 2022; Meyssignac et al., 2019), and should be considered in future establishments of the Earth heat inventory.

From the year 2000 onwards, the in situ component of the GOOS was revolutionized with the implementation of an international program of profiling floats targeting global hydrographic measurements of the upper 2000m depth (Riser et al., 2016; Roemmich et al., 2019) – a target which was largely reached in 2005 for the ocean area between 60°S-60°N and fully realized in 2006 (Riser et al. 2016). The opportunity for improved OHC estimates provided by Argo is tremendous and has led to major advancements in climate science, particularly on the discussion of the EEI (Cheng et al., 2019; Forster et al., 2022; Hansen et al., 2011; Johnson et al., 2016; Loeb et al., 2012, 2021; Trenberth & Fasullo, 2010). The near global coverage of the Argo network also provides an excellent test bed for the long-term OHC reconstruction extending back well before the Argo period (Allison et al., 2019; Cheng, Trenberth, Fasullo, Boyer, et al., 2017). Moreover, these evaluations inform further observing system recommendations for global climate studies, i.e., gaps in the deep ocean layers below 2000m depth, in marginal seas, in shelf areas and in the polar regions (von Schuckmann et al., 2016; 2020). Gap implementations are underway, for example, for the deep Argo array (Johnson et al., 2019). Different research groups have developed gridded products of subsurface temperature fields using different processing methodologies, and

[7] www.iquod.org

https://doi.org/10.5194/essd-2022-239
Preprint. Discussion started: 1 August 2022

an exhaustive list can be found in (Abraham et al., 2013; Boyer et al., 2016; Savita et al., 2022; Cheng et al., 2022; Gulev et al., 2021). Additionally, specific Argo-based products are listed on the Argo web page (http://www.argo.ucsd.edu/, last access: 12 July 2022). Albeit the tremendous improvement of in situ subsurface temperature measurements over time, estimates of global OHC remain an area of active research to minimize effects from different data processing techniques of the irregular in situ database, the choice of the climatology used in the mapping process, and data bias corrections, which today induce discrepancies between the different estimates (Boyer et al., 2016; Cheng et al., 2019; Good, 2017; Gouretski & Cheng, 2020; Savita et al., 2022). Ocean reanalysis systems have also been used to deliver estimates of near-global OHC (Trenberth et al., 2016; von Schuckmann et al., 2018), and their international assessments show increased agreement with increasing in situ data availability for the assimilation, particularly after 2005, i.e. when Argo had achieved nearly global scale data sampling (Palmer et al., 2017; Storto et al., 2018, 2019).

This initiative relies on the availability of regular updates of data products, their temporal extensions and direct interactions with the different research groups. A complete view of all subsurface ocean temperature products can be only achieved through a concerted international effort and over time, particularly accounting for the continued development of new or improved OHC products. In this study, we do not achieve a holistic view of all available products but present a starting point for future international regular assessments of global OHC. A first established international ensemble mean and standard deviation of near global OHC up to 2018 was established in von Schuckmann et al. (2020), which has now been updated up to 2020, and further extended with the addition of 4 new products (Fig. 3). The ensemble spread gives an indication of the agreement among products and can be used as a proxy for uncertainty. Compared to the results in von Schuckmann et al. (2020), the spread has increased by about 0.1 W m^{-2} the recent period 2006-2020 for the 0-2000m and 700-2000m integration depth layers. Concerns about common errors in the products remain. Accurate understanding of the uncertainties of the product is an essential element in their use. So far, a basic assumption is that the error distribution for the observations is Gaussian with a mean of zero, which has been approximated by an ensemble of various products. However, a more complete understanding of any apparent trends requires determination of systematic errors (e.g., systematic calibration errors), or the impacts of changing observation densities, and of instrument technologies (Wong et al., 2020). These elements can result in biases across the ensemble, or produce artificial changes in the energetics of the system (Wunsch, 2020). The uncertainty can also be estimated in other ways including some purely statistical methods (Cheng et al., 2019; Levitus et al., 2012; MacIntosh et al., 2017) or methods explicitly accounting for the error sources (Gaillard et al., 2016; Lyman & Johnson, 2014; von Schuckmann & Le Traon, 2011). Each method has its caveats; for example, the error covariances are mostly unknown, and must be estimated a priori. For this study, adopting a straightforward method with a “data democracy” strategy (i.e., all OHC estimates have been given equal weights) has been chosen as a starting point, differently from the ensemble approach adopted in AR6 (Forster et al., 2022).

https://doi.org/10.5194/essd-2022-239
Preprint. Discussion started: 1 August 2022

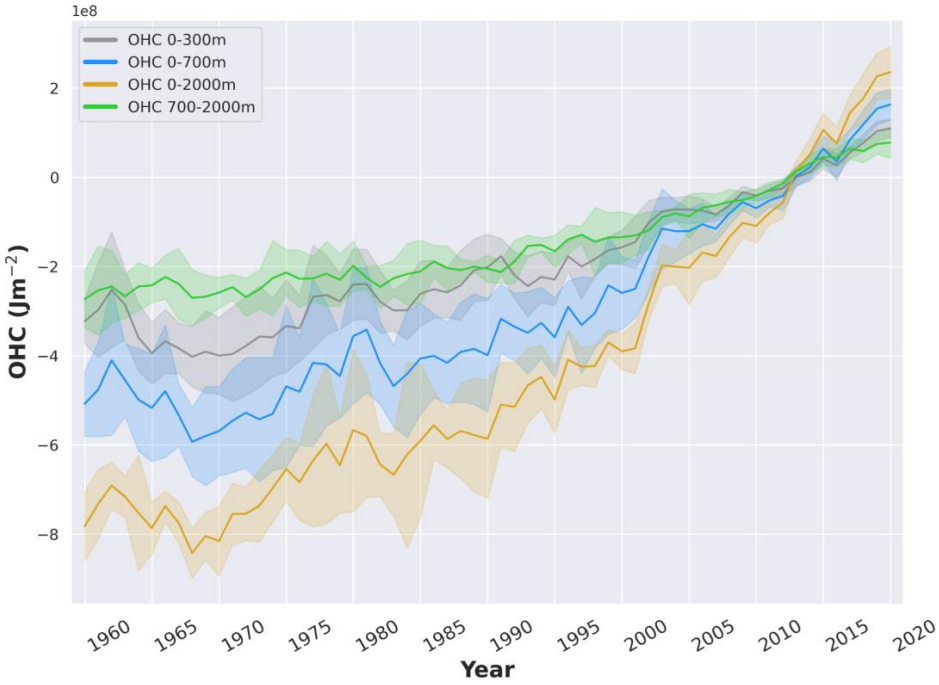

Figure 2. Ensemble mean time series and ensemble standard deviation (2-σ, shaded) of global ocean heat content (OHC) anomalies relative to the 2005–2020 climatology for the 0–300m (gray), 0–700m (blue), 0–2000m (yellow) and 700–2000m depth layer (green). The ensemble mean is an outcome of an international assessment initiative, and all products used are referenced in the legend of Fig. 3. The trends derived from the time series are given in Table 1. Note that values are given for the ocean surface area between 60°S and 60°N and are limited to the 300m bathymetry of each product.

https://doi.org/10.5194/essd-2022-239
Preprint. Discussion started: 1 August 2022

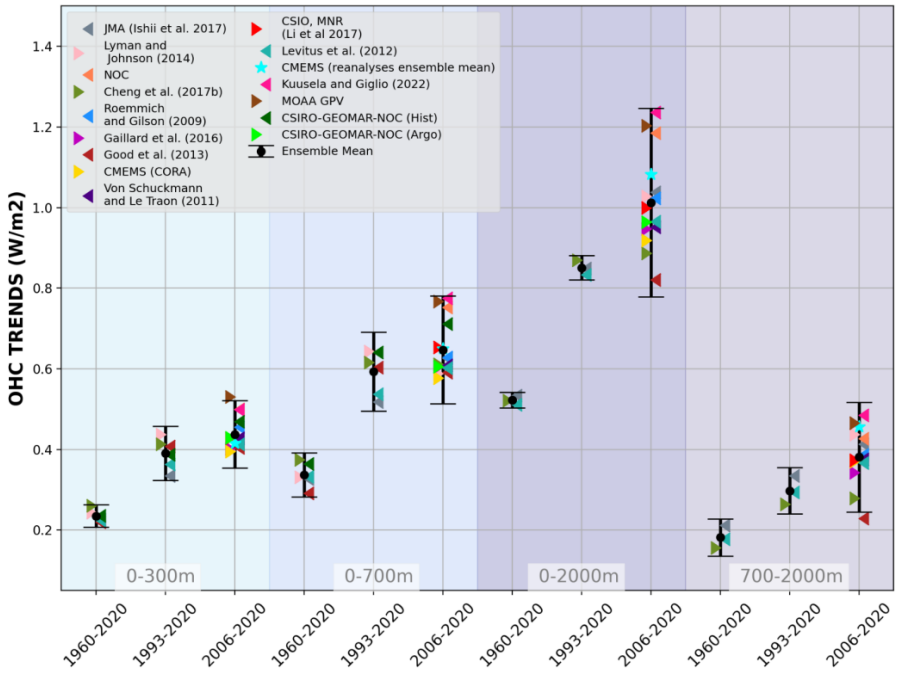

Figure 3. Trends of global ocean heat content (OHC) as derived from different products (colors), and using LOWESS (see text for more details). References are given in the figure legend, except, CMEMS (CORA and ARMOR-3D, http://marine.copernicus.eu/science-learning/ocean-monitoring-indicators, last access: 28 June 2022), CSIRO-GEOMAR-NOC (Argo) (Domingues et al., 2008; Roemmich et al., 2015; Wijffels et al., 2016), CSIRO-GEOMAR-NOC (hist) (Church et al., 2011; Domingues et al., 2008), NOC (National Oceanographic Institution) (Desbruyères et al., 2017) and the Argo dataset MOAA GPV (Hosoda et al., 2008). The ensemble mean and standard deviation (2 σ) are indicated in black. The shaded areas show trends from different depth layer integrations, i.e., 0–300m (light turquoise), 0–700m (light blue), 0–2000m (purple) and 700–2000m (light purple). For each integration depth layer, trends are evaluated over the three study periods, i.e., historical (1960–2020), altimeter era (1993–2020) and golden Argo era (2006–2020). See text for more details on the international assessment criteria. Note that values are given for the ocean surface area (see text for more details). References as indicated in the legend include (Cheng, Trenberth, Fasullo, Boyer, et al., 2017; Gaillard et al., 2016; Good et al., 2013; Ishii et al., 2017; Kuusela & Giglio, 2022; Levitus et al., 2012; Li et al., 2017; Lyman & Johnson, 2014; Roemmich & Gilson, 2009; von Schuckmann & Le Traon, 2011).

The continuity of this activity will help to further expand international collaboration and to unravel uncertainties due to the community's collective efforts on data quality as well as on detecting and reducing processing errors (e.g., IQuOD). It also provides up-to-date scientific knowledge of ocean warming. Products used for this assessment are referenced in the caption of Fig. 3. Estimates of OHC have been provided by the different research groups under largely homogeneous criteria. All

https://doi.org/10.5194/essd-2022-239
Preprint. Discussion started: 1 August 2022

estimates use a coherent ocean volume limited by the 300m isobath of each product and are limited to 60°S–60°N since most observational products exclude high latitude ocean areas because of the low observational coverage, and only annual averages have been used. The ocean areas within 60°S–60°N includes 91% of the global ocean surface area, and limiting to the 300m isobath neglects the contributions from coastal and shallow waters, so the resultant OHC trends will be underestimated if these ocean regions are warming. For example, neglecting shallow waters is discussed to account for more than 10% for 0–2000m OHC trends (Savita et al., 2022; von Schuckmann et al., 2014), and about 4% for the Arctic area (Mayer et al., 2021). The assessment is based on three distinct periods to account for the evolution of the observing system, i.e., 1960–2020 (i.e., "historical"), 1993–2020 (i.e., "altimeter era") and 2006–2020 (i.e., "golden Argo era"). All time series go up to 2020 – which was one of the principal limitations for the inclusion of some products. Our final estimates of OHC for the 0-300m, 0-700m, 700-2000m and 0-2000 m depth layers are the ensemble average of all products, with the uncertainty range defined by the standard deviation (2σ) of the corresponding estimates used (Fig. 2).

For the trend evaluation we have followed the most recent study of (Cheng et al., 2022), and used a Locally Weighted Scatterplot Smoothing (LOWESS) approach to reduce the effect of high-frequency variability (e.g., year-to-year variability), data noise or changes in the GCOS as it relies on a weighted regression (Cleveland, 1979) within a prescribed span width of 25 years for the historical and altimeter era, and 15 years for the recent period 2006-2020. The change in OHC(t) over a specific period, ΔOHC, is then calculated by subtracting the first value to the last value of the fitted time series, $OHC_{LOWESS(t)}$, to obtain the trend while dividing by the considered period. To obtain an uncertainty range on the trend estimate, and take into account the sensitivity of the calculation to interannual variability, we implement a Monte-Carlo simulation to generate 1000 surrogate series $OHC_{random}(t)$, under the assumption of a given mean (our "true" time series OHC(t)) (Cheng et al., 2022). Each surrogate $OHC_{random}(t)$ consists of the "true" time serie OHC(t) plus a randomly generated residual which follows a normal (Gaussian) distribution, and which is included in an envelope equal to 2 times the uncertainty associated to the time series. Then, a LOWESS fitted line is estimated for each of the 1000 surrogates. The 95% confidence interval for the trend is then calculated based on ± 2 times the standard deviation (± 2-σ) of all 1000 trends of the surrogates. However, the use of either trend estimates following a linear, or LOWESS approach, or the approach discussed in (Palmer et al., 2021) lead to consistent results within uncertainties (not shown).

In agreement with (Cheng et al., 2019; Gulev et al., 2021), our results reveal a continuous increase of ocean warming over the entire study period (Fig. 2). Moreover, rates of global ocean warming have increased over the 3 different study periods, i.e., historical up to the recent decadal change. The trend values are all given in Table 1. The major fraction of heat is stored in the upper ocean (0–300 m and 0–700 m depth). However, heat storage at intermediate depth (700–2000 m) increases at a nearly comparable rate as reported for the 0–300 m depth layer (Table 1, Fig. 3). There is a general agreement among the 16 international OHC estimates (Fig. 3). However, for some periods and depth layers the standard deviation reaches maxima to about 0.3 W m^{-2}. All products agree on the fact that global ocean warming rates have increased in the past decades and doubled since the beginning of the altimeter era (1993–2020 compared with 1960–2020) (Fig. 3). Moreover, there is a clear indication that heat sequestration into the deeper ocean layers below 700 m depth took place over the past 6 decades linked to an increase in OHC trends over time (Fig.

https://doi.org/10.5194/essd-2022-239
Preprint. Discussion started: 1 August 2022

3). Ocean warming rates for the 0–2000 m depth layer reached record rates of 1.0 (0.7) ±0.3 W m^{-2} over the period 2006-2020 for the ocean (global) area.

	Ocean Heat Content linear trends (W/m^2)			
	0-300m	**0-700m**	**0-2000m**	**700-2000m**
1960-2020	0.24 ± 0.1	0.34 ± 0.1	0.53 ± 0.1	0.18 ± 0.04
1971-2020	0.30 ± 0.1	0.44 ± 0.1	0.62 ± 0.1	0.21 ± 0.03
1993-2020	0.39 ± 0.1	0.60 ± 0.1	0.86 ± 0.2	0.30 ± 0.04
2006-2020	0.44 ± 0.1	0.64 ± 0.1	1.00 ± 0.3	0.38 ± 0.1

Table 1: *OHC trends using LOWESS (Locally Weighted Scatterplot Smoothing, see text for more details) as derived from the ensemble mean (Fig. 2) for different time intervals, as well as different integration depths. The regression was done for each time period (1960 - 2020, 1971 - 2020, 1993 - 2020, 2006 -2020). A time window of 25 years was used for the periods that allowed it (1960 - 2020, 1971 - 2020, 1993 - 2020). For the period 2006 - 2020, a time window of 15 years was used. Note that values are given in* Wm^{-2} *relative to the ocean surface area between 60°S and 60°N and are limited to the 300 m bathymetry of each product. See also text and Fig. 2-3 for more details.*

For the deep OHC changes below 2000 m, we adapted an updated estimate from (Purkey & Johnson, 2010) (PG10 hereinafter) from 1991 to 2020, which is a constant linear trend estimate (0.97 ± 0.48 ZJ yr^{-1}, 0.06 ±0.03 W m^{-2}) derived from a global integration of OHC below 2000 m using basin scale deep ocean temperature trends from repeated hydrographic sections. Some recent studies strengthened the results in PG10 (Desbruyères et al., 2016; Zanna et al., 2019). Desbruyères et al. (2016) examined the decadal change of the deep and abyssal OHC trends below 2000 m in the 1990s and 2000s, suggesting that there has not been a significant change in the rate of decadal global deep/abyssal warming from the 1990s to the 2000s and the overall deep ocean warming rate is consistent with PG10. Using a Green's function method and ECCO reanalysis data, Zanna et al. (2019) reported a deep ocean warming rate of ~0.06 W m^{-2} during the 2000s, consistent with PG10 used in this study. Zanna et al. (2019) shows a fairly weak global trend during the 1990s, different from observation-based estimates. This mismatch might come from how surface-deep connections are represented in ECCO reanalysis data and the use of time-mean Green's functions in Zanna et al. (2019), as well as from the sparse coverage of the observational network for relatively short time spans. Furthermore, combining hydrographic and deep-Argo floats, a recent study (Johnson et al., 2019) reported an accelerated warming in the South Pacific Ocean in recent years, but a global estimate of the OHC rate of change over time is not available yet, and the rates of warming may vary by ocean basin.

Before 1990, we assume zero OHC trend below 2000 m due to insufficient global observations below 2000m, following the methodology in some studies (Cheng et al. 2017; 2022), IPCC-AR5 (Rhein et al., 2013) and IPCC-AR6 (Forster et al., 2022; Gulev et al. 2021). The deep warming is likely driven by decadal variability in deep water formation rates, which could have been in a non-steady state mode prior to 1990, introducing additional uncertainty to the pre-1990 OHC estimates. Using surface temperature observations and assuming the heat is advected by mean circulation,

https://doi.org/10.5194/essd-2022-239
Preprint. Discussion started: 1 August 2022

Zanna et al. (2019) shows a near-zero (small cooling trend) OHC trend below 2000 m from the 1960s to 1980s, suggesting the assumption of zero-trend before 1990 might be small. The derived time following PG10 series after 1991 and zero-trend before 1990 is used for the Earth energy inventory in Sect. 5. A centralized (around the year 2006) uncertainty approach has been applied for the deep (>2000 m depth) OHC estimate following the method of Cheng et al. (2017), which allows us to extract an uncertainty range over the period 1993–2018 within the given [lower (0.96–0.48 ZJ yr^{-1}), upper (0.96+0.48 ZJ yr^{-1})] range of the deep OHC trend estimate. We then extend the obtained uncertainty estimate back from 1993 to 1960, with 0 OHC anomaly.

3. Heat available to warm the atmosphere

The heat content of the atmosphere is small in absolute terms, since its heat capacity as a gas is small compared to the one of the other Earth subsystems discussed in this paper. Yet it is by no means negligible, since in relative terms, the atmospheric heat gain is rapid over the recent decades and has a high impact on human life (Fig. 1). As for Earth's surface, widespread and rapid changes are ongoing in the atmosphere due to human-induced climate change (IPCC, 2021).

Atmospheric observations show a warming of the troposphere and a cooling and contraction of the stratosphere since at least 1979 (Pisoft et al., 2021; Steiner et al., 2020). In the tropics, the upper troposphere has warmed faster than the near-surface atmosphere since at least 2001, as seen with the new observation technique of GPS radio occultation (Gulev et al., 2021; Steiner et al., 2020a; 2020b), while observations based on microwave soundings have likely underestimated tropospheric temperature trends in the past (Santer et al., 2021; Zou et al., 2021).

Recently, a continuous rise of the tropopause has been observed for 1980 to 2020 over the northern hemisphere (Meng et al., 2022). The increase is equally due to tropospheric warming and stratospheric cooling in the period 1980 to 2000 while the rise after 2000 resulted primarily from enhanced tropospheric heat gain. Moreover, indications exist on a widening of the tropical belt (Fu et al., 2019; Grise et al., 2019; Staten et al., 2020) as well as on changes in the seasonal cycle (Santer et al., 2022). However, changes in atmospheric circulation and conditions for extreme weather are still subject to uncertainty (Cohen et al., 2020) while the occurrence of heat-related extreme weather events has clearly increased over the recent decades (Cohen et al., 2020; IPCC, 2021), with high risks for society, economy, and the environment (Fischer et al., 2021).

A regular assessment of atmospheric heat content changes is hence critical for a complete overview of energy and mass exchanges with other climate components and for a complete energy budgeting of Earth's climate system.

3.1 Atmospheric heat content

In a globally averaged and vertically integrated sense, heat accumulation in the atmosphere arises from a small imbalance between net energy fluxes at the top-of-atmosphere (TOA) and the surface (denoted *s*). The heat energy budget of the vertically integrated and globally averaged atmosphere (indicated by the global averaging operator <.>) reads as follows (Mayer et al., 2017):

https://doi.org/10.5194/essd-2022-239
Preprint. Discussion started: 1 August 2022

$$\frac{\partial AE}{\partial t} > N_{TOA} > -F_s > -F_{snow} > -F_{PE} >, (1)$$

where the vertically integrated atmospheric energy content *AE* per unit surface area [Jm^{-2}] reads

$$AE = \int_{z_s}^{z_{TOA}} \rho \left(c_v T + g(z - z_s) + L_e q + \frac{1}{2} V^2 \right) dz. (2)$$

In Equation (1), formulated in mean-sea-level altitude (z) coordinates used here for integrating over observational data, N_{TOA} is the net radiation at top of the atmosphere, F_s is the net surface energy flux defined as the sum of net surface radiation and latent and sensible heat fluxes, F_{snow} denotes the latent heat flux associated with snowfall, and F_{PE} additionally accounts for sensible heat of precipitation. See Mayer et al. (2017) or von Schuckmann et al. (2020) for a discussion of the latter two terms, which are small on a global scale and hence often neglected.

Equation (2) provides a decomposition of *AE* into sensible heat energy (sum of the first two terms, internal heat energy and gravity potential energy), latent heat energy (third term), and kinetic energy (fourth term), where ρ is the air density, c_v the specific heat for moist air at constant volume, T the air temperature, g the acceleration of gravity, L_e the temperature-dependent effective latent heat of condensation L_v or sublimation L_s (the latter relevant below 0 °C), q the specific humidity of the moist air, and V the wind speed. We neglect atmospheric liquid water droplets and ice particles as separate species, as their amounts and especially their trends are small.

In computing *AE* for the purpose of this update to the von Schuckmann et al. (2020) heat storage assessment, we continued to use the formulations described therein, including that we refer to the (geographically aggregated) *AE* as atmospheric heat content (AHC) in this context, acknowledging the dominance of the heat-related terms in Eq. (2). Briefly, in deriving the AHC from observational datasets, we accounted for the intrinsic temperature-dependence of the latent heat of water vapor in formulating L_e (for details see Gorfer, 2022) while the reanalysis derivations approximated L_e by constant values of L_v, as this simplification is typically also made in the assimilating models (e.g., ECMWF-IFS, 2015). As another small difference, the observational estimations neglected the kinetic energy term in Eq. (2) while the reanalysis estimations accounted for it. The resulting differences in AHC anomalies from any of these differences are negligibly small, however, especially when considering trends over time.

3.2 Datasets and heat content estimation

Turning to the actual datasets used, the AHC and its changes and trends over time can be quantified using various data sources, observation-based and reanalyses. Reassessing possible data sources, we extended the high-quality datasets that we used in the initial von Schuckmann et al. (2020) assessment. In particular, we updated the time period from 2018 to 2020 and improved the back-extension from 1980 to 1960. Specifically, the adopted datasets and the related AHC data record preparations can be summarized as follows.

Atmospheric reanalyses combine observational information from various sources (radiosondes, satellites, weather stations, etc.) and a dynamical model in a statistically optimal way. These data have reached a high level of maturity, thanks to continuous improvement work since the early 1990s (Hersbach et al., 2018). Especially reanalyzed thermodynamic state variables, like

https://doi.org/10.5194/essd-2022-239
Preprint. Discussion started: 1 August 2022

567 temperature and water vapor that are most relevant for AHC computation, are of high quality and
568 suitable for climate studies, although temporal discontinuities introduced from changing observing
569 systems continue to deserve due attention (Berrisford et al., 2011; Chiodo & Haimberger, 2010;
570 Hersbach et al., 2020; Mayer et al., 2021).

571 We use the latest generation of reanalyses, including ECMWF's Fifth generation reanalysis ERA5
572 (Bell et al., 2021; Hersbach et al., 2020), JMA's reanalysis JRA55 (Kobayashi et al., 2015), and
573 NASA's Modern-Era Retrospective analysis for Research and Applications version 2 (MERRA2)
574 (Gelaro et al., 2017). ERA5 and JRA55 are both available over the full joint timeframe of this heat
575 storage assessment from 1960 to 2020, while MERRA2 complements these from 1980 to 2020.
576 The additional JRA55C reanalysis variant of JRA55, included for initial inter-comparison in von
577 Schuckmann et al. (2020), is no longer used since it is available to 2012 only and due to its
578 similarity to JRA55 is not adding appreciable complementary value.

579 In addition to these three reanalyses, the datasets from two climate-quality observation techniques
580 are used, for complementary observational AHC estimates. These include the Wegener Center
581 (WEGC) multi-satellite radio occultation (RO) data record, WEGC OPSv5.6 (Angerer et al., 2017;
582 Steiner et al., 2020b), over 2002-2020 and its radiosonde (RS) data record derived from the high-
583 quality Vaisala sondes RS80/RS92/VS41, WEGC Vaisala (Ladstädter et al., 2015), covering 1996-
584 2020. These RO and RS data sets provide atmospheric profiles of temperature, specific humidity,
585 and density that are vertically completed by collocated ERA5 profiles in domains not fully covered
586 by the data (e.g., in the lower troposphere for RO or at polar latitudes for RS). Similar to dropping
587 the JRA55C reanalysis variant for no longer adding value, the microwave sounding unit (MSU)
588 observational data, inter-compared in von Schuckmann et al. (2020), are no longer used.

589 From the observational data, the AHC is estimated by first evaluating Eq. (2) (using all terms for
590 total and the third term only for latent AHC) at each available profile location and subsequently
591 deriving it as volumetric heat content, for up to global scale, from vertical integration, temporal
592 averaging, and geographic aggregation according to the approach summarized in von Schuckmann
593 et al. (2020) and described in detail by (Gorfer, 2022). For the reanalyses, the estimation is based
594 on the full gridded fields. Applying the approach for crosscheck to reanalysis profiles sub-sampled
595 at observation locations only, confirms its validity as it accurately leads to the same AHC results
596 as from the full gridded fields.

597 **3.3 Atmospheric heat content change since 1960 and its amplification**

598 Figure 4 shows the resulting global AHC change inventory over 1960 to 2020 (61 years record),
599 in terms of total AHC anomalies for each data type (Fig. 4a), and for the ensemble mean with
600 trends for selected periods and uncertainty estimates (Fig. 4c). The selected trend periods align
601 with those for ocean data and with availability of atmospheric data sets (see subsection 3.2 above)
602 and represent a reference trend 1961-2000 plus recent trends of the last about 30, 20, and 15 years,
603 respectively. Latent AHC anomalies, a key component of the AHC (Matthews et al., 2022), are
604 also shown (Fig. 4b and 4d). Compared to von Schuckmann et al. (2020), the AHC data have the
605 ENSO signal removed (with ENSO regressed out via the Nino 3.4 Index; and cross-check with
606 non-ENSO-corrected data showing that trend differences are reasonably small). Variability due to

https://doi.org/10.5194/essd-2022-239
Preprint. Discussion started: 1 August 2022

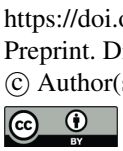

volcanic eruptions is still included, however, and may somewhat influence the trends over 1993-2020, which start in the cold anomaly after the Pinatubo eruption (Santer et al., 2001).

The latent AHC (Fig. 4b and 4d), which accounts for about one-quarter of the total AHC, exhibits a qualitatively similar temporal evolution as total AHC, however with larger relative uncertainty compared to the total AHC. The RO and RS data sets in Fig. 3b show some differences, particularly the low latent AHC values in the 1990s and early 2000s from the RS WEGC Vaisala data set likely stem from known dry biases of the RS80/RS90/RS92 humidity sensors (Verver et al., 2006; Vömel et al., 2007). Estimated trends based on these RS data are thus likely too high, although the overall increase in latent AHC is substantial also in the other datasets.

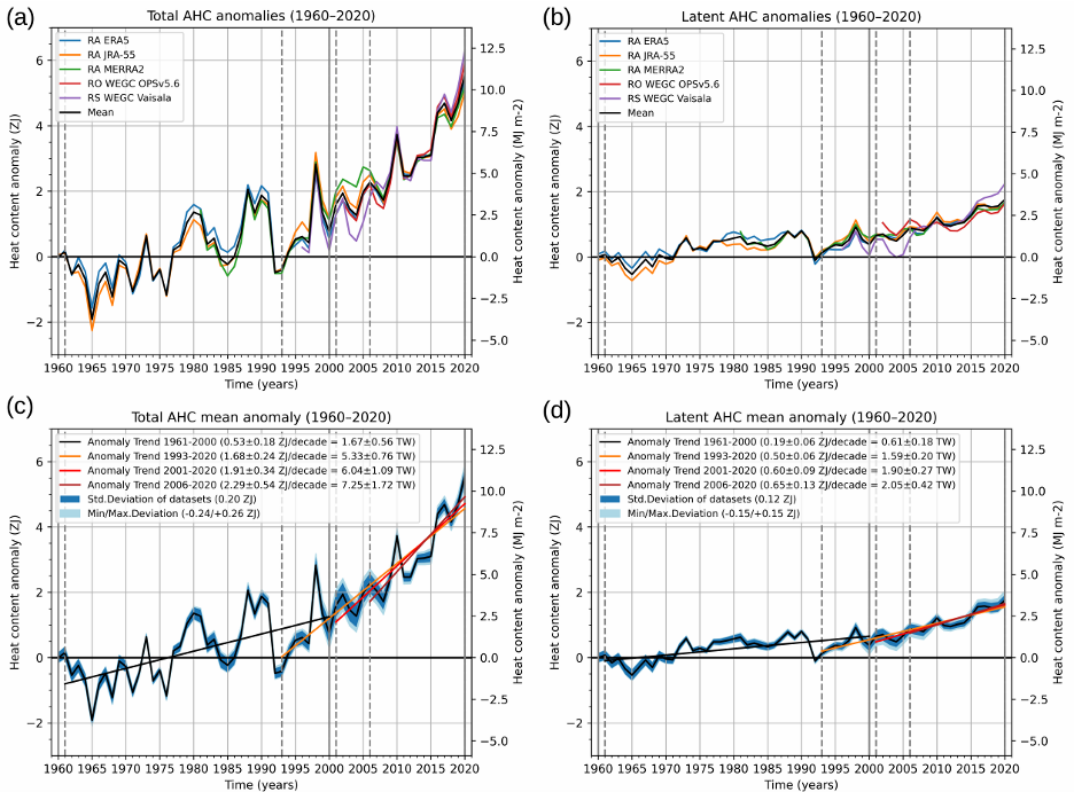

Figure 4. *Annual-mean global AHC anomalies from 1960 to 2020 of total AHC (left) and latent-only AHC (right), respectively, of three different reanalyses and two different observational datasets shown together with their mean (top), and the mean AHC anomaly shown together with four representative AHC trends and ensemble spread measures of its underlying datasets (bottom). The in-panel legends identify the individual datasets (top) and the selected trend periods together with the associated trend values (plus 90 % confidence range) and ensemble spread measures (bottom), the latter including the time-average standard deviation and minimum/maximum deviations of the individual datasets from the mean.*

https://doi.org/10.5194/essd-2022-239
Preprint. Discussion started: 1 August 2022

626

627 The results clearly show that the AHC trends have increased from the earlier decades represented
628 by the 1961-2000 trend of near 1.7 TW. We find the mean trend about 2.5 times higher over 1993-
629 2020 (about 5.3 TW) and about four times higher in the most recent two decades (about 6-7 TW),
630 a period that is already covered also by the RO and RS records. Latent AHC trends in the most
631 recent periods are 3 times larger than the 1961-2000 reference period. Since 1971, the heat gain in
632 the atmosphere amounts to 5 ± 1 ZJ (see also Fig. 8).

633 The remarkable amplification of total AHC and latent AHC trends is highlighted in Figure 4 and
634 summarized in Table 2 for the representative recent periods vs. the 1961-2000 reference period.
635 The 1961-2000 and 1993-2020 periods were covered by reanalysis only, while the WEGC Vaisalä
636 RS dataset additionally covers the 2001-2020 and 2006-2020 periods and the RO dataset the most
637 recent period (see dataset descriptions in subsection 3.2). The larger diversity of recent datasets
638 induces more spread; for example, the RS dataset shows an amplification factor of near 4.5 in the
639 global total AHC gain for 2001-2020, while the amplification factors from the reanalyses range
640 from 2.6 to 3.8. Amplifications are generally largest in the southern hemisphere extratropics and
641 weakest in the tropics. In the most recent period 2006-2020, the amplification factors are strongest,
642 with the RS and RO data sets on the high end of the spread (near factor 5 in global total AHC) and
643 somewhat smaller but still high from the reanalyses (around factor 4).

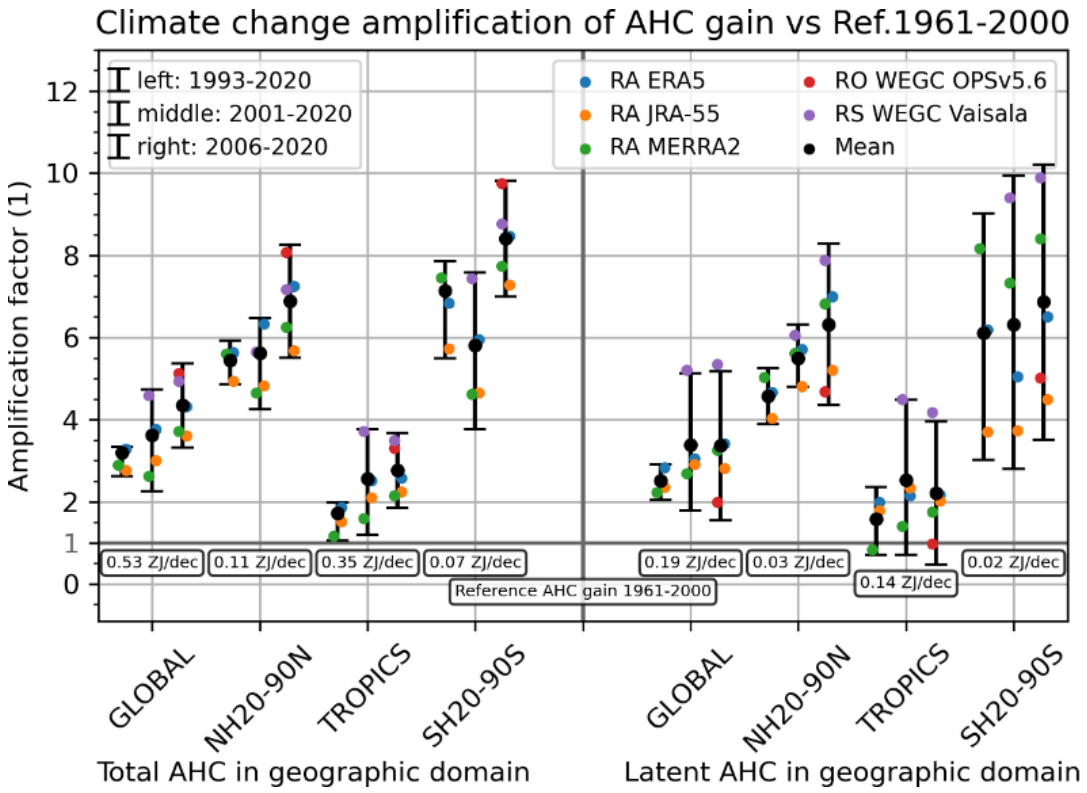

644

https://doi.org/10.5194/essd-2022-239
Preprint. Discussion started: 1 August 2022

Figure 5. *Amplification of long-term trends in AHC anomalies ("AHC gain") for total AHC (left) and latent-only AHC (right) in four geographic domains (global, northern-hemisphere extratropics, tropics, southern-hemisphere extratropics) for three recent time periods (legend upper-left) expressed as a ratio of the trend of each period relative to the trend in the previous-century reference period 1961-2000 (noted below the "amplification factor = 1" reference line). The amplification factor for each recent-trend case (for the four domains of both total and latent AHC) is depicted for the mean anomaly serving as best estimate (larger black circles), the related recent trends in the individual-dataset anomalies (colored circles as per upper-right legend). The related 90 % uncertainty range (black "error bar") is estimated from the spread (standard deviation) of the individual-dataset amplification factors. The trend in the mean anomaly over 1961-2000 is used as the reference AHC gain.*

For the latent AHC amplification factors, we see moderate values in the 1993-2020 period in the global mean and tropics. In the tropics, the lower uncertainty bound for amplification is slightly below 1 during all three recent trend periods. The spread of the amplification factors increases for the most recent periods, which is on the one hand due to the shorter period duration. The range increase is also related to the introduction of the RS and RO data sets after 1993-2020 which contribute the largest and smallest latent AHC gain amplification factors. For 2006-2020, the global mean amplification factor from RO is about 2, whereas from the RS data set it is near 5. Regarding latitudinal bands, the amplification factors are again strongest in the extratropics, exhibiting a large spread especially in the southern extratropics. The relatively large amplification factors of the RS WEGC Vaisala data set are likely exaggerated due to the well documented dry bias of the early RS humidity sensors as noted above (Vömel, 2007; Verver et al., 2006).

Despite the uncertainties and spread described, the overall message from Figure 5 and Table 2 is very clear and substantially reinforcing the evidence from the initial von Schuckmann et al. (2020) assessment: the trends in the AHC, including in its latent heat component, show that atmospheric heat gain has accelerated over the recent decades at an unprecedented rate.

		Total AHC Gain		Latent AHC Gain	
Domain	Time range	Gain ZJ/decade (TW)	Amplification vs Ref.	Gain ZJ/decade (TW)	Amplification vs Ref.
GLOBAL	1993-2020	1.68±0.24 (5.33±0.76)	3.19 [2.63 to 3.34]	0.50±0.06 (1.59±0.20)	2.51 [2.05 to 2.91]
	2001-2020	1.91±0.34 (6.04±1.09)	3.62 [2.27 to 4.73]	0.60±0.09 (1.90±0.27)	3.39 [1.79 to 5.13]
	2006-2020	2.29±0.54 (7.25±1.72)	4.35 [3.33 to 5.36]	0.65±0.13 (2.05±0.42)	3.37 [1.55 to 5.18]
	Ref. 1961-2000	0.53±0.18 (1.67±0.56)	1.0	0.19±0.06 (0.61±0.18)	1.0
NH20-90N	1993-2020	0.62±0.11 (1.97±0.35)	5.44 [4.86 to 5.92]	0.16±0.02 (0.50±0.08)	4.57 [3.90 to 5.26]
	2001-2020	0.64±0.15 (2.03±0.47)	5.62 [4.26 to 6.48]	0.18±0.03 (0.58±0.11)	5.50 [4.79 to 6.31]
	2006-2020	0.79±0.25 (2.49±0.80)	6.89 [5.51 to 8.26]	0.22±0.05 (0.70±0.17)	6.32 [4.36 to 8.28]
	Ref. 1961-2000	0.11±0.08 (0.36±0.24)	1.0	0.03±0.02 (0.11±0.05)	1.0
TROPICS	1993-2020	0.60±0.13 (1.90±0.41)	1.72 [1.05 to 1.98]	0.24±0.04 (0.75±0.12)	1.58 [0.71 to 2.36]
	2001-2020	0.89±0.15 (2.82±0.47)	2.56 [1.20 to 3.77]	0.31±0.05 (1.00±0.16)	2.52 [0.70 to 4.49]
	2006-2020	0.96±0.24 (3.04±0.77)	2.76 [1.86 to 3.67]	0.31±0.07 (0.99±0.22)	2.22 [0.48 to 3.96]
	Ref. 1961-2000	0.35±0.08 (1.10±0.25)	1.0	0.14±0.03 (0.45±0.11)	1.0
SH20-90S	1993-2020	0.46±0.09 (1.46±0.29)	7.14 [5.49 to 7.86]	0.11±0.02 (0.33±0.05)	6.11 [3.02 to 9.02]
	2001-2020	0.37±0.17 (1.18±0.52)	5.80 [3.76 to 7.58]	0.10±0.03 (0.32±0.08)	6.31 [2.81 to 9.95]
	2006-2020	0.54±0.25 (1.71±0.79)	8.40 [6.99 to 9.81]	0.11±0.04 (0.36±0.12)	6.87 [3.52 to 10.22]
	Ref. 1961-2000	0.06±0.06 (0.20±0.18)	1.0	0.02±0.01 (0.05±0.05)	1.0

https://doi.org/10.5194/essd-2022-239
Preprint. Discussion started: 1 August 2022

Table 2. *Long-term trend values in mean AHC anomalies (AHC gains; in units ZJ/decade and TW) and amplification factors vs. the 1961-2000 reference gain (grey "Ref." lines), for total AHC (left block) and latent-only AHC (right block) for the three recent time periods in four geographic domains as illustrated in Figure 4. The AHC gain and amplification values are listed together with their 90 % confidence ranges.*

4. Heat available to warm land

In previous studies the land term of the Earth heat inventory was considered as the heat used to warm the continental subsurface (Hansen et al. 2011; Rhein et al. 2013; von Schuckmann et al. 2020). Temperature changes within the continental subsurface are typically retrieved by analyzing the global network of temperature-depth profiles, measured mostly in the northern hemisphere, southern Africa, and Australia. Each temperature profile records changes in subsurface temperatures caused by the heat propagated through the ground due to alterations in the surface energy balance (Cuesta-Valero et al., 2022a). Such perturbations in the subsurface temperature profiles can be analyzed to recover the changes in past surface conditions that generated the measured profile, allowing a reconstruction of the evolution of ground surface temperatures and ground heat fluxes at decadal to centennial time scales (Beltrami et al., 2002; Beltrami & Mareschal, 1992; Demezhko & Gornostaeva, 2015; Hartmann & Rath, 2005; Hopcroft et al., 2007; Jaume-Santero et al., 2016; Lane, 1923; Pickler et al., 2016; Shen et al., 1992). Although previous estimates only considered changes in ground temperatures for representing the heat storage by exposed land, ground heat storage has been found to be the second largest term of the Earth heat inventory accounting for 4 % to 6 % of the total heat in the Earth System (von Schuckmann et al. 2020, section 6).

The ground heat is, nevertheless, not the only energy component of the continental landmasses. Other processes with large thermodynamic coefficients, such as permafrost thawing and the warming of inland water bodies, occur across large areas, leading to the exchange of large amounts of heat with their surroundings over time. To account for those heat exchanges, a recent study (Cuesta-Valero et al., 2022a) has estimated the heat uptake by permafrost thawing and the warming of inland water bodies, as well as ground heat storage from subsurface temperature profiles, resulting in a comprehensive estimate of continental heat storage. The authors used the same global network of subsurface temperature profiles as in von Schuckmann et al. (2020) to estimate ground heat storage but applied an improved inversion technique to analyze the profiles. This new technique is based on combining bootstrapping sampling with a widely-used Singular Value Decomposition (SVD) algorithm (e.g., Beltrami et al., 1992) to retrieve past changes in surface temperatures and ground heat fluxes, which also resulted in smaller uncertainty estimates for global results (Cuesta-Valero et al., 2022b). Heat uptake from permafrost thawing was estimated using a large ensemble of simulations performed with the CryoGridLite permafrost model (Nitzbon et al., 2022). Ground stratigraphies required for this purpose, including ground ice distributions, were generated using various global ground datasets. Latent heat storage due to melting of ground ice is evaluated to a depth of 550 m over the Arctic region. Uncertainty ranges are evaluated using 100 parameter ensemble simulations with strongly varied soil properties and soil ice distributions. The climate forcing at the surface is based on a paleoclimate simulation

https://doi.org/10.5194/essd-2022-239
Preprint. Discussion started: 1 August 2022

performed by the Commonwealth Scientific and Industrial Research Organization (CSIRO) providing the initialization of the permafrost model, and data from the ERA-Interim reanalysis since 1979 onwards. Heat storage by inland water bodies was estimated by integrating water temperature anomalies in natural lakes and reservoirs from a set of Earth System Model (ESM) simulations participating in the Inter-Sectoral Impact Model Intercomparison Project phase 2b (ISIMP2b) (Frieler et al., 2017; Golub et al., 2022; Grant et al., 2021). Heat storage is then computed using simulations with four global lake models following the methodology presented in (Vanderkelen et al., 2020), but replacing the cylindrical lake assumption in that study for a more detailed lake morphometry, which leads to a more realistic representation of lake volume.

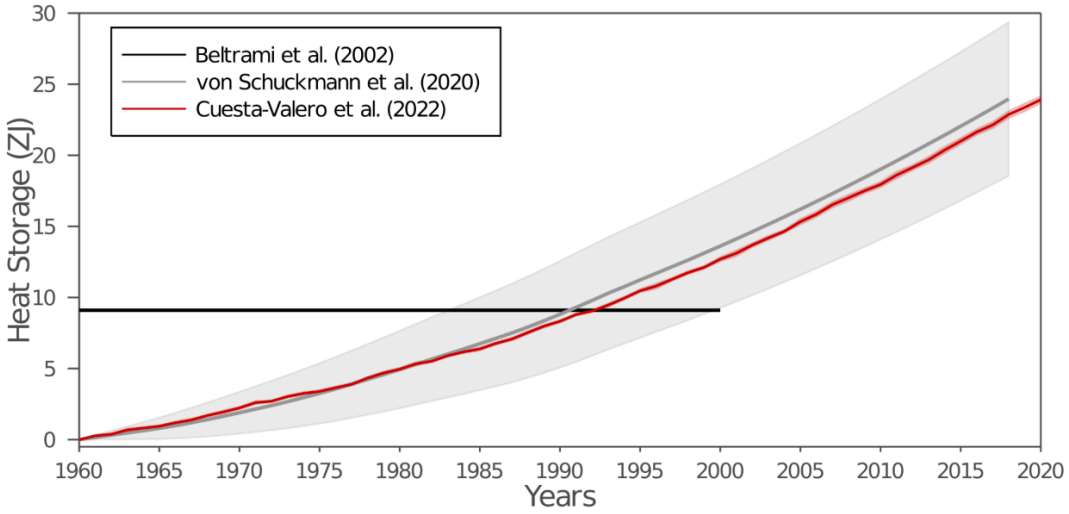

Figure 6: *Continental heat storage from Beltrami et al. (2002) (black), von Schuckmann et al. (2020) (gray), and Cuesta-Valero et al. (2022a) (red). Gray and red shadows show the uncertainty range of the heat storage from von Schuckmann et al. (2020) and Cuesta-Valero et al. (2022a), respectively.*

Figure 6 shows the three main estimates of heat gain by the continental landmasses since 1960. The first global estimate of continental heat storage was provided by Beltrami et al. (2002), consisting of changes in ground heat content for the period 1500-2000 as time steps of 50 years (black line in Figure 6). These estimates were retrieved by inverting 616 subsurface temperature profiles constituting the global network of subsurface temperature profiles in 2002, yielding a heat gain of 9.1 ZJ during the second half of the 20th century. A comprehensive update was included in von Schuckmann et al. (2020) using the results of (Cuesta-Valero et al., 2021) (gray line in Figure 6), with the main difference consisting in the use of a larger dataset with 1079 subsurface temperature profiles. Since many of these new profiles were measured at a later year than those in Beltrami et al. (2002), the inversions from this new data set were able to include the recent warming of the continental subsurface, yielding higher ground heat content than those from Beltrami et al. (2002). Concretely, the estimates in von Schuckmann et al. (2020) showed a heat gain of 24 ± 5 ZJ from 1960 to 2018.

https://doi.org/10.5194/essd-2022-239
Preprint. Discussion started: 1 August 2022

Recently, a new estimate of continental heat gain including the heat used in permafrost thawing and in warming inland water bodies was presented in Cuesta-Valero et al. (2022a) (red line in Figure 6), achieving a heat gain of 24 ± 1 ZJ since 1960, and 22 ± 1 ZJ since 1971 (see also Fig. 8). Although this estimate uses the same 1079 measurement sites as in von Schuckmann et al. (2020) and includes inland water bodies and permafrost thawing, it yields similar values of heat content to those in von Schuckmann et al. (2020). These similar results are caused by the different aggregation techniques used to derive the change in global ground heat storage in von Schuckmann et al. (2020) and in Cuesta-Valero et al. (2022a). There is a difference of ~ 3 ZJ between the average ground heat storage in Cuesta-Valero et al. (2022a) (21.6 ± 0.2 ZJ) and in von Schuckmann et al. (2020) (24 ± 5 ZJ), which is similar to the heat storage in inland water bodies and the heat storage due to permafrost thawing together (see below). Another important result is the narrower confidence interval in estimates from Cuesta-Valero et al. (2022a), which is directly related to the new bootstrap technique used to invert the subsurface temperature profiles (Cuesta-Valero et al., 2022b). Heat storage within inland water bodies has reached 0.2 ± 0.4 ZJ since 1960, with permafrost thawing accounting for 2 ± 2 ZJ. Therefore, ground heat storage is the main contributor to continental heat storage (90 %), with inland water bodies accounting for 0.7 % of the total heat, and permafrost thawing accounting for 9 %. Despite the smaller proportion of heat stored in inland water bodies and permafrost thawing, several important processes affecting both society and ecosystems depend on the warming of lakes and reservoirs, and on the thawing of ground ice (Gädeke et al., 2021). Therefore, it is important to continue quantifying and monitoring the evolution of heat storage in all three components of the continental landmasses.

5. Heat utilized to melt ice

Changes in Earth's cryosphere affect almost all other elements of the environment including the global sea level, ocean currents, marine ecosystems, atmospheric circulation, weather patterns, freshwater resources and the planetary albedo (Abram et al., 2019). The cryosphere includes frozen components of the Earth system that are at or below the land and ocean surface: snow, glaciers, ice sheets, ice shelves, icebergs, sea ice, lake ice, river ice, permafrost and seasonally frozen ground (IPCC, 2019). In this study, we estimate the heat uptake by the melting of ice sheets (including both floating and grounded ice), glaciers and sea ice at global scale (Fig. 7). Notwithstanding the important role snow cover plays in the Earth's energy surface budget as a result of changes in the albedo (de Vrese et al., 2021; Qu & Hall, 2007; Weihs et al., 2021), or its influence on the temperature of underlying permafrost (Jan & Painter, 2020; Park et al., 2015), or on sea ice in the Arctic (Perovich et al., 2017; Webster et al., 2021) and Antarctica (Eicken et al., 1995; Nicolaus et al., 2021; Shen et al., 2022), estimates of changes in global snow cover are still highly uncertain and not included in this inventory. However, they should be considered in future estimates. Similarly, changes in lake ice cover (Grant et al., 2021) are not taken into account here and warrant more attention in the future. Permafrost is accounted for in the land component (see section 4).

https://doi.org/10.5194/essd-2022-239
Preprint. Discussion started: 1 August 2022

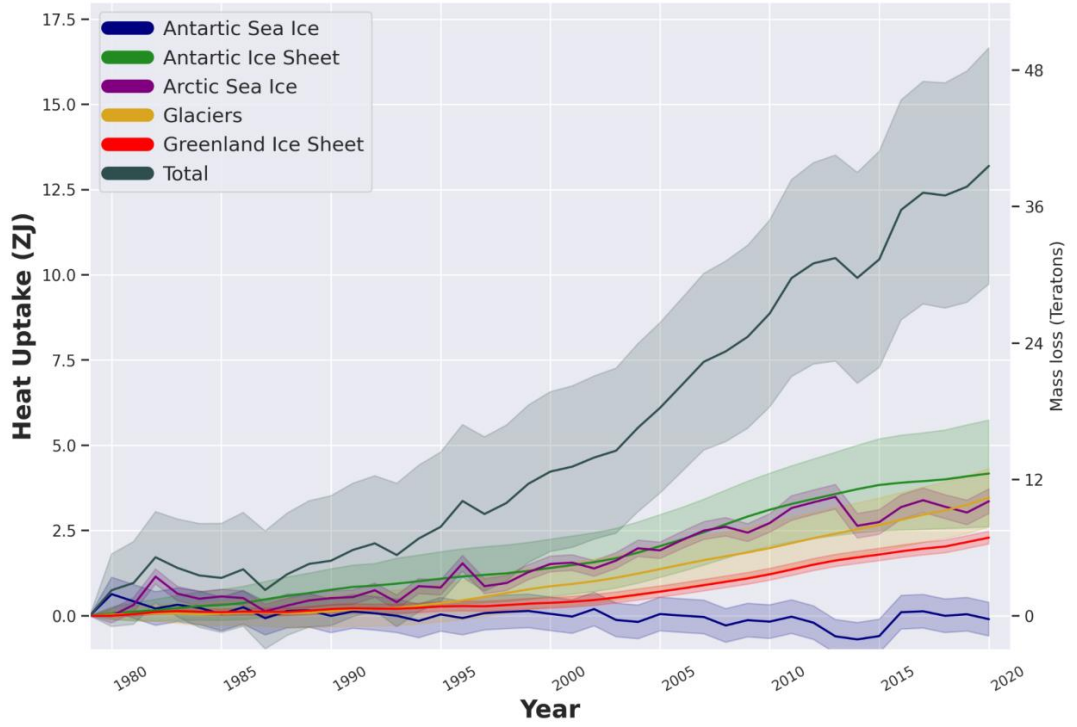

Figure 7: *Heat uptake (in ZJ) and Mass Loss (Trillions of tons) for the Antarctic Ice Sheet (grounded and floating ice, green), Glaciers (orange), Arctic sea ice (purple), Greenland Ice Sheet (grounded and floating ice, red) and Antarctic sea ice (blue), together with the sum of the energy uptake within each one of its components (total, black). Uncertainties are 95% confidence intervals provided as shaded areas, respectively. See text for more details.*

We equate the energy uptake by the cryosphere (glaciers, grounded and floating ice of the Antarctic and Greenland Ice Sheets, and sea-ice) with the energy needed to drive the estimated mass loss. In doing so we assume that the energy change associated with the temperature change of the remaining ice is negligible. As a result, the energy uptake by the cryosphere is directly proportional to the mass of melted ice:

$$E = \Delta M*(L+c*\Delta T),$$

where, for any given component, ΔM is the mass of ice loss, L is the latent heat of fusion, c is the specific heat capacity of the ice and ΔT is the rise in temperature needed to bring the ice to the melting point. For consistency with previous estimates (Ciais et al., 2014; Slater et al., 2021; von Schuckmann et al., 2020), we use a constant latent heat of fusion of $3.34\times105\ J\ kg^{-1}$, a specific heat capacity of $2.01\times103\ J/(kg\ °C)$ and, a density of ice of $917\ kg/m^3$. Estimating the energy used to warm the ice to its melting point requires knowledge of the mean ice temperature for each component. Here we assume a temperature of -15 °C for floating ice in Greenland, -2 °C for the floating ice in Antarctica, -20 ± 10 °C for grounded ice in Antarctica and Greenland and 0 °C for

https://doi.org/10.5194/essd-2022-239
Preprint. Discussion started: 1 August 2022

812 sea-ice and glaciers. Although this assumption is poorly constrained, the energy required to melt
813 ice is primarily associated with its phase transition and the fractional energy required for warming
814 is a small percentage (< 1% °C $^{-1}$) of the total energy uptake (Slater et al., 2021). Nevertheless, we
815 include an additional uncertainty of ±10 °C on the assumed initial ice temperature within our
816 estimate of the energy uptake.
817
818 Grounded ice losses from the Greenland and Antarctic Ice Sheets from 1992 to 2020 are estimated
819 from a combination of 50 satellite-based estimates of ice sheet mass balance produced from
820 observations of changes in ice sheet volume, flow and gravitational attraction, compiled by the Ice
821 Sheet Mass Balance Intercomparison Exercise (IMBIE[8]) (Shepherd et al., 2018, 2019). To extend
822 those time-series further back in time, we use ice sheet mass balance estimates produced using the
823 input-output method, which combines estimates of solid ice discharge with surface mass balance
824 estimates. Satellite estimates of ice velocity are available from the Landsat historical archive from
825 1972 allowing the calculation of ice discharge before the 1990s while surface mass balance is
826 estimated from regional climate models. We extend the IMBIE mass balance time-series
827 backwards to 1979 for Greenland using (Mouginot et al., 2019) and (Mankoff et al., 2019) and for
828 Antarctica from 1972 to 1991 using (Rignot et al., 2019).
829
830 Changes in Antarctic floating ice shelves due to thinning between 1994 and 2017 are derived from
831 satellite altimetry reconstructions (Adusumilli et al., 2020). There were no estimates of ice shelf
832 thinning between 1979 and 1993, therefore we assume zero mass loss from ice shelf thinning
833 during that period. Changes in Antarctic ice shelves due to increased calving in the Antarctic
834 Peninsula and the Amundsen Sea sector are derived from ERS-1 radar altimetry (Adusumilli et al.
835 2020) for 1994-2017. For the 1979-1994 period, we only have data for changes in the extent of the
836 Antarctic Peninsula ice shelves from (Cook & Vaughan, 2010). These are converted to changes in
837 mass using an ice shelf thickness of 140 +/- 110 m ice equivalent which represents the range of
838 ice thickness values for the portions of Antarctic Peninsula ice shelves that have collapsed since
839 1994 (Adusumilli et al. 2020). Once icebergs calve off large Antarctic floating ice shelves, the
840 timescales of dissolution of the icebergs are largely unknown; therefore, we assumed a linear rate
841 of energy uptake between 1979–2018. For icebergs, we use an initial temperature of -16°C, which
842 was the mean ice temperature in the Ross Ice Shelf J-9 ice core (Clough & Hansen, 1979). There
843 are no large-scale observations or manifestations of significant firn layer temperature change for
844 the Antarctic ice shelf; for example, there is no significant trend in the observationally-constrained
845 model outputs of surface melt described in (Smith et al., 2020). Therefore, the change in
846 temperature of any ice that does not melt is assumed to be negligible.
847
848 Changes in the floating portions of the Greenland Ice Sheet include ice shelf collapse, ice shelf
849 thinning and tidewater glacier retreat. As in von Schuckmann et al. 2020, we assume no ice shelf
850 mass loss pre-1997 and estimate a loss of 13 Gt/yr post-1997 based on studies of Zacharie Isstrom,
851 C. H. Ostenfeld, Petermann, Jakobshavn, 79N and Ryder Glaciers (Moon & Joughin, 2008;
852 Motyka et al., 2011; Mouginot et al., 2015; Münchow et al., 2014; Wilson et al., 2017). We assign
853 a generous uncertainty of 50% to this value. For tidewater glacier retreat we note a mean retreat
854 rate of 37.6 m/yr during 1992-2000 and 141.7 m/yr during 2000-2010. We assume the former
855 estimate is also valid for 1979-1991 and the latter estimate is valid for 2011-2020. Assuming a

[8] https://imbie.org

https://doi.org/10.5194/essd-2022-239
Preprint. Discussion started: 1 August 2022

mean glacier width of 4 km and thickness of 400 m we estimate mass loss from glacier retreat to be 9.3 Gt/yr during 1979-2000 and 35.1 Gt/yr during 2000-2020. Based on firn modeling we assessed that warming of Greenland's firn has not yet contributed significantly to its energy uptake (Ligtenberg et al., 2018).

The contributions from both the Antarctic and Greenland Ice Sheets to the EEI are obtained by summing the mass loss from the individual components (ice shelf mass, grounded ice mass, and ice shelf extent) for each ice sheet separately and, given that the datasets used for each component are independent, the uncertainties were summed in quadrature. This is then converted to an energy uptake according to the equation above.

Glaciers are another part of the land-based ice, and we here include glaciers found in the periphery of Greenland and Antarctica, but distinct from the ice sheets, in our estimate. We build our estimate on the international efforts to compile and reconcile measurements of glacier mass balance, under the lead of the World Glacier Monitoring Service (WGMS[9]). Up to 2016, the results are based on (Zemp et al., 2019), who combine geodetic mass balance observations from DEM differencing on long temporal and large spatial scales with in-situ glaciological observations, which are spatially less representative, but provide information of higher temporal resolution. Through this combination, they achieve coverage that is globally complete yet retains the interannual variability well. For 2017 to 2021, the numbers are based on the ad-hoc method of (Zemp et al., 2020), which corrects for the spatial bias of the limited number of recent in-situ glaciological observations that are available with short delay (WGMS, 2021), to derive globally representative estimates. Error bars include uncertainties related to the in-situ and spaceborne observations, extrapolation to unmeasured glaciers, density conversion, as well as to glacier area and its changes. For the conversion from mass loss to energy uptake, only the latent heat uptake is considered, which is based on the assumption of ice at the melting point, due to lack of glacier temperature data at the global scale. Moreover, since the absolute mass change estimates are based on geodetic mass balances, mass loss of ice below floatation is neglected. While this is a reasonable approximation concerning the glacier contribution to sea-level rise, it implies a systematic underestimation of the glacier heat uptake. While to our knowledge there are no quantitative estimates available of glacier mass loss below sea level on the global scale, it is reasonable to assume that this effect is minor, based on the volume-altitude distribution of glacier mass (Farinotti et al., 2019; Millan et al., 2022). Further efforts are under way within the Glacier Mass Balance Intercomparison Exercise (GlaMBIE[10]), particularly to reconcile global glacier mass changes including also estimates from gravimetry and altimetry, and to further assess related sources of uncertainties (Zemp et al., 2019).

Sea ice, formed from freezing ocean water, and further thickened by snow accumulation is not only another important aspect of the albedo effect (Kashiwase et al., 2017; R. Zhang et al., 2019) and water formation processes (Moore et al., 2022), but also provides essential services for polar ecosystems and human systems in the Arctic (Abram et al., 2019). Observations of sea-ice extent are available over the satellite era, i.e. since the 1970s, but ice thickness data - required to obtain changes in volume - have only recently become available through the launch of CryoSat-2 and ICESat-2. For the Arctic, we use a combination of sea ice thickness estimates from from the Pan-

[9] https://wgms.ch
[10] https://glambie.org

https://doi.org/10.5194/essd-2022-239
Preprint. Discussion started: 1 August 2022

Arctic Ice Ocean Modeling and Assimilation System (PIOMAS) between 1980 and 2011 (Schweiger et al., 2019; Zhang & Rothrock, 2003) and CryoSat-2 satellite radar altimeter measurements between 2011 and 2020 when they are available (Slater et al., 2021; Tilling et al., 2018). PIOMAS assimilates ice concentration and sea surface temperature data and is validated with most available thickness data (from submarines, oceanographic moorings, and remote sensing) and against multidecadal records constructed from satellite (Labe et al., 2018; Laxon et al., 2013; Wang et al., 2016). We note that the PIOMAS domain does not extend sufficiently far south to include all regions covered by sea ice in winter (Perovich et al., 2017). Given that the entirety of the regions that are unaccounted for (e.g., the Sea of Okhotsk and the Gulf of St. Lawrence) are only seasonally ice covered since the start of the record, this should not influence the results. We convert monthly estimates of sea ice volume from CryoSat-2 satellite altimetry to mass using densities of 882 and 916.7 kg/m^3 in regions of multi- and first-year ice respectively (Tilling et al., 2018). During the summer months (May to September) the presence of melt ponds on Arctic sea ice makes it difficult to discriminate between radar returns from leads and sea ice floes, preventing the retrieval of summer sea ice thickness from radar altimetry (Tilling et al., 2018). As a result, we use the winter-mean (October to April) mass trend across the Arctic for both CryoSat-2 and PIOMAS estimates for consistency. According to PIOMAS, winter Arctic sea ice mass estimates are 19 Gt/yr (6 %) smaller than the annual mass trend between 1980 and 2011 (-324 Gt/yr) and so are a conservative estimate of Arctic sea ice mass change (Slater et al., 2021). The uncertainty on monthly Arctic sea ice volume measurements from CryoSat-2 ranges from 14.5 % in October to 13 % in April (Slater et al., 2021; Tilling et al., 2018), and is estimated as $\pm 1.8 \times 10^3$ km^3 for PIOMAS (Schweiger et al., 2011).

Satellite radar altimeter retrievals of sea ice thickness in the Southern Ocean are complicated by the presence of thick snow layers with unknown radar backscatter properties on Antarctic sea ice floes. As a result, no remote sensing estimates are available for Antarctic sea ice and we use sea ice volume anomalies from the Global Ice-Ocean Modeling and Assimilation System (GIOMAS, Zhang & Rothrock, 2003), the global equivalent to PIOMAS. GIOMAS output has been recently validated against in-situ and satellite data by (Liao et al., 2022). We compute Antarctic sea ice trends as annual averages between January and December. In the absence of a detailed characterization of uncertainties for these estimates, we attribute the same uncertainty to GIOMAS estimates as for PIOMAS ($\pm 1.8 \times 10^3$ km^3). For future updates of the GCOS Earth heat inventory, we also aim to include observation-based (remote sensing) estimates in the Southern Ocean (Lavergne et al., 2019).

Our estimate of the total heat gain in the cryosphere amounts to 14 ± 4 ZJ over the period 1971-2020 (see also Fig. 8 and section 6), (assuming negligible contribution before 1979 according to the data availability limitation), which is consistent with the estimate obtained in (von Schuckmann et al., 2020) within uncertainties. Approximately half of the cryosphere's energy uptake is associated with the melting of grounded ice, while the remaining half is associated with the melting of floating ice (ice shelves in Antarctica and Greenland, Arctic sea ice). Compared to earlier estimates, and in particular the 8.83 ZJ estimate from Ciais et al. (2013), this larger estimate is a result both of the longer period of time considered and, also, the improved estimates of ice loss across all components, especially the ice shelves in Antarctica. Contributions to the total cryosphere heat gain are dominated by the Antarctic Ice Sheet (including the floating and grounded ice, 33 ± 11%) and Arctic Sea ice (26 ± 3%), directly followed by the heat utilized to melt glaciers

https://doi.org/10.5194/essd-2022-239
Preprint. Discussion started: 1 August 2022

(25 ± 7%). The Greenland Ice Sheet amounts to 17 ± 2%, whereas Antarctic sea ice is accounted for with a non-significant contribution of 0.2 ± 4%.

6. The Earth heat inventory: where does the energy go?

Evaluations of the heat storage in the different Earth system components as performed in section 2-5 allow now for the establishment of the Earth heat inventory. Our results reconfirm a continuous accumulation of heat in the Earth system since our estimate begins (Fig. 8). The total Earth system heat gain in this study amounts to 380±62 ZJ over the period 1971–2020. For comparison, the heat gain obtained in IPCC AR6 obtained a total heat gain of 434.9 [324.5 to 545.5] ZJ for the period 1971-2018, and is hence consistent with our estimate within uncertainties (Forster et al., 2021). However, it is important to note that our estimate still excludes some aspects of Earth heat accumulation, such as for example the shallow areas of the ocean. Although some estimates and discussions have been provided to account for the relative contributions of these areas, these results are still hampered by a number of assumptions and are challenging to be quantified with respect to gaps in the observing system.

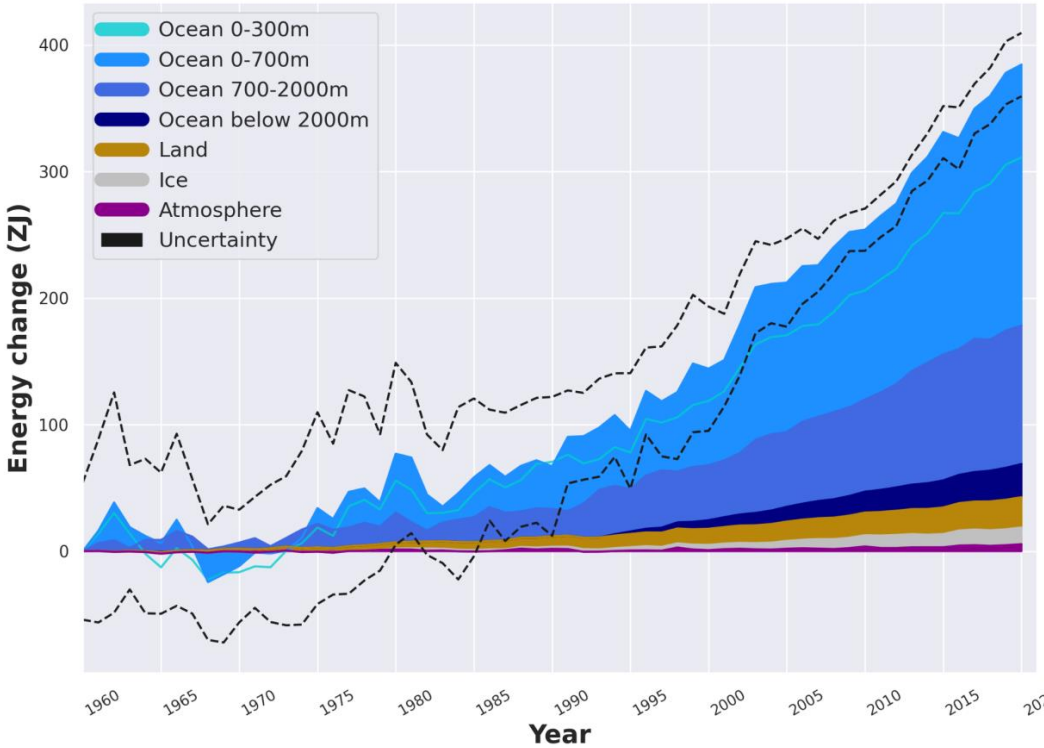

Figure 8: *Total Earth system heat gain in ZJ (1 ZJ =10^{21} J) relative to 1960 and from 1960 to 2020. The upper ocean (0–300 m, light blue line, and 0–700 m, light blue shading) accounts for the largest amount of heat gain, together with the intermediate ocean (700–2000 m, blue shading) and the deep ocean below 2000 m depth (dark blue shading). The second largest contributor is the*

https://doi.org/10.5194/essd-2022-239
Preprint. Discussion started: 1 August 2022

storage of heat on land (orange shading), followed by the gain of heat to melt grounded and floating ice in the cryosphere (gray shading), and heating of the atmosphere (magenta shading). Uncertainty in the ocean estimate also dominates the total uncertainty (dot-dashed lines derived from the standard deviations (2σ) for the ocean, cryosphere, land and atmosphere). See sections 2-5 for more details of the different estimates. The dataset for the Earth heat inventory is published at the German Climate Computing Centre (DKRZ, https://www.dkrz.de/) (see section 7). Consistent with von Schuckmann et al. (2020), we obtain a total heat gain of 380±62 ZJ over the period 1971–2020, which is equivalent to a heating rate (i.e., the EEI) of 0.48±0.1 W m^{-2} applied continuously over the surface area of the Earth (5.10×10^{14} m^2). The corresponding EEI over the period 2006–2020 amounts to 0.76±0.2 W m^{-2}. The LOWESS method and associated uncertainty evaluations have been used as described in section 2.

The estimate of heat storage in all Earth system components not only allows for obtaining a measure of how much and where heat is available for inducing changes in the Earth system (Fig. 1), but also to improve the accuracy of the Earth's system total heat gain. In 1971-2020 and for the total heat gain, the ocean accounts for the largest contributor with a 89 ± 17% fraction of the global inventory. The second largest component in the Earth heat inventory relies on heat stored in land with a 6 ± 0.1% contribution. The cryosphere component accounts for 4 ± 1%, and the atmosphere 1 ± 0.2%. For the most recent era of best available GCOS data for the Earth heat inventory since the year 2006, the fractions amount to 89 ± 20 % for the ocean, 5 ± 1% for land, 4 ± 3 % for the cryosphere, and 2 ± 0.4% for the atmosphere.

The change of the Earth heat inventory over time allows for an estimate of the absolute value of the Earth energy imbalance. Our results of the total heat gain in the Earth system over the period 1971-2020 is equivalent to a heating rate of 0.48±0.1 W m^{-2}, and is applied continuously over the surface area of the Earth (5.10×10^{14} m^2). For comparison, the heat gain obtained in IPCC AR5 amounts to 274 ± 78 ZJ and 0.4 W m^{-2} over the period 1971–2010 (Rhein et al., 2013). In IPCC AR6, the total heat rate has been assessed by 0.57 [0.43 to 0.72] W m^{-2} for the period 1971-2018 (Forster et al., 2021). We further infer a total heating rate of 0.76 ± 0.2 W m^{-2} for the most recent era 2006-2020.

Thus, the number of how fast heat has been accumulated in the Earth system has increased during the most recent era as compared to the long-term estimate – an outcome which reconfirms the earlier finding in von Schuckmann et al. (2020), and which had then been concurrently and independently confirmed in Foster et al. (2021), Hakuba et al. (2021), Loeb et al. (2021) and Kramer et al. (2021). The drivers of a larger EEI in the 2000s than in the long-term period since 1971 are still unclear, and several mechanisms are discussed in literature. For example, Loeb et al. (2021) argue for a decreased reflection of energy back into space by clouds and sea-ice, and increases in well-mixed greenhouse gases (GHG) and water vapor to account for this increase in EEI. (Kramer et al., 2021) refers to a combination of rising concentrations of well-mixed GHG and recent reductions in aerosol emissions accounting for the increase, and (Liu et al., 2020) addresses changes in surface heat flux together with planetary heat re-distribution and changes in ocean heat storage. Future studies are needed to further explain the drivers of this change, together with its implications for changes in the Earth system.

https://doi.org/10.5194/essd-2022-239
Preprint. Discussion started: 1 August 2022

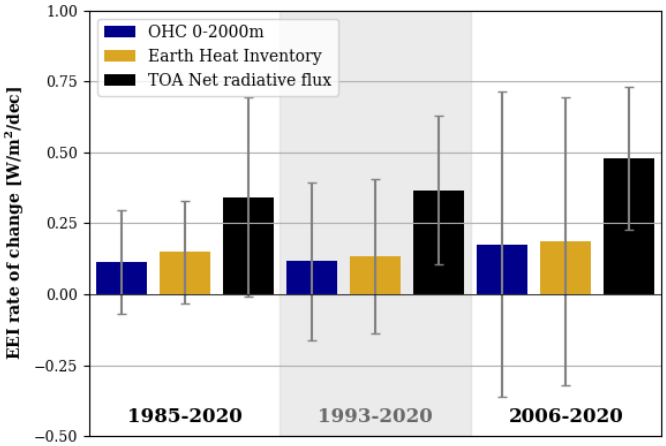

Figure 9: *Decadal scale rate of change for the Earth Energy Imbalance (EEI) in Wm^{-2}/decade as derived from the Earth heat inventory in Fig. 8 (yellow), OHC of the 0-2000m depth layer (blue, see section 2) and net flux at the top of the atmosphere (TOA, black) based on the estimates of Liu et al. (2020) and Loeb et al. (2021) for three different periods, 1985-2020 (i.e., the full available net flux at TOA estimate), 1993-2020 (i.e., the altimeter era) and 2006-2020 (i.e., the GCOS golden period for the Earth heat inventory). See Liu et al. (2020) and Loeb et al. (2021) on more details of the uncertainty estimate, and note that satellite instrument drift error is not considered. A linear regression has been applied to obtain the rate of change.*

With respect to the current status of the GCOS, we further want to emphasize the fact that today the Earth heat inventory is the best estimate for the absolute value of the Earth energy imbalance. This is explained by the fact that satellite derived measurements for the net flux at the top of the atmosphere (TOA) have to be anchored by an absolute value, which is done through the use of the Earth heat inventory, and for which mostly global OHC is used (Loeb et al., 2012; 2021; Liu et al., 2020). However, the temporal change of the EEI can be best estimated from the net flux at TOA from remote sensing data as these are superior in terms of temporal stability. To further discuss the temporal change of the EEI, we compare our results of the Earth heat inventory with the satellite derived net flux at TOA. Consistent with the results of Loeb et al. (2021), the net flux estimates at TOA show a change in the EEI at a significant rate of 0.48 ± 0.3 Wm^{-2}/decade during the period 2006-2020. In 1985-2020 (1993-2020), the value amounts to 0.3 ± 0.4 Wm^{-2}/decade (0.4 ± 0.3 Wm^{-2}/decade) (Fig. 9).

For the Earth heat inventory, the results show that uncertainties for estimating temporal changes of the EEI are still too large to obtain significant results, even during the GCOS ‘golden period’ for the Earth heat inventory in 2006-2020 (Loeb et al., 2022). In other words, this comparison highlights the strength of the complementary use of different independent GCOS components. But the results also show that the current status of the GCOS does not allow for unraveling the rate of change of heat stored in the Earth system components, which is critical information to further understand associated changes in the Earth system (Fig. 1), and to validate climate models for

https://doi.org/10.5194/essd-2022-239
Preprint. Discussion started: 1 August 2022

improving projections of these changes into the future. Hence, these results further underpin the need for sustaining and further extending the GCOS for improving our knowledge and monitoring capacity of estimates for how much and where heat is stored in the Earth system.

Besides heat, which is the focus of this study, Earth also stores energy chemically through photosynthesis in living and dead biomass with plant growth. Recent studies (Crisp et al., 2022; Denning, 2022; Friedlingstein et al., 2022) on the Global Carbon Budget and cycle show that approximately 25% of the added anthropogenic CO2 is removed from the atmosphere by increased plant growth, which is a result of fertilization by rising atmospheric CO2 and Nitrogen inputs and of higher temperatures and longer growing seasons in northern temperate and boreal areas (Friedlingstein et al., 2022). This significant increase in carbon uptake by the biosphere indicates that more energy is stored inside biomass, together with the stored carbon. The quantification of the additional amount of energy stored inside the biosphere is outside the scope of this study.

7. Data availability

The time series of the Earth heat inventory are published at DKRZ (https://www.dkrz.de/, last access: 20 July 2020) under https://www.wdc-climate.de/ui/entry?acronym=GCOS_EHI_1960-2020, more precisely for:

- (von Schuckmann et al., 2022); data for ocean heat content (section 2), and the total heat inventory as presented in section 6 are integrated.
- (Kirchengast et al., 2022) ; data for the atmospheric heat content are distributed (section 3).
- (Cuesta Valero et al., 2022c); data for the ground heat storage, together with the total continental heat gain are provided (section 4)
- (Vanderkelen et al., 2022); data for inland freshwater heat storage is included (section 4)
- (Nitzbon et al., 2022b); data for permafrost are delivered (section 4).
- (Adusumilli et al., 2022); data for the cryosphere heat inventory are provided.

Persistent identifiers (PIDs) for the specific data access are provided in Table 2.

Earth heat inventory component	PID	Reference
Ocean heat content; Total Earth heat inventory	https://hdl.handle.net/21.14106/9b2fddbe4637e3bb9fbf2414c55e6aad0e3923b0	von Schuckmann et al., 2022
Atmospheric heat content	https://hdl.handle.net/21.14106/2c4e7216177fcb742f324eae2792c43faf8361f1	Kirchengast et al., 2022
Continental heat content	https://hdl.handle.net/21.14106/302a4aedadcabf09d5f432003361275e9102a48a	Cuesta Valero et al., 2022c
Inland water heat content	https://hdl.handle.net/21.14106/e095f83398baa6e5b355ba88ae97cd7dedd008de	Vanderkelen et al., 2022
Heat available to melt permafrost	https://hdl.handle.net/21.14106/a9654c3d10c0002da4dde3ef080f6503e2deebf5	Nitzbon et al., 2022b
Heat available to melt the cryosphere	https://hdl.handle.net/21.14106/b9829ba3230f0631d3545a66a88e1c89803510ee	Adusumilli et al., 2022

https://doi.org/10.5194/essd-2022-239
Preprint. Discussion started: 1 August 2022

Table 2: *Overview on persistent identifiers (PIDs) for data access for each component of the Earth heat inventory. The results are presented in Fig. 8.*

8. Conclusion

This study builds on the first internationally and multidisciplinary driven Earth heat inventory in 2020 (von Schuckmann et al., 2020) and provides an update on total Earth system heat accumulation, heat storage in all Earth system components (ocean, land, cryosphere, atmosphere) and the Earth energy imbalance up to the year 2020. Moreover, this study succeeded to improve estimates, to further extent and foster international collaboration, and to continue to move towards a more complete view on where and how much heat is stored in the Earth system through the addition of new estimates such as for permafrost thawing, inland freshwater (section 4) and Antarctic sea ice (section 5). Results obtained reveal a total Earth system heat gain of 380±62 ZJ over the period 1971–2020, with an associated total heating rate of 0.48±0.1 W m^{-2}. 89 ± 17 % of this heat stored in the ocean, 6 ± 0.1 % on land, 4 ± 1% in the cryosphere and 1 ± 0.2 % in the atmosphere (Fig. 8, 11). The analysis additionally reconfirms an increased heating rate which amounts to 0.76 ± 0.2 W/m^{-2} for the most recent era 2006-2020. These results are consistent with previous estimates, which is again demonstrated through a comprehensive assessment of estimates for the EEI published in peer-reviewed literature (Fig. 10). Albeit the drivers for this change still need to be elucidated and most likely reflect the interplay between natural variability and anthropogenic change (Loeb et al., 2021; Kramer et al., 2021; Liu et al., 2020), their implications for changes in the Earth system are reflected in the many record levels of change in the 2000s reported elsewhere, e.g., (Cheng et al., 2022; Forster et al., 2022; Gulev et al., 2021; WMO, 2022).

The recent Glasgow Climate Pact (UNFCCC, 2021) is '*Acknowledging that climate change is a common concern of humankind …*' and '*Recognizing … the importance of international cooperation in addressing climate change and its impacts…*', and '*Recognizes the importance of the best available science for effective climate action and policy making*'. The UN 2030 Agenda for Sustainable Development[11] states that climate change is "*one of the greatest challenges of our time …*" and warns *"… the survival of many societies, and of the biological support systems of the planet, is at risk*". The outcome document of the Rio+20 Conference, The Future We Want[12], defines climate change as "*an inevitable and urgent global challenge with long-term implications for the sustainable development of all countries*". The Paris Agreement builds upon the United Nations Framework Convention on Climate Change and for the first time all nations agreed to undertake ambitious efforts to combat climate change, with the central aim to keep global temperature rise this century well below 2 °C above pre industrial levels and to limit the temperature increase even further to 1.5 °C. Article 14 of the Paris Agreement requires the Conference of the Parties serving as the meeting of the Parties to the Paris Agreement (CMA) to periodically take stock of the implementation of the Paris Agreement and to assess collective

[11] https://sustainabledevelopment.un.org/content/documents/21252030%20Agenda%20for%20Sustainable%20Development%20web.pdf

[12] https://sustainabledevelopment.un.org/content/documents/733FutureWeWant.pdf

https://doi.org/10.5194/essd-2022-239
Preprint. Discussion started: 1 August 2022

progress towards achieving the purpose of the agreement and its long-term goals through the so-called Global Stocktake of the Paris Agreement (GST)[13] based on best available science.

The Earth heat inventory provides information on how much and where heat is accumulated and stored in the Earth system. Moreover, it provides a measure of how much the Earth is out of energy balance, and when combined with directly measured net flux at the top of the atmosphere, enables also to understand the change of the EEI over time. This in turn allows for assessing the portion of the anthropogenic forcing that the Earth's climate system has not yet responded to (Hansen et al., 2005) and defines additional global warming that will occur without further change in human-induced forcing (Hansen et al., 2017). The Earth heat inventory is thus one of the key critical global climate change indicators defining the prospects for continued global warming and climate change (Hansen et al., 2011; von Schuckmann et al., 2016; 2020) Hence, we call for an implementation of the Earth heat inventory into the global stocktake.

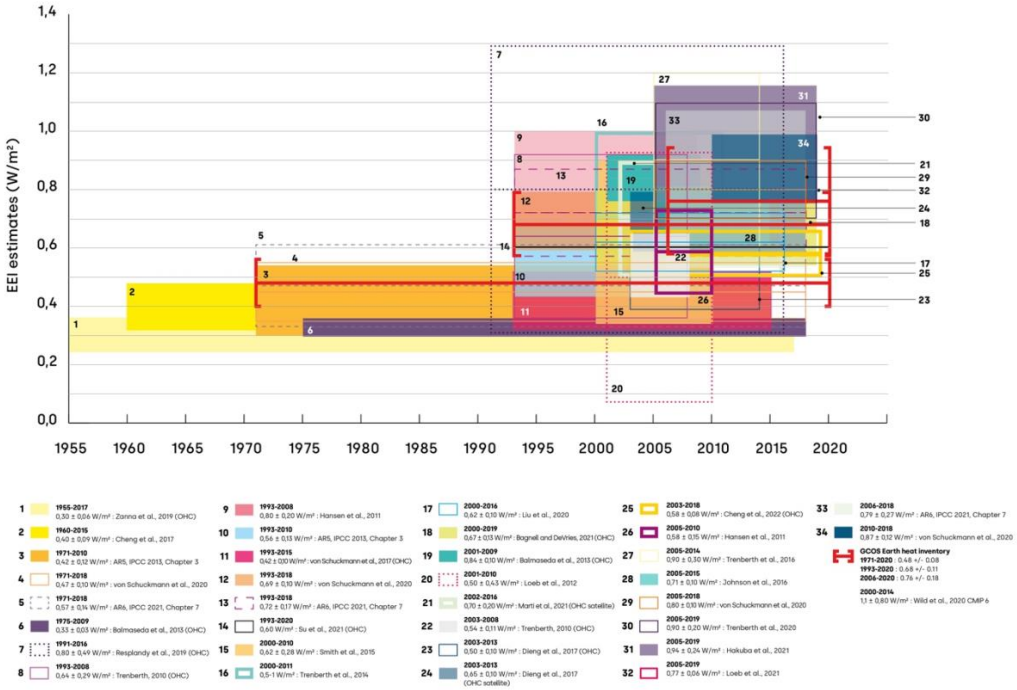

Figure 10: *Overview on EEI and d(OHC)/dt (indicated with (OHC) in the legend) estimates as obtained from previous publications; references are listed in the figure legend. The color bars take into account the uncertainty ranges provided in each publication, respectively. For comparison,*

[13] https://unfccc.int/topics/global-stocktake/global-stocktake#:~:text=The%20global%20stocktake%20of%20the,term%20goals%20(Article%2014).

https://doi.org/10.5194/essd-2022-239
Preprint. Discussion started: 1 August 2022

the estimates of our Earth heat inventory based on the results of Fig. 8 have been added (red lines) for the periods 1971–2020, 1993–2020 and 2006–2020.

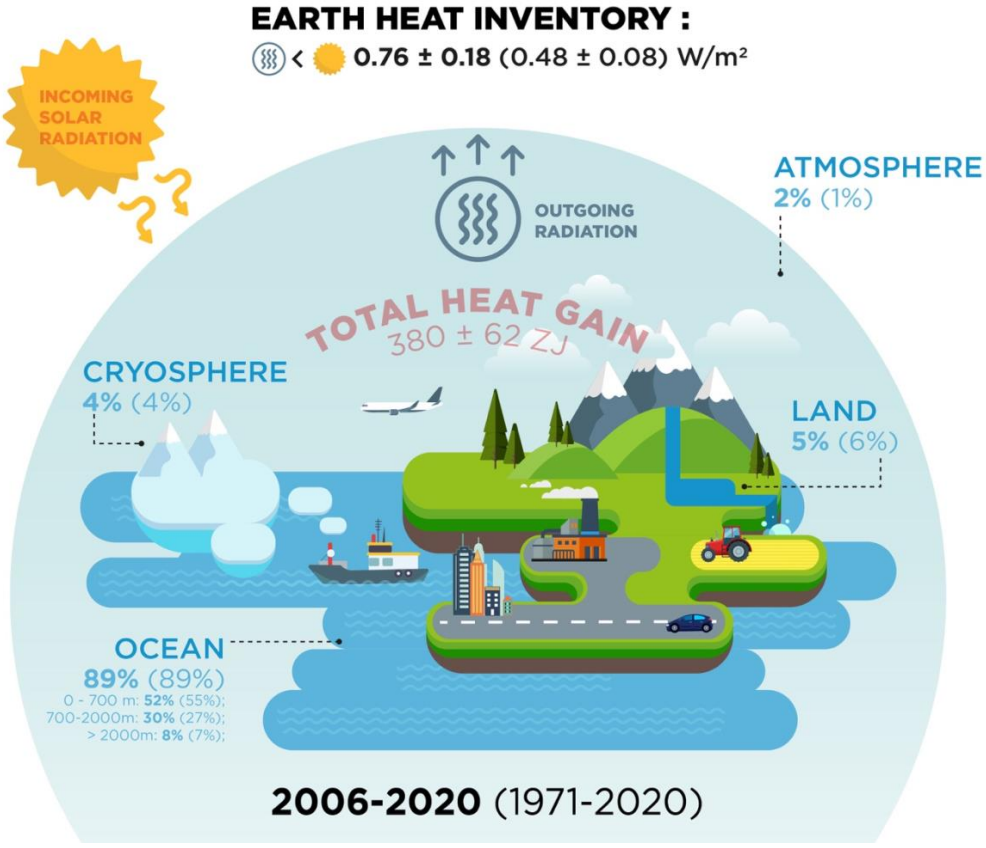

Figure 11: *Schematic presentation on the Earth heat inventory for the current anthropogenically driven positive Earth energy imbalance at the top of the atmosphere (TOA). The relative partition (in %) of the Earth heat inventory presented in Fig. 8 for the different components is given for the ocean (upper: 0–700 m, intermediate: 700–2000 m, deep: >2000 m), land, cryosphere (grounded and floating ice) and atmosphere, for the periods 2006–2020 and 1971–2020 (for the latter period values are provided in parentheses), as well as for the EEI. The total heat gain (in red) over the period 1971–2020 is obtained from the Earth heat inventory as presented in Fig. 8.*

The quantifications presented in this study are the result of multidisciplinary global-scale collaboration and demonstrate the critical importance of concerted international efforts for climate change monitoring and community-based recommendations for the GCOS. For the GOOS, the core Argo sampling needs to be sustained – which includes the maintenance of shipboard collection of reference data for validation - and complemented by remote sensing data. Extensions

https://doi.org/10.5194/essd-2022-239
Preprint. Discussion started: 1 August 2022

such as into the deep ocean layer need to be further fostered, and technical developments for the measurements under ice and in shallower areas need to be sustained and extended. Moreover, continued efforts are needed to further advance bias correction methodologies, uncertainty evaluations, data recovery and processing of the historical dataset.

For the ground heat storage, the estimate had been hampered by a lack of subsurface temperature profiles in the southern hemisphere, as well as by the fact that most of the profiles were measured before the 2000s. Subsurface temperature data are direct and independent (not proxy) measurements of temperature yielding information on the temporal variation of the ground surface temperature and ground heat flux at the land surface. A larger spatial scale dataset of the thermal state of the subsurface from the last millennium to the present will aid in the continuing monitoring of continental heat storage, provide initial conditions for Land Surface Model (LSM) components of Earth System Models (ESMs) (Cuesta-Valero et al., 2019), and serve as a dataset for validation of climate models' simulations (Cuesta-Valero et al., 2021; Cuesta-Valero et al., 2016). Progress in understanding climate variability through the last millennium must lean on additional data acquisition as the only way to reduce uncertainty in the paleoclimatic record and on changes to the current state of the continental energy reservoir. Remote sensing data are expected to be very valuable to retrieve recent past and future changes in ground heat flux at short-time scales with near global coverage. However, collecting subsurface temperature data is urgent as we must make a record of the present thermal state of the subsurface before the subsurface climate baseline is affected by the downward propagating thermal signal from current climate heating. Furthermore, an international organization should take responsibility to gather and curate all measured subsurface temperature profiles currently available and those that will be measured in the future, as the current practices, in which individual researchers are responsible for measuring, storing and distributing the data, have led to fragmented datasets, restrictions in the use of data, and loss of the original datasets. Support from GCOS for an international data acquisition and curating efforts would be extremely important in this context.

For the permafrost estimates, the primary sources of uncertainty arise from lacking information about the amount and distribution of ground ice in permafrost regions, as well as measurements of liquid water content (Nitzbon et al., 2022). Permafrost heat storage is defined as the required heat to change the mass of ground ice at a certain location, thus monitoring changes in ground ice and water contents would be required to improve estimates of this component of the continental heat storage. Nevertheless, the current monitoring system for permafrost soils is focused on soil temperature, and the distribution of stations is still relatively scarce in comparison with the vast areas that need to be surveyed (Biskaborn et al., 2015). Due to the current limitations in the observational data, a permafrost model was used to estimate the heat uptake by thawing of ground ice. This approach retrieves latent heat fluxes in extensive areas and at depths relevant to analyze the long-term change in ground ice mass, but at the cost of ignoring other relevant processes, such as ground subsidence, to balance model performance with computational resources. Including permafrost heat storage in the Tibetan Plateau is a priority for the next iteration of this work, as well as to explore new methods to evaluate model simulations using the available observations in permafrost areas.

For inland water heat storage, a better representation of lake and reservoir volume would be possible by better accounting for lake bathymetry using the GLOBathy (Khazaei et al., 2022)

https://doi.org/10.5194/essd-2022-239
Preprint. Discussion started: 1 August 2022

dataset and results from the upcoming Surface Water and Ocean Topography (SWOT) mission. These improvements in the representation of lake volume, and an updated lake mask will be available in the upcoming ISIMIP3 simulation round, next to improved meteorological forcing data (Golub et al., 2022). In contrast to (Vanderkelen et al., 2020), the heat storage in rivers is not included in this analysis due to the high uncertainties in simulated river water volume. To reduce the uncertainty in river heat storage, the estimation of river water storage should be improved, together with an explicit representation of water temperature in the global hydrological models (Wanders et al., 2019). These improvements will be incorporated in ISIMIP3 and will lead to better estimates of inland water heat storage, thus enhancing future estimates of continental heat storage. In the long run, these model-based estimates could be supplemented or replaced by observation-based estimates, which would however require a large, global-scale effort to monitor lake and river temperatures at high spatial resolution and over long time periods.

For the cryosphere, sustained remote sensing for all of the cryosphere components is critical in quantifying future changes over these vast and inaccessible regions; in situ observations are also needed for process understanding and in order to properly calibrate and validate them. For sea ice, observations of the albedo, the area and ice thickness are all essential - the continuation of satellite altimeter missions with high inclination, polar focused orbits is critical in our ability to monitor sea ice thickness in particular. Observations of snow thickness with multi-frequency altimeters are essential for further constraining sea ice thickness estimates. For ice sheets and glaciers, reliable gravimetric, geodetic, and ice velocity measurements, knowledge of ice thickness and extent, snow/firn thickness and density, and the continuation of the now three-decade long satellite altimeter record are essential in understanding changes in the mass balance of grounded and floating ice. The recent failure of Sentinel-1b, which in tandem with Sentinel-1a could be used to systematically measure ice speed changes every 6 days, means that images are now being acquired every 12 days and thus an earlier launch of Sentinel-1c should be encouraged to regain the ability to monitor ice speed changes over short time-scales. The estimate of glacier heat uptake is particularly affected by lacking knowledge of ice melt below sea level, and to a lesser degree, lacking knowledge of firn and ice temperatures. This lack of observations is likely related to most studies on glaciers focussing on their contribution to sea-level rise or seasonal water availability, where melt below sea level and warming of ice do not matter much. However, it becomes obvious here that this gap introduces a systematic bias in the estimate of cryospheric energy uptake, which is presumably small compared to the other components, but unconstrained. Although the Antarctic sea ice change and the warming of Greenland and Antarctic firn are poorly constrained or have not significantly contributed to this assessment, they may become increasingly important over the coming decades. Similarly, there exists the possibility for rapid change associated with positive ice dynamical feedbacks at the marine margins of the Antarctic Ice Sheet. Sustained monitoring of each of these components will, therefore, serve the dual purpose of furthering the understanding of the dynamics and quantifying the contribution to Earth's energy budget. In addition to data collection, open access to the data and data synthesis products, as well as coordinated international efforts, are key to the continued monitoring of the ice loss from the cryosphere and its related energy uptake.

For the atmosphere, there is a need to sustain and enhance a coherent operational long-term monitoring system for the provision of climate data records of essential climate variables. Observations from radiosonde stations within the GCOS reference upper air network (GRUAN)

https://doi.org/10.5194/essd-2022-239
Preprint. Discussion started: 1 August 2022

and from satellite-based GNSS radio occultation deliver thermodynamic profiling observations of benchmark quality and stability from surface to stratopause. For climate monitoring, it is of critical importance to ensure continuity of such observations with global coverage over all local times. This continuity of radio occultation observations in the future is not sufficiently guaranteed as we are facing an imminent observational gap in mid- to high latitudes for most local times(IROWG, 2021), which is a major concern. Thus, there is an urgent need for satellite missions in high inclination orbits to provide full global and local time coverage in order to ensure global climate monitoring. Operational radio occultation missions need to be maintained as backbone for a global climate observing system and long-term availability and archiving of measurement data, metadata and processing information needs to be ensured.

In summary, we also call for urgently needed actions for enabling continuity, archiving, rescuing and calibrating efforts to assure improved and long-term monitoring capacity of the GCOS for the Earth heat inventory. Particularly, the summarized recommendations include

- Need to sustain, reinforce or even to establish data repositories for historical climate data (archiving)
- Need to reinforce efforts for recovery projects for historical data and associated meta-data information (rescuing)
- Need to sustain and reinforce the GCOS for assuring the monitoring of the Earth heat inventory targets (continuity)
- Need to foster calibration measurements (in situ) for assuring quality and reliability of large-scale measurement techniques (e.g., remote sensing, autonomous components (eg argo) (calibrating)

A continuous effort to regularly update the Earth heat inventory is important as this global climate indicator crosses multidisciplinary boundaries and calls for the inclusion of new science knowledge from the different disciplines involved, including the evolution of climate observing systems and associated data products, uncertainty evaluations, and processing tools. The outcomes have further demonstrated how we are able to evolve our estimates for the Earth heat inventory while bringing together different expertise and major climate science advancements through a concerted international effort. All of these component estimates are at the leading edge of climate science. Their union has provided a new and unique insight on the inventory of heat in the Earth system, its evolution over time and the absolute values. The data product of this effort is made available and can be thus used for model validation purposes.

This study has demonstrated the unique value of such a concerted international effort, and we thus call for a regular evaluation of the Earth heat inventory. This updated attempt presented here has been focused on the global area average only, and evolving into regional heat storage and redistribution, the inclusion of various timescales (e.g., seasonal, year to year) and other climate study tools (e.g., indirect methods, ocean reanalyses) would be an important asset of this much needed regular international framework for the Earth heat inventory. This would also respond directly to the request of GCOS to establish the observational requirements needed to further monitor the Earth's cycles and the global energy budget (GCOS, 2021). The outcome of this study will therefore directly feed into GCOS' assessments of the status of the global climate observing system, and the identified observation requirements will guide the development of the next

https://doi.org/10.5194/essd-2022-239
Preprint. Discussion started: 1 August 2022

generation of in situ and satellite global climate observations as specified by GCOS by all national meteorological services and space agencies and other oceanic and terrestrial networks.

Acknowledgements.

Ocean: OHC estimate from the product ISAS (Gaillard et al., 2016) was provided by 'Service National d'Observation Argo France' (INSU/CNRS) at OSU IUEM (https://www.argo-france.fr/).
Atmosphere: We acknowledge the WEGC EOPAC team for providing the OPSv5.6 RO data (available online at https://doi.org/10.25364/WEGC/OPS5.6:2020.1) as well as quality-processed Vaisala RS data, UCAR/CDAAC (Boulder, CO, USA) for access to RO phase and orbit data, ECMWF (Reading, UK) for access to operational analysis and forecast data, ERA5 reanalysis data, and RS data from the ERA-Interim archive, JMA (Tokyo, Japan) for provision of the JRA55 and JRA55C reanalysis data, and NASA GMAO (Greenbelt, MD, USA) for access of the MERRA-2 reanalysis data.

Financial support.

Maximilian Gorfer was supported by WEGC atmospheric remote sensing and climate system research group young scientist funds. Michael Mayer was supported by Austrian Science Fund project P33177.

Donata Giglio and Mikael Kuusela acknowledge support from NOAA (Award NA21OAR4310261).
L.C. acknowledges financial supports from the Strategic Priority Research Program of the Chinese Academy of Sciences (XDB42040402), National Natural Science Foundation of China (grant number 42122046, 42076202).

J.C. and Y.L. were supported by the Centre for Southern Hemisphere Oceans Research (CSHOR), jointly funded by the Qingdao National Laboratory for Marine Science and Technology (QNLM, China) and the Commonwealth Scientific and Industrial Research Organisation (CSIRO, Australia), and the Australian Research Council's Discovery Project funding scheme (project DP190101173). TMcD and PMB gratefully acknowledge Australian Research Council support through grant FL150100090. This paper contributes to the tasks of the Joint SCOR/IAPSO/IAPWS Committee on the Thermophysical Properties of Seawater.

Hugo Beltrami was supported by grants from the National Sciences and Engineering Research Council of Canada Discovery Grant (NSERC DG 140576948) and the Canada Research Chairs Program (CRC 230687). Hugo Beltrami holds a Canada Research Chair in Climate Dynamics

Francisco José Cuesta-Valero is an Alexander von Humboldt Research Fellow at the Helmholtz Centre for Environmental Research (UFZ).

Richard P. Allan is funded by the National Centre for Earth Observation RCUK grant NE/RO16518/1.

References

Abraham, J. P., Baringer, M., Bindoff, N. L., Boyer, T., Cheng, L. J., Church, J. A., Conroy, J. L., Domingues, C. M., Fasullo, J. T., Gilson, J., Goni, G., Good, S. A., Gorman, J. M., Gouretski, V., Ishii, M., Johnson, G. C., Kizu, S., Lyman, J. M., Macdonald, A. M., … Willis, J. K. (2013). A review of global ocean temperature observations: Implications for ocean heat content estimates and climate change. *Reviews of Geophysics*, *51*(3), 450–483. https://doi.org/10.1002/rog.20022

Abram, N., Gattuso, J.-P., Prakash, A., Cheng, L., Chidichimo, M. P., Crate, S., Enomoto, H.,

https://doi.org/10.5194/essd-2022-239
Preprint. Discussion started: 1 August 2022

1341 Garschagen, M., Gruber, N., Harper, S., Holland, E., Kudela, R. M., Rice, J., Steffen, K., &
1342 von Schuckmann, K. (2019). Framing and Context of the Report. In H. O. Pörtner, D. C.
1343 Roberts, V. Masson-Delmotte, P. Zhai, M. Tignor, E. Poloczanska, K. Mintenbeck, A.
1344 Alegría, M. Nicolai, A. Okem, J. Petzold, B. Rama, & N. M. Weyer (Eds.), *IPCC Special*
1345 *Report on the Ocean and Cryosphere in a Changing Climate* (pp. 73–129). in press.
1346 https://www.ipcc.ch/srocc/
1347 Adusumilli, Susheel; Hendricks, Stefan; Korosov, Anton; Straneo, Fiammetta; Lavergne,
1348 Thomas; Lawrence, Isobel; Marzeion, Ben; Otosaka, Inès; Schweiger, Axel; Shepherd,
1349 Andrew; Slater, Donald; Slater, Thomas; Timmermanns, Mary-Louise; Zemp, Michael
1350 (2022). Heat stored in the Earth system 1960-2020: Where does the energy go?, submitted
1351 to Earth System Science Data. (2022). World Data Center for Climate (WDCC) at DKRZ.
1352 https://www.wdc-climate.de/ui/entry?acronym=GCOS_EHI_1960-2020_CrHC
1353 Adusumilli, S., Fricker, H. A., Medley, B., Padman, L., & Siegfried, M. R. (2020). Interannual
1354 variations in meltwater input to the Southern Ocean from Antarctic ice shelves. *Nature*
1355 *Geoscience*, *13*(9), 616–620. https://doi.org/10.1038/s41561-020-0616-z
1356 Allison, L. C., Roberts, C. D., Palmer, M. D., Hermanson, L., Killick, R. E., Rayner, N. A.,
1357 Smith, D. M., & Andrews, M. B. (2019). Towards quantifying uncertainty in ocean heat
1358 content changes using synthetic profiles. *Environmental Research Letters*, *14*(8), 084037.
1359 https://doi.org/10.1088/1748-9326/ab2b0b
1360 Angerer, B., Ladstädter, F., Scherllin-Pirscher, B., Schwärz, M., Steiner, A. K., Foelsche, U., &
1361 Kirchengast, G. (2017). Quality aspects of the Wegener Center multi-satellite GPS radio
1362 occultation record OPSv5.6. *Atmospheric Measurement Techniques*, *10*(12), 4845–4863.
1363 https://doi.org/10.5194/amt-10-4845-2017
1364 Bell, B., Hersbach, H., Simmons, A., Berrisford, P., Dahlgren, P., Horányi, A., Muñoz-Sabater,
1365 J., Nicolas, J., Radu, R., Schepers, D., Soci, C., Villaume, S., Bidlot, J.-R., Haimberger, L.,
1366 Woollen, J., Buontempo, C., & Thépaut, J.-N. (2021). The ERA5 global reanalysis:
1367 Preliminary extension to 1950. *Quarterly Journal of the Royal Meteorological Society*,
1368 *147*(741), 4186–4227. https://doi.org/https://doi.org/10.1002/qj.4174
1369 Beltrami, H., & Mareschal, J.-C. (1992). Ground temperature histories for central and eastern
1370 Canada from geothermal measurements: Little Ice Age signature. *Geophysical Research*
1371 *Letters*, *19*(7), 689–692. https://doi.org/10.1029/92GL00671
1372 Beltrami, H., Smerdon, J. E., Pollack, H. N., & Huang, S. (2002). Continental heat gain in the
1373 global climate system. *Geophysical Research Letters*, *29*(8), 8-1-8–3.
1374 https://doi.org/10.1029/2001GL014310
1375 Berrisford, P., Kållberg, P., Kobayashi, S., Dee, D., Uppala, S., Simmons, A. J., Poli, P., & Sato,
1376 H. (2011). Atmospheric conservation properties in ERA-Interim. *Quarterly Journal of the*
1377 *Royal Meteorological Society*, *137*(659), 1381–1399. https://doi.org/10.1002/qj.864
1378 Biskaborn, B. K., Lanckman, J.-P., Lantuit, H., Elger, K., Streletskiy, D. A., Cable, W. L., &
1379 Romanovsky, V. E. (2015). The new database of the Global Terrestrial Network for
1380 Permafrost (GTN-P). *Earth Syst. Sci. Data*, *7*(2), 245–259. https://doi.org/10.5194/essd-7-
1381 245-2015
1382 Boyer, T., Domingues, C. M., Good, S. A., Johnson, G. C., Lyman, J. M., Ishii, M., Gouretski,
1383 V., Willis, J. K., Antonov, J., Wijffels, S., Church, J. A., Cowley, R., & Bindoff, N. L.
1384 (2016). Sensitivity of Global Upper-Ocean Heat Content Estimates to Mapping Methods,
1385 XBT Bias Corrections, and Baseline Climatologies. *Journal of Climate*, *29*(13), 4817–4842.
1386 https://doi.org/10.1175/JCLI-D-15-0801.1

https://doi.org/10.5194/essd-2022-239
Preprint. Discussion started: 1 August 2022

1387 Cabanes, C., Grouazel, A., von Schuckmann, K., Hamon, M., Turpin, V., Coatanoan, C., Paris,
1388 F., Guinehut, S., Boone, C., Ferry, N., de Boyer Montégut, C., Carval, T., Reverdin, G.,
1389 Pouliquen, S., & Le Traon, P.-Y. (2013). The CORA dataset: validation and diagnostics of
1390 in-situ ocean temperature and salinity measurements. *Ocean Sci.*, *9*(1), 1–18.
1391 https://doi.org/10.5194/os-9-1-2013
1392 Castelao, G. P. (2020). A Framework to Quality Control Oceanographic Data. Journal of Open
1393 Source Software. *Journal of Open Source Software*, *5*(48), 2063.
1394 https://doi.org/https://doi.org/10.21105/joss.02063
1395 Castelão, G. P. (2021). A machine learning approach to quality control oceanographic data.
1396 *Computers & Geosciences*, *155*, 104803.
1397 https://doi.org/https://doi.org/10.1016/j.cageo.2021.104803
1398 Cheng, L., Abraham, J., Hausfather, Z., & Trenberth, K. E. (2019). How fast are the oceans
1399 warming? *Science*, *363*(6423), 128. https://doi.org/10.1126/science.aav7619
1400 Cheng, L., Foster, G., Hausfather, Z., Trenberth, K. E., & Abraham, J. (2022). Improved
1401 Quantification of the Rate of Ocean Warming. *Journal of Climate*, *35*(14), 4827–4840.
1402 https://doi.org/10.1175/JCLI-D-21-0895.1
1403 Cheng, L., Luo, H., Boyer, T., Cowley, R., Abraham, J., Gouretski, V., Reseghetti, F., & Zhu, J.
1404 (2018). How Well Can We Correct Systematic Errors in Historical XBT Data? *Journal of*
1405 *Atmospheric and Oceanic Technology*, *35*(5), 1103–1125. https://doi.org/10.1175/JTECH-
1406 D-17-0122.1
1407 Cheng, L., Schuckmann, K. von, Abraham, J., Trenberth, K., Mann, M., Zanna, L., England, M.
1408 H., Zika, J. D., Fasullo, J., Yu1, Y., Pan, Y., Zhu, J., Newsom, E., Bronselaer, B., & Lin, X.
1409 (2022). Past and future ocean warming. *Nature*, *under revi*.
1410 Cheng, L., Trenberth, K. E., Fasullo, J., Boyer, T., Abraham, J., & Zhu, J. (2017). Improved
1411 estimates of ocean heat content from 1960 to 2015. *Science Advances*, *3*(3), e1601545.
1412 https://doi.org/10.1126/sciadv.1601545
1413 Cheng, L., Trenberth, K., Fasullo, J., Abraham, J., Boyer, T., von Schuckmann, K., & Zhu, J.
1414 (2017). Taking the Pulse of the Planet. *Eos*. https://doi.org/10.1029/2017EO081839
1415 Chiodo, G., & Haimberger, L. (2010). Interannual changes in mass consistent energy budgets
1416 from ERA-Interim and satellite data. *Journal of Geophysical Research: Atmospheres*,
1417 *115*(D2). https://doi.org/10.1029/2009JD012049
1418 Church, J. A., White, N. J., Konikow, L. F., Domingues, C. M., Cogley, J. G., Rignot, E.,
1419 Gregory, J. M., van den Broeke, M. R., Monaghan, A. J., & Velicogna, I. (2011). Revisiting
1420 the Earth's sea-level and energy budgets from 1961 to 2008. *Geophysical Research Letters*,
1421 *38*(18). https://doi.org/10.1029/2011GL048794
1422 Ciais, P., Sabine, C., Bala, G., Bopp, L., Brovkin, V., Canadell, J., Chhabra, A., DeFries, R.,
1423 Galloway, J., Heimann, M., Jones, C., Le Quéré, C., Myneni, R. B., Piao, S., & Thornton, P.
1424 (2014). *Carbon and Other Biogeochemical Cycles. In Climate Change 2013 – The Physical*
1425 *Science Basis: Working Group I Contribution to the Fifth Assessment Report of the*
1426 *Intergovernmental Panel on Climate Change*. Cambridge University Press.
1427 https://doi.org/https://doi.org/DOI: 10.1017/CBO9781107415324.015
1428 Cleveland, W. S. (1979). Robust Locally Weighted Regression and Smoothing Scatterplots. *J.*
1429 *Am.Stat.Assoc.*, *74*, 829–836.
1430 Clough, W. J., & Hansen, L. B. (1979). The Ross Ice Shelf Project. *Science*, *203*(4379), 433–
1431 434. https://doi.org/10.1126/science.203.4379.433
1432 Cohen, J., Zhang, X., Francis, J., Jung, T., Kwok, R., Overland, J., Ballinger, T., Bhatt, U. S.,

https://doi.org/10.5194/essd-2022-239
Preprint. Discussion started: 1 August 2022

1433 Chen, H. W., Coumou, D., Feldstein, S., Handorf, D., Henderson, G., Ionita, M.,
1434 Kretschmer, M., Laliberte, F., Lee, S., Linderholm, H. W., Maslowski, W., … Yoon, J.
1435 (2020). Divergent consensuses on Arctic amplification influence on midlatitude severe
1436 winter weather. *Nature Climate Change*, *10*, 20–29. https://doi.org/10.1038/s41558-019-
1437 0662-y
1438 Cook, A. J., & Vaughan, D. G. (2010). Overview of areal changes of the ice shelves on the
1439 Antarctic Peninsula over the past 50 years. *The Cryosphere*, *4*(1), 77–98.
1440 https://doi.org/10.5194/tc-4-77-2010
1441 Cowley, R., Killick, R. E., Boyer, T., Gouretski, V., Reseghetti, F., Kizu, S., Palmer, M. D.,
1442 Cheng, L., Storto, A., Le Menn, M., Simoncelli, S., Macdonald, A. M., & Domingues, C.
1443 M. (2021). International Quality-Controlled Ocean Database (IQuOD) v0.1: The
1444 Temperature Uncertainty Specification . In *Frontiers in Marine Science* (Vol. 8).
1445 https://www.frontiersin.org/articles/10.3389/fmars.2021.689695
1446 Crisp, D., Dolman, H., Tanhua, T., McKinley, G. A., Hauck, J., Bastos, A., Sitch, S., Eggleston,
1447 S., & Aich, V. (2022). How Well Do We Understand the Land-Ocean-Atmosphere Carbon
1448 Cycle? *Reviews of Geophysics*, *60*(2), e2021RG000736.
1449 https://doi.org/https://doi.org/10.1029/2021RG000736
1450 Cuesta-Valero, F. J., Beltrami, H., García-García, A., Krinner, G., Langer, M., MacDougall, A.,
1451 Nitzbon, J., Peng, J., von Schuckmann, K., Seneviratne, S. I., Smith, N., Thiery, W.,
1452 Vanderkelen, I., & Wu, T. (2022). Continental Heat Storage: Contributions from Ground,
1453 Inland Waters, and Permafrost Thawing, submitted. *Earth System Dynamics*, *submitted*.
1454 Cuesta-Valero, F. J., Beltrami, H., Gruber, S., García-García, A., & González-Rouco, J. F.
1455 (2022). A new bootstrap technique to quantify uncertainty in estimates of ground surface
1456 temperature and ground heat flux histories from geothermal data. Submitted. *Geoscientific*
1457 *Model Development*, *submitted*.
1458 Cuesta-Valero, Francisco; Beltrami, Hugo; García-García, Almudena; Krinner, Gerhard; Langer,
1459 Moritz; MacDougall, Andrew; Nitzbon, Jean; Peng, Jian; von Schuckmann, Karina;
1460 Seneviratne, Sonia; Smith, Noah; Thiery, Wim; Vanderkelen, Inne; Wu, Tonghua (2022).
1461 Continental heat storage: Contributions from the ground, inland waters, and permafrost
1462 thawing, submitted to Earth System Dynamics (2022c). World Data Center for Climate
1463 (WDCC) at DKRZ. https://www.wdc-climate.de/ui/entry?acronym=GCOS_EHI_1960-
1464 2020_CoHC
1465 Cuesta-Valero, F J, García-García, A., Beltrami, H., & Finnis, J. (2021). First assessment of the
1466 earth heat inventory within CMIP5 historical simulations. *Earth Syst. Dynam.*, *12*(2), 581–
1467 600. https://doi.org/10.5194/esd-12-581-2021
1468 Cuesta-Valero, F J, Garcia-Garcia, A., Beltrami, H., González-Rouco, J. F., & Garcia-
1469 Bustamante, E. (2021). Long-Term Global Ground Heat Flux and Continental Heat Storage
1470 from Geothermal Data. *Climate of the Past*, *17*(1), 451–468. https://doi.org/10.5194/cp-17-
1471 451-2021
1472 Cuesta-Valero, F J, García-García, A., Beltrami, H., Zorita, E., & Jaume-Santero, F. (2019).
1473 Long-term Surface Temperature (LoST) database as a complement for GCM preindustrial
1474 simulations. *Clim. Past*, *15*(3), 1099–1111. https://doi.org/10.5194/cp-15-1099-2019
1475 Cuesta-Valero, Francisco José, Beltrami, H., Burke, E., García-García, A., MacDougall, A.,
1476 Peng, J., Schuckmann, K. von, Seneviratne, S. I., Smith, N., Thiery, W., Vanderkelen, I., &
1477 Wu, T. (2022). Continental Heat Storage: Contributions from the Ground, Inland Waters,
1478 and Permafrost Thawing. *Submitted to Earth System Data*.

https://doi.org/10.5194/essd-2022-239
Preprint. Discussion started: 1 August 2022

1479 Cuesta-Valero, Francisco José, García-García, A., Beltrami, H., & Smerdon, J. E. (2016). First
1480 assessment of continental energy storage in CMIP5 simulations. *Geophysical Research*
1481 *Letters*, *43*(10), 5326–5335. https://doi.org/10.1002/2016GL068496
1482 de Vrese, P., Stacke, T., Caves Rugenstein, J., Goodman, J., & Brovkin, V. (2021). Snowfall-
1483 albedo feedbacks could have led to deglaciation of snowball Earth starting from mid-
1484 latitudes. *Communications Earth & Environment*, *2*(1), 91. https://doi.org/10.1038/s43247-
1485 021-00160-4
1486 Demezhko, D. Y., & Gornostaeva, A. A. (2015). Late Pleistocene–Holocene ground surface heat
1487 flux changes reconstructed from borehole temperature data. *Climate of the Past*, *11*(4), 647–
1488 652. https://doi.org/D O I: 10.5194/cp 11-647-2015
1489 Denning, A. S. (2022). Where Has All the Carbon Gone? *Annual Review of Earth and Planetary*
1490 *Sciences*, *50*(1), 55–78. https://doi.org/10.1146/annurev-earth-032320-092010
1491 Desbruyères, D. G., Purkey, S. G., McDonagh, E. L., Johnson, G. C., & King, B. A. (2016).
1492 Deep and abyssal ocean warming from 35 years of repeat hydrography. *Geophysical*
1493 *Research Letters*, *43*(19), 10, 310–356, 365. https://doi.org/10.1002/2016GL070413
1494 Desbruyères, D., McDonagh, E. L., King, B. A., & Thierry, V. (2017). Global and Full-Depth
1495 Ocean Temperature Trends during the Early Twenty-First Century from Argo and Repeat
1496 Hydrography. *Journal of Climate*, *30*(6), 1985–1997. https://doi.org/10.1175/JCLI-D-16-
1497 0396.1
1498 Dieng, H. B., Cazenave, A., Meyssignac, B., & Ablain, M. (2017). New estimate of the current
1499 rate of sea level rise from a sea level budget approach. *Geophysical Research Letters*, *44*(8),
1500 3744–3751. https://doi.org/10.1002/2017GL073308
1501 Domingues, C. M., Church, J. A., White, N. J., Gleckler, P. J., Wijffels, S. E., Barker, P. M., &
1502 Dunn, J. R. (2008). Improved estimates of upper-ocean warming and multi-decadal sea-
1503 level rise. *Nature*, *453*(7198), 1090–1093. https://doi.org/10.1038/nature07080
1504 Dorigo, W., Dietrich, S., Aires, F., Brocca, L., Carter, S., Cretaux, J.-F., Dunkerley, D.,
1505 Enomoto, H., Forsberg, R., Güntner, A., Hegglin, M. I., Hollmann, R., Hurst, D. F.,
1506 Johannessen, J. A., Kummerow, C., Lee, T., Luojus, K., Looser, U., Miralles, D. G., …
1507 Aich, V. (2021). Closing the Water Cycle from Observations across Scales: Where Do We
1508 Stand? *Bulletin of the American Meteorological Society*, *102*(10), E1897–E1935.
1509 https://doi.org/10.1175/BAMS-D-19-0316.1
1510 Eicken, H., Fischer, H., & Lemke, P. (1995). Effects of the snow cover on Antarctic sea ice and
1511 potential modulation of its response to climate change. *Annals of Glaciology*, *21*, 369–376.
1512 https://doi.org/DOI: 10.3189/S0260305500016086
1513 Farinotti, D., Huss, M., Fürst, J. J., Landmann, J., Machguth, H., Maussion, F., & Pandit, A.
1514 (2019). A consensus estimate for the ice thickness distribution of all glaciers on Earth.
1515 *Nature Geoscience*, *12*, 168–173. https://doi.org/10.1038/s41561-019-0300-3
1516 Fischer, E. M., Sippel, S., & Knutti, R. (2021). Increasing probability of record-shattering
1517 climate extremes. *Nature Climate Change*, *11*(8), 689–695. https://doi.org/10.1038/s41558-
1518 021-01092-9
1519 Forster, P., Storelvmo, T., Armour, K., Collins, W., Dufresne, J.-L., Frame, D., Lunt, D. J.,
1520 Mauritsen, T., Palmer, M. D., Watanabe, M., Wild, M., & Zhang, H. (2022). *The Earth's*
1521 *Energy Budget, Climate Feedbacks, and Climate Sensitivity. In Climate Change 2021: The*
1522 *Physical Science Basis. Contribution of Working Group I to the Sixth Assessment Report of*
1523 *the Intergovernmental Panel on Climate Change* (V. Masson-Delmotte, P. Zhai, A. Pirani,
1524 S. L. Connors, C. Péan, S. Berger, N. Caud, Y. Chen, L. Goldfarb, M. I. Gomis, M. Huang,

https://doi.org/10.5194/essd-2022-239
Preprint. Discussion started: 1 August 2022

1525 K. Leitzell, E. Lonnoy, J. B. R. Matthews, T. K. Maycock, T. Waterfield, O. Yelekçi, R.
1526 Yu, & B. Zhou (eds.)). Cambridge University Press, Cambridge, United Kingdom and New
1527 York, NY, USA. https://doi.org/10.1017/9781009157896.009
1528 Friedlingstein, P., Jones, M. W., O'Sullivan, M., Andrew, R. M., Bakker, D. C. E., Hauck, J., Le
1529 Quéré, C., Peters, G. P., Peters, W., Pongratz, J., Sitch, S., Canadell, J. G., Ciais, P.,
1530 Jackson, R. B., Alin, S. R., Anthoni, P., Bates, N. R., Becker, M., Bellouin, N., … Zeng, J.
1531 (2022). Global Carbon Budget 2021. *Earth Syst. Sci. Data*, *14*(4), 1917–2005.
1532 https://doi.org/10.5194/essd-14-1917-2022
1533 Frieler, K., Lange, S., Piontek, F., Reyer, C., Schewe, J., Warszawski, L., Zhao, F., Chini, L.,
1534 Denvil, S., Emanuel, K., Geiger, T., Halladay, K., Hurtt, G., Mengel, M., Murakami, D.,
1535 Ostberg, S., Popp, A., Riva, R., Stevanovic, M., & Yamagata, Y. (2017). Assessing the
1536 impacts of 1.5°C global warming - Simulation protocol of the Inter-Sectoral Impact Model
1537 Intercomparison Project (ISIMIP2b). *Geoscientific Model Development*, *10*, 4321–4345.
1538 https://doi.org/10.5194/gmd-10-4321-2017
1539 Fu, Q., Solomon, S., Pahlavan, H. A., & Lin, P. (2019). Observed changes in Brewer–Dobson
1540 circulation for 1980–2018. *Environmental Research Letters*, *14*(11), 114026.
1541 https://doi.org/10.1088/1748-9326/ab4de7
1542 Gädeke, A., Langer, M., Boike, J., Burke, E. J., Chang, J., Head, M., Reyer, C. P. O., Schaphoff,
1543 S., Thiery, W., & Thonicke, K. (2021). Climate change reduces winter overland travel
1544 across the Pan-Arctic even under low-end global warming scenarios. *Environmental*
1545 *Research Letters*, *16*(2), 24049. https://doi.org/10.1088/1748-9326/abdcf2
1546 Gaillard, F., Reynaud, T., Thierry, V., Kolodziejczyk, N., & von Schuckmann, K. (2016). In
1547 Situ–Based Reanalysis of the Global Ocean Temperature and Salinity with ISAS:
1548 Variability of the Heat Content and Steric Height. *Journal of Climate*, *29*(4), 1305–1323.
1549 https://doi.org/10.1175/JCLI-D-15-0028.1
1550 GCOS. (2016). *The Global Observing System for Climate: Implementation needs, World*
1551 *Meteorological Organization, Geneva, Switzerland*.
1552 GCOS. (2021). *The Status of the Global Climate Observing System 2021: Executive Summary.*
1553 *(GCOS-239)*.
1554 Gelaro, R., McCarty, W., Suárez, M. J., Todling, R., Molod, A., Takacs, L., Randles, C. A.,
1555 Darmenov, A., Bosilovich, M. G., Reichle, R., Wargan, K., Coy, L., Cullather, R., Draper,
1556 C., Akella, S., Buchard, V., Conaty, A., da Silva, A. M., Gu, W., … Zhao, B. (2017). The
1557 Modern-Era Retrospective Analysis for Research and Applications, Version 2 (MERRA-2)
1558 (I200, trans.). *Journal of Climate*, *30*(14), 5419–5454. https://doi.org/10.1175/JCLI-D-16-
1559 0758.1
1560 Golub, M., Thiery, W., Marcé, R., Pierson, D., Vanderkelen, I., Mercado-Bettín, D., Woolway,
1561 R., Grant, L., Jennings, E., Kraemer, B., Schewe, J., Zhao, F., Frieler, K., Mengel, M.,
1562 Bogomolov, V., Bouffard, D., Côté, M., Couture, R.-M., Debolskiy, A., & Zdorovennova,
1563 G. (2022). A framework for ensemble modelling of climate change impacts on lakes
1564 worldwide: the ISIMIP Lake Sector. *Geoscientific Model Development*, *15*, 4597–4623.
1565 https://doi.org/10.5194/gmd-15-4597-2022
1566 Goni, G. J., Sprintall, J., Bringas, F., Cheng, L., Cirano, M., Dong, S., Domingues, R., Goes, M.,
1567 Lopez, H., Morrow, R., Rivero, U., Rossby, T., Todd, R. E., Trinanes, J., Zilberman, N.,
1568 Baringer, M., Boyer, T., Cowley, R., Domingues, C. M., … Volkov, D. (2019). More Than
1569 50 Years of Successful Continuous Temperature Section Measurements by the Global
1570 Expendable Bathythermograph Network, Its Integrability, Societal Benefits, and Future.

https://doi.org/10.5194/essd-2022-239
Preprint. Discussion started: 1 August 2022

Frontiers in Marine Science, *6*, 452. https://www.frontiersin.org/article/10.3389/fmars.2019.00452

Good, S. A. (2017). The impact of observational sampling on time series of global 0–700 m ocean average temperature: a case study. *International Journal of Climatology*, *37*(5), 2260–2268. https://doi.org/10.1002/joc.4654

Good, S. A., Martin, M. J., & Rayner, N. A. (2013). EN4: Quality controlled ocean temperature and salinity profiles and monthly objective analyses with uncertainty estimates (I5197, trans.). *Journal of Geophysical Research: Oceans*, *118*(12), 6704–6716. https://doi.org/10.1002/2013JC009067

GOOS. (2019). *The Global Ocean Observing System Strategy. GOOS Report No. 239, IOC Brochure 2019-5 (IOC/Bro/2019/5 rev.2)*. https://www.goosocean.org/index.php?option=com_oe&task=viewDocumentRecord&docID=24590

Gorfer, M. (2022). *Monitoring of climate change and variability in atmospheric heat content based on climate records and reanalyses, Sci. Rep. 94-2022*. Wegener Center Verlag. https://wegcenter.uni-graz.at/wegener-center-verlag/2022

Gould, J., Sloyan, B., & Visbeck, M. (2013). Chapter 3 - In Situ Ocean Observations: A Brief History, Present Status, and Future Directions. In G. Siedler, S. M. Griffies, J. Gould, & J. A. Church (Eds.), *Ocean Circulation and Climate* (Vol. 103, pp. 59–81). Academic Press. https://doi.org/https://doi.org/10.1016/B978-0-12-391851-2.00003-9

Gouretski, V., & Cheng, L. (2020). Correction for Systematic Errors in the Global Dataset of Temperature Profiles from Mechanical Bathythermographs. *Journal of Atmospheric and Oceanic Technology*, *37*(5), 841–855. https://doi.org/10.1175/JTECH-D-19-0205.1

Grant, L., Vanderkelen, I., Gudmundsson, L., Tan, Z., Perroud, M., Stepanenko, V. M., Debolskiy, A. V, Droppers, B., Janssen, A. B. G., Woolway, R. I., Choulga, M., Balsamo, G., Kirillin, G., Schewe, J., Zhao, F., del Valle, I. V., Golub, M., Pierson, D., Marcé, R., … Thiery, W. (2021). Attribution of global lake systems change to anthropogenic forcing. *Nature Geoscience*, *14*(11), 849–854. https://doi.org/10.1038/s41561-021-00833-x

Gregory, J. M., & Andrews, T. (2016). Variation in climate sensitivity and feedback parameters during the historical period. *Geophysical Research Letters*, *43*(8), 3911–3920. https://doi.org/10.1002/2016GL068406

Grise, K. M., Davis, S. M., Simpson, I. R., Waugh, D. W., Fu, Q., Allen, R. J., Rosenlof, K. H., Ummenhofer, C. C., Karnauskas, K. B., Maycock, A. C., Quan, X. W., Birner, T., & Staten, P. W. (2019). Recent tropical expansion: Natural variability or forced response? *Journal of Climate*, *32*(5), 1551–1571. https://doi.org/10.1175/JCLI-D-18-0444.1

Guinehut, S., Dhomps, A.-L., Larnicol, G., & Le Traon, P.-Y. (2012). High resolution 3-D temperature and salinity fields derived from in situ and satellite observations. *Ocean Sci.*, *8*(5), 845–857. https://doi.org/10.5194/os-8-845-2012

Gulev, S. K., Thorne, P. W., Ahn, J., Dentener, F. J., Domingues, C. M., Gerland, S., Gong, D., Kaufman, D. S., Nnamchi, H. C., Quaas, J., Rivera, J. A., Sathyendranath, S., Smith, S. L., Trewin, B., Schuckmann, K. von, & Vose, R. S. (2021). *Changing State of the Climate System Supplementary Material. In Climate Change 2021: The Physical Science Basis. Contribution of Working Group I to the Sixth Assessment Report of the Intergovernmental Panel on Climate Change* (V. Masson-Delmotte, P. Zhai, A. Pirani, S. L. Connors, C. Péan, S. Berger, N. Caud, Y. Chen, L. Goldfarb, M. I. Gomis, M. Huang, K. Leitzell, E. Lonnoy, J. B. R. Matthews, T. K. Maycock, T. Waterfield, O. Yelekçi, R. Yu, & B. Zhou (eds.)).

https://doi.org/10.5194/essd-2022-239
Preprint. Discussion started: 1 August 2022

Cambridge University Press,. https://doi.org/10.1017/9781009157896.004

Hakuba, M. Z., Frederikse, T., & Landerer, F. W. (2021). Earth's Energy Imbalance From the Ocean Perspective (2005–2019). *Geophysical Research Letters*, *48*(16), e2021GL093624. https://doi.org/https://doi.org/10.1029/2021GL093624

Hansen, J, Sato, M., Kharecha, P., & von Schuckmann, K. (2011). Earth's energy imbalance and implications. *Atmos. Chem. Phys.*, *11*(24), 13421–13449. https://doi.org/10.5194/acp-11-13421-2011

Hansen, J, Sato, M., Kharecha, P., von Schuckmann, K., Beerling, D. J., Cao, J., Marcott, S., Masson-Delmotte, V., Prather, M. J., Rohling, E. J., Shakun, J., Smith, P., Lacis, A., Russell, G., & Ruedy, R. (2017). Young people's burden: requirement of negative CO2 emissions. *Earth Syst. Dynam.*, *8*(3), 577–616. https://doi.org/10.5194/esd-8-577-2017

Hansen, James, Nazarenko, L., Ruedy, R., Sato, M., Willis, J., Del Genio, A., Koch, D., Lacis, A., Lo, K., Menon, S., Novakov, T., Perlwitz, J., Russell, G., Gavin A., S., & Tausnev, N. (2005). Earth's Energy Imbalance: Confirmation and Implications. *Science*, *308*(5727), 1431–1435. https://doi.org/10.1126/science.1110252

Hartmann, A., & Rath, V. (2005). Uncertainties and shortcomings of ground surface temperature histories derived from inversion of temperature logs. *Journal of Geophysics and Engineering*, *2*(4), 299–311. https://doi.org/10.1088/1742-2132/2/4/S02

Hersbach, H., de Rosnay, P., Bell, B., Schepers, D., Simmons, A., Soci, C., Abdalla, S., Alonso-Balmaseda, M., Balsamo, G., Bechtold, P., Berrisford, P., Bidlot, J.-R., de Boisséson, E., Bonavita, M., Browne, P., Buizza, R., Dahlgren, P., Dee, D., Dragani, R., … Zuo, H. (2018). *Operational global reanalysis: progress, future directions and synergies with NWP*. https://www.ecmwf.int/node/18765

Hersbach, Hans, Bell, B., Berrisford, P., Hirahara, S., Horányi, A., Muñoz-Sabater, J., Nicolas, J., Peubey, C., Radu, R., Schepers, D., Simmons, A., Soci, C., Abdalla, S., Abellan, X., Balsamo, G., Bechtold, P., Biavati, G., Bidlot, J., Bonavita, M., … Thépaut, J. N. (2020). The ERA5 global reanalysis. *Quarterly Journal of the Royal Meteorological Society*, *146*, 1999–2049. https://doi.org/10.1002/qj.3803

Hopcroft, P. O., Gallagher, K., & Pain, C. C. (2007). Inference of past climate from borehole temperature data using Bayesian Reversible Jump Markov chain Monte Carlo. *Geophysical Journal International*, *171*(3), 1430–1439. https://doi.org/10.1111/j.1365-246X.2007.03596.x

Hosoda, S., Ohira, T., & Nakamura, T. (2008). *A monthly mean dataset of global oceanic temperature and salinity derived from Argo float observations*. http://www.jamstec.go.jp/ARGO/argo_web/ancient/MapQ/Hosoda_etal_MOAA_GPV.pdf

IPCC. (2019). *IPCC Special Report on the Ocean and Cryosphere in a Changing Climate* (H.-O. Pörtner, D. C. Roberts, V. Masson-Delmotte, P. Zhai, M. Tignor, E. Poloczanska, K. Mintenbeck, A. Alegría, M. Nicolai, A. Okem, J. Petzold, B. Rama, & N. M. Weyer (eds.)). Cambridge University Press. https://doi.org/https://doi.org/10.1017/9781009157964

IPCC. (2021). *Summary for Policymakers. In: Climate Change 2021: The Physical Science Basis. Contribution of Working Group I to the Sixth Assessment Report of the Intergovernmental Panel on Climate Change* (V. Masson-Delmotte, P. Zhai, A. Pirani, S. L. Connors, C. Péan, S. Berger, N. Caud, Y. Chen, L. Goldfarb, M. I. Gomis, M.Huang, K. Leitzell, E. Lonnoy, J. B. R. Matthews, T. K. Maycock, T. Waterfield, O. Yelekçi, R. Yu, & B. Zhou (eds.)). Cambridge University Press. https://doi.org/10.1017/9781009157896.001

IPCC. (2022a). *Climate Change 2022: Impacts, Adaptation, and Vulnerability. Contribution of*

https://doi.org/10.5194/essd-2022-239
Preprint. Discussion started: 1 August 2022

Working Group II to the Sixth Assessment Report of the Intergovernmental Panel on Climate Change (H.-O. Pörtner, D. C. Roberts, M. Tignor, E. S. Poloczanska, K. Mintenbeck, A. Alegría, M. Craig, S. Langsdorf, S. Löschke, V. Möller, A. Okem, & B. Rama (eds.)). Cambridge University Press, Cambridge, UK and New York, NY, USA. https://doi.org/in press

IPCC. (2022b). *Climate Change 2022: Mitigation of Climate Change. Contribution of Working Group III to the Sixth Assessment Report of the Intergovernmental Panel on Climate Change* (P. R. Shukla, J. Skea, R. Slade, A. Al Khourdajie, R. van Diemen, D. McCollum, M. Pathak, S. Some, P. Vyas, R. Fradera, M. Belkacemi, A. Hasija, G. Lisboa, S. Luz, & J. Malley (eds.)). Cambridge University Press, Cambridge, UK and New York, NY, USA. https://doi.org/10.1017/9781009157926

IPCC. (2022c). *Summary for Policymakers, In: Climate Change 2022: Impacts, Adaptation, and Vulnerability. Contribution of Working Group II to the Sixth Assessment Report of the Intergovernmental Panel on Climate Change* (H.-O. Pörtner, D. C. Roberts, M. Tignor, E. S. Poloczanska, K. Mintenbeck, A. Alegría, M. Craig, S. Langsdorf, S. Löschke, V. Möller, A. Okem, & B. Rama (eds.)). Cambridge University Press. https://doi.org/in press

IROWG. (2021). *Report of IROWG activities: Outcome and recommendations from the IROWG-8 Workshop, CGMS-49 IROWG-WP-01 V3, 28 April 2021, International Radio Occultation Working Group*. https://irowg.org/wpcms/wp-content/uploads/2021/07/CGMS-49-IROWG-WP-01.pdf

Ishii, M., Fukuda, Y., Hirahara, S., Yasui, S., Suzuki, T., & Sato, K. (2017). Accuracy of Global Upper Ocean Heat Content Estimation Expected from Present Observational Data Sets. *SOLA*, *13*, 163–167. https://doi.org/10.2151/sola.2017-030

Jan, A., & Painter, S. L. (2020). Permafrost thermal conditions are sensitive to shifts in snow timing. *Environmental Research Letters*, *15*(8), 084026. https://doi.org/10.1088/1748-9326/ab8ec4

Jaume-Santero, F., Pickler, C., Beltrami, H., & Mareschal, J.-C. (2016). North American regional climate reconstruction from ground surface temperature histories. *Clim. Past*, *12*(12), 2181–2194. https://doi.org/10.5194/cp-12-2181-2016

Johnson, G. C., Lyman, J. M., & Loeb, N. G. (2016). Improving estimates of Earth's energy imbalance. *Nature Climate Change*, *6*(7), 639–640. https://doi.org/10.1038/nclimate3043

Johnson, G. C., Purkey, S. G., Zilberman, N. V, & Roemmich, D. (2019). Deep Argo Quantifies Bottom Water Warming Rates in the Southwest Pacific Basin. *Geophysical Research Letters*, *46*(5), 2662–2669. https://doi.org/10.1029/2018GL081685

Kashiwase, H., Ohshima, K. I., Nihashi, S., & Eicken, H. (2017). Evidence for ice-ocean albedo feedback in the Arctic Ocean shifting to a seasonal ice zone. *Scientific Reports*, *7*(1), 8170. https://doi.org/10.1038/s41598-017-08467-z

Khazaei, B., Read, L. K., Casali, M., Sampson, K. M., & Yates, D. N. (2022). GLOBathy, the global lakes bathymetry dataset. *Scientific Data*, *9*(1), 36. https://doi.org/10.1038/s41597-022-01132-9

King, B. A., Firing, E., & Joyce, T. (2001). Chapter 3.1 Shipboard observations during WOCE. *Int. Geophys.*, *77*, 99–122. https://doi.org/https://doi.org/10.1016/S0074-6142(01)80114-5

Kirchengast, Gottfried; Gorfer, Maximilian; Haimberger, Leopold; Mayer, Michael; Steiner, Andrea; Allan, Richard (2022). Heat stored in the Earth system 1960-2020: Where does the energy go?, submitted to Earth System Science Data. (2022). World Data Center for Climate (WDCC) at DKRZ. https://www.wdc-

climate.de/ui/entry?acronym=GCOS_EHI_1960-2020_AHC

Kobayashi, S., Ota, Y., Harada, Y., Ebita, A., Moriya, M., Onoda, H., Onogi, K., Kamahori, H., Kobayashi, C., Endo, H., MiyaokaI, K., & Takahashi, K. (2015). The JRA-55 Reanalysis: General Specifications and Basic Characteristics. *Journal of the Meteorological Society of Japan. Ser. II*, *93*(1), 5–48. https://doi.org/10.2151/jmsj.2015-001

Kramer, R. J., He, H., Soden, B. J., Oreopoulos, L., Myhre, G., Forster, P. M., & Smith, C. J. (2021). Observational Evidence of Increasing Global Radiative Forcing. *Geophysical Research Letters*, *48*(7), e2020GL091585. https://doi.org/https://doi.org/10.1029/2020GL091585

Kuhlbrodt, T., & Gregory, J. M. (2012). Ocean heat uptake and its consequences for the magnitude of sea level rise and climate change. *Geophysical Research Letters*, *39*(18). https://doi.org/10.1029/2012GL052952

Kuusela, M., & Giglio, D. (2022). *Global Ocean Heat Content Anomalies based on Argo data*. https://doi.org/10.5281/ZENODO.6131625

Labe, Z., Magnusdottir, G., & Stern, H. (2018). Variability of Arctic Sea Ice Thickness Using PIOMAS and the CESM Large Ensemble. *Journal of Climate*, *31*(8), 3233–3247. https://doi.org/10.1175/JCLI-D-17-0436.1

Ladstädter, F., Steiner, A. K., Schwärz, M., & Kirchengast, G. (2015). Climate intercomparison of GPS radio occultation, RS90/92 radiosondes and GRUAN from 2002 to 2013. *Atmospheric Measurement Techniques*, *8*(4), 1819–1834. https://doi.org/10.5194/amt-8-1819-2015

Lane, A. C. (1923). Geotherms of Lake Superior Copper Country. *GSA Bulletin*, *34*(4), 703–720. https://doi.org/10.1130/GSAB-34-703

Lavergne, T., Macdonald Sørensen, A., Kern, S., Tonboe, R., Notz, D., Aaboe, S., Bell, L., Dybkjær, G., Eastwood, S., Gabarro, C., Heygster, G., Anne Killie, M., Brandt Kreiner, M., Lavelle, J., Saldo, R., Sandven, S., & Pedersen, L. T. (2019). Version 2 of the EUMETSAT OSI SAF and ESA CCI sea-ice concentration climate data records. *Cryosphere*, *13*(1), 49–78. https://doi.org/10.5194/tc-13-49-2019

Laxon, S. W., Giles, K. A., Ridout, A. L., Wingham, D. J., Willatt, R., Cullen, R., Kwok, R., Schweiger, A., Zhang, J., Haas, C., Hendricks, S., Krishfield, R., Kurtz, N., Farrell, S., & Davidson, M. (2013). CryoSat-2 estimates of Arctic sea ice thickness and volume (I326, trans.). *Geophysical Research Letters*. https://doi.org/10.1002/grl.50193

Leahy, T. P., Llopis, F. P., Palmer, M. D., & Robinson, N. H. (2018). Using Neural Networks to Correct Historical Climate Observations (I6042, trans.). *Journal of Atmospheric and Oceanic Technology*, *35*(10), 2053–2059. https://doi.org/10.1175/JTECH-D-18-0012.1

Levitus, S., Antonov, J. I., Boyer, T. P., Baranova, O. K., Garcia, H. E., Locarnini, R. A., Mishonov, A. V, Reagan, J. R., Seidov, D., Yarosh, E. S., & Zweng, M. M. (2012). World ocean heat content and thermosteric sea level change (0–2000 m), 1955–2010. *Geophysical Research Letters*, *39*(10). https://doi.org/10.1029/2012GL051106

Li, H., Xu, F., Zhou, W., Wang, D., Wright, J. S., Liu, Z., & Lin, Y. (2017). Development of a global gridded Argo data set with Barnes successive corrections. *Journal of Geophysical Research: Oceans*, *122*(2), 866–889. https://doi.org/https://doi.org/10.1002/2016JC012285

Liao, S., Luo, H., Wang, J., Shi, Q., Zhang, J., & Yang, Q. (2022). An evaluation of Antarctic sea-ice thickness from the Global Ice-Ocean Modeling and Assimilation System based on in situ and satellite observations. *The Cryosphere*, *16*(5), 1807–1819. https://doi.org/10.5194/tc-16-1807-2022

https://doi.org/10.5194/essd-2022-239
Preprint. Discussion started: 1 August 2022

Ligtenberg, S. R. M., Kuipers Munneke, P., Noël, B. P. Y., & van den Broeke, M. R. (2018). Brief communication: Improved simulation of the present-day Greenland firn layer (1960–2016). *The Cryosphere*, *12*(5), 1643–1649. https://doi.org/10.5194/tc-12-1643-2018

Liu, C., Allan, R. P., Mayer, M., Hyder, P., Desbruyères, D., Cheng, L., Xu, J., Xu, F., & Zhang, Y. (2020). Variability in the global energy budget and transports 1985–2017. *Climate Dynamics*, *55*(11), 3381–3396. https://doi.org/10.1007/s00382-020-05451-8

Llovel, W., Willis, J. K., Landerer, F. W., & Fukumori, I. (2014). Deep-ocean contribution to sea level and energy budget not detectable over the past decade. *Nature Climate Change*, *4*(11), 1031–1035. https://doi.org/10.1038/nclimate2387

Loeb, N. G., Johnson, G. C., Thorsen, T. J., Lyman, J. M., Rose, F. G., & Kato, S. (2021). Satellite and Ocean Data Reveal Marked Increase in Earth's Heating Rate. *Geophysical Research Letters*, *48*(13), e2021GL093047. https://doi.org/https://doi.org/10.1029/2021GL093047

Loeb, N. G., Lyman, J. M., Johnson, G. C., Allan, R. P., Doelling, D. R., Wong, T., Soden, B. J., & Stephens, G. L. (2012). Observed changes in top-of-the-atmosphere radiation and upper-ocean heating consistent within uncertainty. *Nature Geoscience*, *5*(2), 110–113. https://doi.org/10.1038/ngeo1375

Loeb, N. G., Mayer, M., Kato, S., Fasullo, J. T., Zuo, H., Senan, R., Lyman, J. M., Johnson, G. C., & Balmaseda, M. (2022). Evaluating Twenty-Year Trends in Earth's Energy Flows From Observations and Reanalyses. *Journal of Geophysical Research: Atmospheres*, *127*(12), e2022JD036686. https://doi.org/https://doi.org/10.1029/2022JD036686

Lyman, J. M., & Johnson, G. C. (2014). Estimating Global Ocean Heat Content Changes in the Upper 1800 m since 1950 and the Influence of Climatology Choice. *Journal of Climate*, *27*(5), 1945–1957. https://doi.org/10.1175/JCLI-D-12-00752.1

MacIntosh, C. R., Merchant, C. J., & von Schuckmann, K. (2017). Uncertainties in Steric Sea Level Change Estimation During the Satellite Altimeter Era: Concepts and Practices. *Surveys in Geophysics*, *38*(1), 59–87. https://doi.org/10.1007/s10712-016-9387-x

Mankoff, K. D., Colgan, W., Solgaard, A., Karlsson, N. B., Ahlstrøm, A. P., van As, D., Box, J. E., Khan, S. A., Kjeldsen, K. K., Mouginot, J., & Fausto, R. S. (2019). Greenland Ice Sheet solid ice discharge from 1986 through 2017. *Earth Syst. Sci. Data*, *11*(2), 769–786. https://doi.org/10.5194/essd-11-769-2019

Marti, F., Blazquez, A., Meyssignac, B., Ablain, M., Barnoud, A., Fraudeau, R., Jugier, R., Chenal, J., Larnicol, G., Pfeffer, J., Restano, M., & Benveniste, J. (2022). Monitoring the ocean heat content change and the Earth energy imbalance from space altimetry and space gravimetry. *Earth Syst. Sci. Data*, *14*(1), 229–249. https://doi.org/10.5194/essd-14-229-2022

Matthews, T., Byrne, M., Horton, R., Murphy, C., Pielke Sr, R., Raymond, C., Thorne, P., & Wilby, R. L. (2022). Latent heat must be visible in climate communications. *WIREs Climate Change*, *13*(4), e779. https://doi.org/https://doi.org/10.1002/wcc.779

Mayer, J., Mayer, M., & Haimberger, L. (2021). Consistency and Homogeneity of Atmospheric Energy, Moisture, and Mass Budgets in ERA5. *Journal of Climate*, *34*(10), 3955–3974. https://doi.org/10.1175/JCLI-D-20-0676.1

Mayer, M., Lien, V. S., Mork, K. A., von Schuckmann, K., Monier, M., & Greiner, E. (2021). Ocean heat content in the High North, in Copernicus Marine Service Ocean State Report, Issue 5. *Journal of Operational Oceanography*, *14:sup1*, 17–23. https://doi.org/10.1080/1755876X.2021.1946240

https://doi.org/10.5194/essd-2022-239
Preprint. Discussion started: 1 August 2022

Mayer, Michael, Haimberger, L., Edwards, J. M., & Hyder, P. (2017). Toward Consistent Diagnostics of the Coupled Atmosphere and Ocean Energy Budgets. *Journal of Climate*, *30*(22), 9225–9246. https://doi.org/10.1175/JCLI-D-17-0137.1

Meng, L., Liu, J., Tarasick, D. W., Randel, W. J., Steiner, A. K., Wilhelmsen, H., Wang, L., & Haimberger, L. (2022). Continuous rise of the tropopause in the Northern Hemisphere over 1980–2020. *Science Advances*, *7*(45), eabi8065. https://doi.org/10.1126/sciadv.abi8065

Meyssignac, B., Boyer, T., Zhao, Z., Hakuba, M. Z., Landerer, F. W., Stammer, D., Köhl, A., Kato, S., L'Ecuyer, T., Ablain, M., Abraham, J. P., Blazquez, A., Cazenave, A., Church, J. A., Cowley, R., Cheng, L., Domingues, C. M., Giglio, D., Gouretski, V., … Zilberman, N. (2019). Measuring Global Ocean Heat Content to Estimate the Earth Energy Imbalance. *Frontiers in Marine Science*, *6*, 432. https://www.frontiersin.org/article/10.3389/fmars.2019.00432

Mieruch, S., Demirel, S., Simoncelli, S., Schlitzer, R., & Seitz, S. (2021). SalaciaML: A Deep Learning Approach for Supporting Ocean Data Quality Control . In *Frontiers in Marine Science* (Vol. 8). https://www.frontiersin.org/articles/10.3389/fmars.2021.611742

Millan, R., Mouginot, J., Rabatel, A., & Morlighem, M. (2022). Ice velocity and thickness of the world's glaciers. *Nature Geoscience*, *15*(2), 124–129. https://doi.org/10.1038/s41561-021-00885-z

Moltmann, T., Turton, J., Zhang, H.-M., Nolan, G., Gouldman, C., Griesbauer, L., Willis, Z., Piniella, Á. M., Barrell, S., Andersson, E., Gallage, C., Charpentier, E., Belbeoch, M., Poli, P., Rea, A., Burger, E. F., Legler, D. M., Lumpkin, R., Meinig, C., … Zhang, Y. (2019). A Global Ocean Observing System (GOOS), Delivered Through Enhanced Collaboration Across Regions, Communities, and New Technologies . In *Frontiers in Marine Science* (Vol. 6, p. 291). https://www.frontiersin.org/article/10.3389/fmars.2019.00291

Moon, T., & Joughin, I. (2008). Changes in ice front position on Greenland's outlet glaciers from 1992 to 2007. *Journal of Geophysical Research: Earth Surface*, *113*(F2). https://doi.org/https://doi.org/10.1029/2007JF000927

Moore, G. W. K., Våge, K., Renfrew, I. A., & Pickart, R. S. (2022). Sea-ice retreat suggests re-organization of water mass transformation in the Nordic and Barents Seas. *Nature Communications*, *13*(1), 67. https://doi.org/10.1038/s41467-021-27641-6

Motyka, R. J., Truffer, M., Fahnestock, M., Mortensen, J., Rysgaard, S., & Howat, I. (2011). Submarine melting of the 1985 Jakobshavn Isbræ floating tongue and the triggering of the current retreat. *Journal of Geophysical Research: Earth Surface*, *116*(F1). https://doi.org/https://doi.org/10.1029/2009JF001632

Mouginot, J., Rignot, E., Bjørk, A., van den Broeke, M., Millan, R., Morlighem, M., Noël, B., Scheuchl, B., & Wood, M. (2019). Forty-six years of Greenland Ice Sheet mass balance from 1972 to 2018. *Proceedings of the National Academy of Sciences*, *116*(19), 9239–9244. https://doi.org/10.1073/pnas.1904242116

Mouginot, J., Rignot, E., Scheuchl, B., Fenty, I., Khazendar, A., Morlighem, M., Buzzi, A., & Paden, J. (2015). Fast retreat of Zachariæ Isstrøm, northeast Greenland. *Science*, *350*(6266), 1357–1361. https://doi.org/10.1126/science.aac7111

Münchow, A., Padman, L., & Fricker, H. A. (2014). Interannual changes of the floating ice shelf of Petermann Gletscher, North Greenland, from 2000 to 2012. *Journal of Glaciology*, *60*(221), 489–499. https://doi.org/DOI: 10.3189/2014JoG13J135

Nauels, A., Meinshausen, M., Mengel, M., Lorbacher, K., & Wigley, T. M. L. (2017). Synthesizing long-term sea level rise projections – the MAGICC sea level model v2.0.

https://doi.org/10.5194/essd-2022-239
Preprint. Discussion started: 1 August 2022

1847 *Geosci. Model Dev.*, *10*(6), 2495–2524. https://doi.org/10.5194/gmd-10-2495-2017
1848 Nicolaus, M., Hoppmann, M., Arndt, S., Hendricks, S., Katlein, C., Nicolaus, A., Rossmann, L.,
1849 Schiller, M., & Schwegmann, S. (2021). Snow Depth and Air Temperature Seasonality on
1850 Sea Ice Derived From Snow Buoy Measurements . In *Frontiers in Marine Science* (Vol.
1851 8). https://www.frontiersin.org/article/10.3389/fmars.2021.655446
1852 Nitzbon, J., Krinner, G., Schneider von Deimling, T., Werner, M., & Langer, M. (2022).
1853 Quantifying the Permafrost Heat Sink in Earth's Climate System. Submitted. *Geophysical*
1854 *Research Letters*.
1855 Nitzbon, Jean; Krinner, Gerhard; Langer, Moritz (2022b). Quantifying the Permafrost Heat Sink
1856 in Earth's Climate System, doi:/10.1002/essoar.10511600.1, submitted to Geophysical
1857 Research Letters (2022). World Data Center for Climate (WDCC) at DKRZ.
1858 https://www.wdc-climate.de/ui/entry?acronym=GCOS_EHI_1960-2020_PHC
1859 Palmer, M D, & McNeall, D. J. (2014). Internal variability of Earth's energy budget simulated
1860 by CMIP5 climate models. *Environmental Research Letters*, *9*(3), 034016.
1861 https://doi.org/10.1088/1748-9326/9/3/034016
1862 Palmer, M D, Roberts, C. D., Balmaseda, M., Chang, Y.-S., Chepurin, G., Ferry, N., Fujii, Y.,
1863 Good, S. A., Guinehut, S., Haines, K., Hernandez, F., Köhl, A., Lee, T., Martin, M. J.,
1864 Masina, S., Masuda, S., Peterson, K. A., Storto, A., Toyoda, T., … Xue, Y. (2017). Ocean
1865 heat content variability and change in an ensemble of ocean reanalyses. *Climate Dynamics*,
1866 *49*(3), 909–930. https://doi.org/10.1007/s00382-015-2801-0
1867 Palmer, Matthew D, Boyer, T., Cowley, R., Kizu, S., Reseghetti, F., Suzuki, T., & Thresher, A.
1868 (2018). An Algorithm for Classifying Unknown Expendable Bathythermograph (XBT)
1869 Instruments Based on Existing Metadata. *Journal of Atmospheric and Oceanic Technology*,
1870 *35*(3), 429–440. https://doi.org/10.1175/JTECH-D-17-0129.1
1871 Palmer, Matthew D, Domingues, C. M., Slangen, A. B. A., & Boeira Dias, F. (2021). An
1872 ensemble approach to quantify global mean sea-level rise over the 20th century from tide
1873 gauge reconstructions (I3507, trans.). *Environmental Research Letters*, *16*(4), 044043.
1874 https://doi.org/10.1088/1748-9326/abdaec
1875 Park, H., Fedorov, A. N., Zheleznyak, M. N., Konstantinov, P. Y., & Walsh, J. E. (2015). Effect
1876 of snow cover on pan-Arctic permafrost thermal regimes. *Climate Dynamics*, *44*(9), 2873–
1877 2895. https://doi.org/10.1007/s00382-014-2356-5
1878 Perovich, D., Polashenski, C., Arntsen, A., & Stwertka, C. (2017). Anatomy of a late spring
1879 snowfall on sea ice. *Geophysical Research Letters*, *44*(6), 2802–2809.
1880 https://doi.org/https://doi.org/10.1002/2016GL071470
1881 Pickler, C., Beltrami, H., & Mareschal, jean-claude. (2016). Laurentide Ice Sheet basal
1882 temperatures during the last glacial cycle as inferred from borehole data. *Climate of the*
1883 *Past*, *12*, 115–127. https://doi.org/10.5194/cp-12-115-2016
1884 Pisoft, P., Sacha, P., Polvani, L. M., Añel, J. A., de la Torre, L., Eichinger, R., Foelsche, U.,
1885 Huszar, P., Jacobi, C., Karlicky, J., Kuchar, A., Miksovsky, J., Zak, M., & Rieder, H. E.
1886 (2021). Stratospheric contraction caused by increasing greenhouse gases. *Environmental*
1887 *Research Letters*, *16*(6), 64038. https://doi.org/10.1088/1748-9326/abfe2b
1888 Purkey, S. G., & Johnson, G. C. (2010). Warming of Global Abyssal and Deep Southern Ocean
1889 Waters between the 1990s and 2000s: Contributions to Global Heat and Sea Level Rise
1890 Budgets. *Journal of Climate*, *23*(23), 6336–6351. https://doi.org/10.1175/2010JCLI3682.1
1891 Qu, X., & Hall, A. (2007). What Controls the Strength of Snow-Albedo Feedback? *Journal of*
1892 *Climate*, *20*(15), 3971–3981. https://doi.org/10.1175/JCLI4186.1

https://doi.org/10.5194/essd-2022-239
Preprint. Discussion started: 1 August 2022

1893 Rhein, M., RintoulS., Aoki, S., Campos, E., Chambers, D., `, Feely, R., Gulev, S., Johnson, G.,
1894 Josey, S., Kostianoy, A., Mauritzen, C., Roemmich, D., Talley, L., & Wang, F. (2013).
1895 *Chapter 3: Observations: Ocean. In: Climate Change 2013: The Physical Science Basis.*
1896 *Contribution of Working Group I to the Fifth Assessment Report of the Intergovernmental*
1897 *Panel on Climate Change.* (T. Stocker, D. Qin, G.-K. Plattner, M. Tignor, S. Allen, J.
1898 Boschung, A. Nauels, Y. Xia, V. Bex, & P. Midgley (eds.)). Cambridge University Press.
1899 Rignot, E., Mouginot, J., Scheuchl, B., van den Broeke, M., van Wessem, M. J., & Morlighem,
1900 M. (2019). Four decades of Antarctic Ice Sheet mass balance from 1979–2017. *Proceedings*
1901 *of the National Academy of Sciences*, *116*(4), 1095.
1902 https://doi.org/10.1073/pnas.1812883116
1903 Riser, S. C., Freeland, H. J., Roemmich, D., Wijffels, S., Troisi, A., Belbéoch, M., Gilbert, D.,
1904 Xu, J., Pouliquen, S., Thresher, A., Le Traon, P.-Y., Maze, G., Klein, B., Ravichandran, M.,
1905 Grant, F., Poulain, P.-M., Suga, T., Lim, B., Sterl, A., … Jayne, S. R. (2016). Fifteen years
1906 of ocean observations with the global Argo array. *Nature Climate Change*, *6*(2), 145–153.
1907 https://doi.org/10.1038/nclimate2872
1908 Roemmich, D., Alford, M. H., Claustre, H., Johnson, K., King, B., Moum, J., Oke, P., Owens,
1909 W. B., Pouliquen, S., Purkey, S., Scanderbeg, M., Suga, T., Wijffels, S., Zilberman, N.,
1910 Bakker, D., Baringer, M., Belbeoch, M., Bittig, H. C., Boss, E., … Yasuda, I. (2019). On
1911 the Future of Argo: A Global, Full-Depth, Multi-Disciplinary Array . In *Frontiers in*
1912 *Marine Science* (Vol. 6, p. 439).
1913 https://www.frontiersin.org/article/10.3389/fmars.2019.00439
1914 Roemmich, D., Church, J., Gilson, J., Monselesan, D., Sutton, P., & Wijffels, S. (2015).
1915 Unabated planetary warming and its ocean structure since 2006 (I3631, trans.). *Nature*
1916 *Climate Change*, *5*, 240. https://doi.org/10.1038/nclimate2513
1917 Roemmich, D., & Gilson, J. (2009). The 2004–2008 mean and annual cycle of temperature,
1918 salinity, and steric height in the global ocean from the Argo Program. *Progress in*
1919 *Oceanography*, *82*(2), 81–100. https://doi.org/https://doi.org/10.1016/j.pocean.2009.03.004
1920 Santer, B D, Wigley, T. M. L., Doutriaux, C., Boyle, J. S., Hansen, J. E., Jones, P. D., Meehl, G.
1921 A., Roeckner, E., Sengupta, S., & Taylor, K. E. (2001). Accounting for the effects of
1922 volcanoes and ENSO in comparisons of modeled and observed temperature trends. *Journal*
1923 *of Geophysical Research: Atmospheres*, *106*(D22), 28033–28059.
1924 https://doi.org/https://doi.org/10.1029/2000JD000189
1925 Santer, Benjamin D, Po-Chedley, S., Feldl, N., Fyfe, J. C., Fu, Q., Solomon, S., England, M.,
1926 Rodgers, K. B., Stuecker, M. F., Mears, C., Zou, C.-Z., Bonfils, C. J. W., Pallotta, G.,
1927 Zelinka, M. D., Rosenbloom, N., & Edwards, J. (2022). Robust anthropogenic signal
1928 identified in the seasonal cycle of tropospheric temperature. *Journal of Climate*, 1–51.
1929 https://doi.org/10.1175/JCLI-D-21-0766.1
1930 Santer, Benjamin D, Po-Chedley, S., Mears, C., Fyfe, J. C., Gillett, N., Fu, Q., Painter, J. F.,
1931 Solomon, S., Steiner, A. K., Wentz, F. J., Zelinka, M. D., & Zou, C.-Z. (2021). Using
1932 Climate Model Simulations to Constrain Observations. *Journal of Climate*, *34*(15), 6281–
1933 6301. https://doi.org/10.1175/JCLI-D-20-0768.1
1934 Savita, A., Domingues, C. M., Boyer, T., Gouretski, V., Ishii, M., Johnson, G. C., Lyman, J. M.,
1935 Willis, J. K., Marsland, S. J., Hobbs, W., Church, J. A., Monselesan, D. P., Dobrohotoff, P.,
1936 Cowley, R., & Wijffels, S. E. (2022). Quantifying Spread in Spatiotemporal Changes of
1937 Upper-Ocean Heat Content Estimates: An Internationally Coordinated Comparison. *Journal*
1938 *of Climate*, *35*(2), 851–875. https://doi.org/10.1175/JCLI-D-20-0603.1

https://doi.org/10.5194/essd-2022-239
Preprint. Discussion started: 1 August 2022

1939 Schweiger, A. J., Wood, K. R., & Zhang, J. (2019). Arctic Sea Ice Volume Variability over
1940 1901–2010: A Model-Based Reconstruction. *Journal of Climate*, *32*(15), 4731–4752.
1941 https://doi.org/10.1175/JCLI-D-19-0008.1
1942 Schweiger, A., Lindsay, R., Zhang, J., Steele, M., Stern, H., & Kwok, R. (2011). Uncertainty in
1943 modeled Arctic sea ice volume. *Journal of Geophysical Research: Oceans*, *116*(C8).
1944 https://doi.org/10.1029/2011JC007084
1945 Shen, P. Y., Wang, K., Beltrami, H., & Mareschal, J.-C. (1992). A comparative study of inverse
1946 methods for estimating climatic history from borehole temperature data. *Palaeogeography,*
1947 *Palaeoclimatology, Palaeoecology*, *98*(2), 113–127.
1948 https://doi.org/https://doi.org/10.1016/0031-0182(92)90192-8
1949 Shen, X., Ke, C.-Q., & Li, H. (2022). Snow depth product over Antarctic sea ice from 2002 to
1950 2020 using multisource passive microwave radiometers. *Earth Syst. Sci. Data*, *14*(2), 619–
1951 636. https://doi.org/10.5194/essd-14-619-2022
1952 Shepherd, A., Fricker, H. A., & Farrell, S. L. (2018). Trends and connections across the
1953 Antarctic cryosphere. *Nature*, *558*(7709), 223–232. https://doi.org/10.1038/s41586-018-
1954 0171-6
1955 Shepherd, A., Ivins, E., Rignot, E., Smith, B., van den Broeke, M., Velicogna, I., Whitehouse, P.,
1956 Briggs, K., Joughin, I., Krinner, G., Nowicki, S., Payne, T., Scambos, T., Schlegel, N.,
1957 Geruo, A., Agosta, C., Ahlstrøm, A., Babonis, G., Barletta, V. R., … Team, T. I. (2019).
1958 Mass balance of the Greenland Ice Sheet from 1992 to 2018. *Nature*.
1959 https://doi.org/10.1038/s41586-019-1855-2
1960 Slater, T., Lawrence, I. R., Otosaka, I. N., Shepherd, A., Gourmelen, N., Jakob, L., Tepes, P.,
1961 Gilbert, L., & Nienow, P. (2021). Review article: Earth's ice imbalance. *The Cryosphere*,
1962 *15*(1), 233–246. https://doi.org/10.5194/tc-15-233-2021
1963 Smith, B., Fricker, A. H., Gardner, S. A., Medley, B., Nilsson, J., Paolo, S. F., Holschuh, N.,
1964 Adusumilli, S., Brunt, K., Csatho, B., Harbeck, K., Markus, T., Neumann, T., Siegfried, M.,
1965 & Zwally, J. H. (2020). Pervasive ice sheet mass loss reflects competing ocean and
1966 atmosphere processes. *Science*, *368*(6496), 1239–1242.
1967 https://doi.org/10.1126/science.aaz5845
1968 Smith, D. M., Allan, R. P., Coward, A. C., Eade, R., Hyder, P., Liu, C., Loeb, N. G., Palmer, M.
1969 D., Roberts, C. D., & Scaife, A. A. (2015). Earth's energy imbalance since 1960 in
1970 observations and CMIP5 models. *Geophysical Research Letters*, *42*(4), 1205–1213.
1971 https://doi.org/10.1002/2014GL062669
1972 Staten, P. W., Grise, K. M., Davis, S. M., Karnauskas, K. B., Waugh, D. W., Maycock, A. C.,
1973 Fu, Q., Cook, K., Adam, O., Simpson, I. R., Allen, R. J., Rosenlof, K., Chen, G.,
1974 Ummenhofer, C. C., Quan, X.-W., Kossin, J. P., Davis, N. A., & Son, S.-W. (2020).
1975 Tropical Widening: From Global Variations to Regional Impacts. *Bulletin of the American*
1976 *Meteorological Society*, *101*(6), E897–E904. https://doi.org/10.1175/bams-d-19-0047.1
1977 Steiner, A K, Ladstädter, F., Ao, C. O., Gleisner, H., Ho, S.-P., Hunt, D., Schmidt, T., Foelsche,
1978 U., Kirchengast, G., Kuo, Y.-H., Lauritsen, K. B., Mannucci, A. J., Nielsen, J. K.,
1979 Schreiner, W., Schwärz, M., Sokolovskiy, S., Syndergaard, S., & Wickert, J. (2020).
1980 Consistency and structural uncertainty of multi-mission GPS radio occultation records
1981 (I1695, trans.). *Atmospheric Measurement Techniques*, *13*(5), 2547–2575.
1982 https://doi.org/10.5194/amt-13-2547-2020
1983 Steiner, Andrea K., Ladstädter, F., Randel, W. J., Maycock, A. C., Fu, Q., Claud, C., Gleisner,
1984 H., Haimberger, L., Ho, S.-P., Keckhut, P., Leblanc, T., Mears, C., Polvani, L. M., Santer,

https://doi.org/10.5194/essd-2022-239
Preprint. Discussion started: 1 August 2022

B. D., Schmidt, T., Sofieva, V., Wing, R., & Zou, C.-Z. (2020). Observed Temperature Changes in the Troposphere and Stratosphere from 1979 to 2018 (I3342, trans.). *Journal of Climate*, *33*(19), 8165–8194. https://doi.org/10.1175/JCLI-D-19-0998.1

Storto, A., Alvera-Azcárate, A., Balmaseda, M. A., Barth, A., Chevallier, M., Counillon, F., Domingues, C. M., Drevillon, M., Drillet, Y., Forget, G., Garric, G., Haines, K., Hernandez, F., Iovino, D., Jackson, L. C., Lellouche, J.-M., Masina, S., Mayer, M., Oke, P. R., … Zuo, H. (2019). Ocean Reanalyses: Recent Advances and Unsolved Challenges. *Frontiers in Marine Science*, *6*, 418. https://doi.org/10.3389/fmars.2019.00418

Storto, A., Masina, S., Simoncelli, S., Iovino, D., Cipollone, A., Drevillon, M., Drillet, Y., Schuckman, K., Parent, L., Garric, G., Greiner, E., Desportes, C., Zuo, H., Balmaseda, M., & Peterson, K. (2018). The added value of the multi-system spread information for ocean heat content and steric sea level investigations in the CMEMS GREP ensemble reanalysis product. *Climate Dynamics*. https://doi.org/10.1007/s00382-018-4585-5

Tilling, R. L., Ridout, A., & Shepherd, A. (2018). Estimating Arctic sea ice thickness and volume using CryoSat-2 radar altimeter data. *Advances in Space Research*, *62*(6), 1203–1225. https://doi.org/https://doi.org/10.1016/j.asr.2017.10.051

Trenberth, K. E., & Fasullo, J. T. (2010). Tracking Earth's Energy. *Science*, *328*(5976), 316. https://doi.org/10.1126/science.1187272

Trenberth, K. E., Fasullo, J. T., von Schuckmann, K., & Cheng, L. (2016). Insights into Earth's Energy Imbalance from Multiple Sources. *Journal of Climate*, *29*(20), 7495–7505. https://doi.org/10.1175/JCLI-D-16-0339.1

Vanderkelen, Inne; Thiery, Wim (2022). Global Heat Uptake by Inland Waters. Geophysical Research Letters, 47(12). e2020GL087867. D O I: https://doi.org/10.1029/2020GL087867. (2020). World Data Center for Climate (WDCC) at DKRZ. https://www.wdc-climate.de/ui/entry?acronym=GCOS_EHI_1960-2020_IWHC

Vanderkelen, I., van Lipzig, N. P. M., Lawrence, D. M., Droppers, B., Golub, M., Gosling, S. N., Janssen, A. B. G., Marcé, R., Schmied, H. M., Perroud, M., Pierson, D., Pokhrel, Y., Satoh, Y., Schewe, J., Seneviratne, S. I., Stepanenko, V. M., Tan, Z., Woolway, R. I., & Thiery, W. (2020). Global Heat Uptake by Inland Waters. *Geophysical Research Letters*, *47*(12), e2020GL087867. https://doi.org/https://doi.org/10.1029/2020GL087867

Verver, G., Fujiwara, M., Dolmans, P., Becker, C., Fortuin, P., & Miloshevich, L. (2006). Performance of the Vaisala RS80A/H and RS90 Humicap Sensors and the Meteolabor "Snow White" Chilled-Mirror Hygrometer in Paramaribo, Suriname. *Journal of Atmospheric and Oceanic Technology*, *23*(11), 1506–1518. https://doi.org/10.1175/JTECH1941.1

Vömel, H., Selkirk, H., Miloshevich, L., Valverde-Canossa, J., Valdés, J., Kyrö, E., Kivi, R., Stolz, W., Peng, G., & Diaz, J. A. (2007). Radiation Dry Bias of the Vaisala RS92 Humidity Sensor. *Journal of Atmospheric and Oceanic Technology*, *24*(6), 953–963. https://doi.org/10.1175/JTECH2019.1

von Schuckmann, Karina; Minière, Audrey; Gues, Flora; Cuesta-Valero, Francisco; Kirchengast, Gottfried; Adusumilli, Susheel; Straneo, Fiammetta; Allan, Richard; Barker, Paul M.; Beltrami, Hugo; Boyer, Tim; Cheng, Lijing; Church, John; Desbruyeres, Damien; Dolman, Han; Domingues, Catia; García-García, Almudena; Gilson, John; Gorfer, Maximilian; Haimberger, Leopold; Hendricks, Stefan; Hosoda, Shigeki; Johnson, Gregory; Killick, Rachel; King, Brian; Kolodziejczyk, Nicolas; Korosov, Anton; Krinner, Gerhard; Kuusela, Mikael; Langer, Moritz; Lavergne, Thomas; Lawrence, Isobel; Li, Yuehua; Lyman, John;

Marzeion, Ben; Mayer, Michael; MacDougall, Andrew; McDougall, Trevor; Monselesan, Didier; Nitzbon, Jean; Otosaka, Inès; Peng, Jian; Purkey, Sarah; Roemmich, Dean; Sato, Kanako; Sato, Katsunari; Savita, Abhishek; Schweiger, Axel; Shepherd, Andrew; Seneviratne, Sonia; Slater, Donald; Slater, Thomas; Smith, Noah; Steiner, Andrea; Szekely, Tanguy; Suga, Toshio; Thiery, Wim; Timmermanns, Mary-Louise; Vanderkelen, Inne; Wijffels, Susan; Wu, Tonghua; Zemp, Michael; Simons, Leon (2022). Heat stored in the Earth system 1960-2020: Where does the energy go?. World Data Center for Climate (WDCC) at DKRZ. https://www.wdc-climate.de/ui/entry?acronym=GCOS_EHI_1960-2020_OHC

von Schuckmann, K., Palmer, M. D., Trenberth, K. E., Cazenave, A., Chambers, D., Champollion, N., Hansen, J., Josey, S. A., Loeb, N., Mathieu, P.-P., Meyssignac, B., & Wild, M. (2016). An imperative to monitor Earth's energy imbalance. *Nature Climate Change*, *6*(2), 138–144. https://doi.org/10.1038/nclimate2876

von Schuckmann, K, Cheng, L., Palmer, M. D., Hansen, J., Tassone, C., Aich, V., Adusumilli, S., Beltrami, H., Boyer, T., Cuesta-Valero, F. J., Desbruyères, D., Domingues, C., García-García, A., Gentine, P., Gilson, J., Gorfer, M., Haimberger, L., Ishii, M., Johnson, G. C., … Wijffels, S. E. (2020). Heat stored in the Earth system: where does the energy go? *Earth Syst. Sci. Data*, *12*(3), 2013–2041. https://doi.org/10.5194/essd-12-2013-2020

von Schuckmann, K, & Le Traon, P.-Y. (2011). How well can we derive Global Ocean Indicators from Argo data? *Ocean Sci.*, *7*(6), 783–791. https://doi.org/10.5194/os-7-783-2011

von Schuckmann, Karina, Le Traon, P.-Y., Smith, N., Pascual, A., Brasseur, P., Fennel, K., Djavidnia, S., Aaboe, S., Fanjul, E. A., Autret, E., Axell, L., Aznar, R., Benincasa, M., Bentamy, A., Boberg, F., Bourdallé-Badie, R., Nardelli, B. B., Brando, V. E., Bricaud, C., … Zuo, H. (2018). Copernicus Marine Service Ocean State Report. *Journal of Operational Oceanography*, *11*(sup1), S1–S142. https://doi.org/10.1080/1755876X.2018.1489208

Wanders, N., Thober, S., Kumar, R., Pan, M., Sheffield, J., Samaniego, L., & Wood, E. F. (2019). Development and Evaluation of a Pan-European Multimodel Seasonal Hydrological Forecasting System. *Journal of Hydrometeorology*, *20*(1), 99–115. https://doi.org/10.1175/JHM-D-18-0040.1

Wang, X., Key, J., Kwok, R., & Zhang, J. (2016). Comparison of Arctic Sea Ice Thickness from Satellites, Aircraft, and PIOMAS Data. In *Remote Sensing* (Vol. 8, Issue 9). https://doi.org/10.3390/rs8090713

WCRP Global Sea Level Budget Group. (2018). Global sea-level budget 1993–present. *Earth Syst. Sci. Data*, *10*(3), 1551–1590. https://doi.org/10.5194/essd-10-1551-2018

Webster, M. A., DuVivier, A. K., Holland, M. M., & Bailey, D. A. (2021). Snow on Arctic Sea Ice in a Warming Climate as Simulated in CESM. *Journal of Geophysical Research: Oceans*, *126*(1), e2020JC016308. https://doi.org/https://doi.org/10.1029/2020JC016308

Weihs, P., Laimighofer, J., Formayer, H., & Olefs, M. (2021). Influence of snow making on albedo and local radiative forcing in an alpine area. *Atmospheric Research*, *255*, 105448. https://doi.org/https://doi.org/10.1016/j.atmosres.2020.105448

WGMS. (2021). *Fluctuations of Glaciers Database. World Glacier Monitoring Service, Zurich, Switzerland.* https://doi.org/DOI:10.5904/wgms-fog-2021-05

Wijffels, S., Roemmich, D., Monselesan, D., Church, J., & Gilson, J. (2016). Ocean temperatures chronicle the ongoing warming of Earth. *Nature Climate Change*, *6*(2), 116–118. https://doi.org/10.1038/nclimate2924

https://doi.org/10.5194/essd-2022-239
Preprint. Discussion started: 1 August 2022

2077 Willis, J. K., Roemmich, D., & Cornuelle, B. (2004). Interannual variability in upper ocean heat
2078 content, temperature, and thermosteric expansion on global scales. *Journal of Geophysical*
2079 *Research: Oceans*, *109*(C12). https://doi.org/10.1029/2003JC002260
2080 Wilson, N., Straneo, F., & Heimbach, P. (2017). Satellite-derived submarine melt rates and mass
2081 balance (2011–2015) for Greenland's largest remaining ice tongues. *The Cryosphere*, *11*,
2082 2773–2782. https://doi.org/10.5194/tc-11-2773-2017
2083 WMO. (2022). *The State of the Global Climate 2021*.
2084 https://library.wmo.int/index.php?lvl=notice_display&id=22080
2085 Wunsch, C. (2020). Is the Ocean Speeding Up? Ocean Surface Energy Trends. *Journal of*
2086 *Physical Oceanography*, *50*, 3205–3217. https://doi.org/10.1175/JPO-D-20-0082.1
2087 Zanna, L., Khatiwala, S., Gregory, J. M., Ison, J., & Heimbach, P. (2019). Global reconstruction
2088 of historical ocean heat storage and transport. *Proceedings of the National Academy of*
2089 *Sciences*, *116*(4), 1126. https://doi.org/10.1073/pnas.1808838115
2090 Zemp, M., Huss, M., Thibert, E., Eckert, N., McNabb, R., Huber, J., Barandun, M., Machguth,
2091 H., Nussbaumer, S. U., Gärtner-Roer, I., Thomson, L., Paul, F., Maussion, F., Kutuzov, S.,
2092 & Cogley, J. G. (2019). *Global and regional glacier mass changes from 1961 to 2016*.
2093 https://doi.org/10.5281/ZENODO.3557199
2094 Zemp, Michael, Huss, M., Eckert, N., Thibert, E., Paul, F., Nussbaumer, U. S., & Gärtner-Roer,
2095 I. (2020). Brief communication: Ad hoc estimation of glacier contributions to sea-level rise
2096 from the latest glaciological observations (I5946, trans.). *Cryosphere*, *14*(3).
2097 https://doi.org/10.5194/tc-14-1043-2020
2098 Zhang, J., & Rothrock, D. A. (2003). Modeling Global Sea Ice with a Thickness and Enthalpy
2099 Distribution Model in Generalized Curvilinear Coordinates. *Monthly Weather Review*,
2100 *131*(5), 845–861. https://doi.org/10.1175/1520-0493(2003)131<0845:MGSIWA>2.0.CO;2
2101 Zhang, R., Wang, H., Fu, Q., Rasch, J. P., & Wang, X. (2019). Unraveling driving forces
2102 explaining significant reduction in satellite-inferred Arctic surface albedo since the 1980s.
2103 *Proceedings of the National Academy of Sciences*, *116*(48), 23947–23953.
2104 https://doi.org/10.1073/pnas.1915258116
2105 Zou, C.-Z., Xu, H., Hao, X., & Fu, Q. (2021). Post-Millennium Atmospheric Temperature
2106 Trends Observed From Satellites in Stable Orbits. *Geophysical Research Letters*, *48*(13),
2107 e2021GL093291. https://doi.org/https://doi.org/10.1029/2021GL093291
2108